



UMEÅ UNIVERSITY

New Alternatives to Combat
Listeria monocytogenes and
Chlamydia trachomatis

Design, Synthesis, and Evaluation of
Substituted Ring-Fused 2-Pyridones as
Anti-Virulent Agents

Martina Kulén

Department of Chemistry
Umeå University
Umeå, Sweden 2018

Responsible publisher under Swedish law: the Dean of the Faculty of Science and Technology

This work is protected by the Swedish Copyright Legislation (Act 1960:729)

Dissertation for PhD

ISBN: 978-91-7601-920-7

Cover illustration by Robert Svensson

Electronic version available at: <http://umu.diva-portal.org/>

Printed by: Service Center, KBC, Umeå University

Umeå, Sweden 2018

“Walking is man’s best medicine”

Hippocrates
460 BC- 370 BC

Table of Contents

Abstract.....	iii
Preface	v
Abbreviations.....	vii
List of publications.....	ix
Populärvetenskaplig sammanfattning	xi
Antibiotikaresistens – ett globalt problem	xi
2-pyridoner som avväpnare – en ny typ av antibiotika	xii
1. Introduction	1
Antibiotic drugs	1
Antibiotic resistance	1
Anti-virulence drug approach	2
Design and development of ring-fused 2-pyridones.....	3
Similarities and differences of the <i>Listeria monocytogenes</i> and the <i>Chlamydia trachomatis</i> projects	4
<i>Listeria monocytogenes</i>	5
<i>Chlamydia trachomatis</i>	8
2. Objectives	11
3. Structure-based design of ring-fused 2-pyridones targeting <i>Listeria monocytogenes</i> (Paper I)	13
Synthesis of the first compound set	16
Biological screen of compounds.....	20
Design, synthesis, and evaluation of further analogues.....	22
Further evaluation of inhibition candidates.....	23
Summary and concluding remarks.....	27
4. Towards new ring-fused 2-pyridones targeting <i>Listeria monocytogenes</i> (Appendix 1).....	28
Summary and future plans.....	35
5. Ring-fused 2-pyridone amide isosteres inhibiting <i>Chlamydia trachomatis</i> infection (Paper II).....	37
Synthesis of compounds	38
Evaluation of biological activity	42
Summary and concluding remarks	45
6. C8-substituted ring-fused 2-pyridone amide analogues targeting <i>Chlamydia trachomatis</i> infectivity (Paper III)	46
Synthesis of the first set of inhibitor candidates	47
Evaluation of biological effectivity of the first set of inhibitor candidates.....	50
Synthesis and biological evaluation of the second set of inhibitor candidates	53
Summary and concluding remarks	58
7. Formation of ring-fused 4-pyridones (Appendix 2)	59

Summary and concluding remarks	62
8. Summary and future directions	63
Conclusion	66
Appendix 1	67
Appendix 2	73
Acknowledgement.....	77
References	79

Abstract

Antibiotic resistance has become a global health burden with the number of resistant bacteria continuously increasing. Antibiotic drugs act by being either bactericidal (killing bacteria) or bacteriostatic (inhibiting growth of bacteria). However, these modes of action increase the selective pressure on the bacteria. An alternative treatment strategy to antibiotics is anti-virulence therapies that inhibits virulence of the pathogenic bacteria. The term “virulence” summarises a number of factors that the bacteria need to colonise a new niche and as a consequence its ability to infect and cause diseases. By inhibiting virulence, instead of killing, the selective pressure on the bacteria can be reduced and consequently decreases the rapid development of resistance. This thesis describes two projects focusing on development of anti-virulence agents, with the ring-fused 2-pyridone scaffold as the central character, targeting the bacteria *Listeria monocytogenes* and *Chlamydia trachomatis*.

The first project is targeting *L. monocytogenes*, which is the cause for listeriosis in humans. This can develop into life-threatening encephalitis and meningitis as well as cause severe complications for developing fetus. The target in *L. monocytogenes* is the transcriptional regulator PrfA that control almost all virulence factors in this bacterium. We have designed and synthesised potent substituted ring-fused 2-pyridones, which at low micromolar concentrations block activation of the virulence regulator PrfA and thus attenuate the bacterial infection. Co-crystallisation of the active ring-fused 2-pyridones with PrfA resulted in determination of the exact substance interaction site in the protein. This facilitated further structure-based design that resulted in improved compounds capable of attenuating *L. monocytogenes* in an *in vivo* model.

The second project targets *C. trachomatis*, which is the causative agent behind the most common sexually transmitted infection as well as the eye infection trachoma. By structure-activity relationship analysis of previously tested ring-fused 2-pyridones, we have designed and synthesised non-hydrolysable ring-fused 2-pyridone amide isosteres. The most potent analogues inhibit *C. trachomatis* infectivity at low nanomolar concentrations, without showing host cell toxicity or affecting the viability of commensal microbiota. Introduction of heteroatom substituents at specific sites of the ring-fused 2-pyridone scaffold, resulted in improved pharmacokinetic properties of the analogues and further evaluation *in vivo* was performed.

Preface

The central character of this thesis and the work presented, is the ring-fused 2-pyridone scaffold (Figure 1). The thesis is built on two multidisciplinary collaboration projects, where the key focus has been on the development of synthetic strategies towards ring-fused 2-pyridone analogues targeting *Listeria monocytogenes* or *Chlamydia trachomatis*. The overall aim is to explore the structure-activity relationship aiming at potent nontoxic anti-virulence compounds that block virulence, without affecting bacterial proliferation. The thesis is based on published articles and unpublished material included in the chapters and appendices.

The project targeting *Listeria monocytogenes* is a collaboration between three research groups comprising synthetic organic chemistry (Fredrik Almqvist's group), structural biology (Elisabeth Sauer-Eriksson's group), and molecular biology (Jörgen Johansson's group). Based on the known target, the transcriptional regulator PrfA, we have designed and synthesised new substituted ring-fused 2-pyridone analogues with particular focus on the C7- and C8-positions. The compounds have been evaluated by *in vitro* and *in vivo* models and their specific interactions to PrfA has been assessed by determination of crystal structures of PrfA in complex with the compounds (Chapter 3 and 4).

The project targeting *Chlamydia trachomatis* is a collaboration between two research groups focused on synthetic organic chemistry (Fredrik Almqvist's group) and molecular biology (Sven Bergström's group). The target in this project is unknown, thus structure-activity relationship has been the basis of compound design. The main structural investigations have been focused on the positions C3, C7, and C8, in order to improve anti-virulence activity and the pharmacokinetic properties of the compounds (Chapter 5 and 6), which have been evaluated for their biological activity.

The C8-nitrogen analogue chemistry utilised in Paper I was developed by Andrew G. Cairns and further elaborated alongside Anders E. G. Lindgren for Paper III. The isostere synthesis in Paper II was undertaken in collaboration with James A. D. Good.

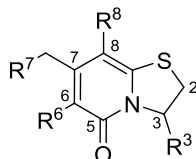


Figure 1. The ring-fused 2-pyridone scaffold with marked substitution sites. The substitution numbering will be the same throughout the thesis.

Abbreviations

ActA	actin assembly-inducing protein
Ac	acetyl
AUC	area under curve
BOC	<i>tert</i> -butyloxycarbonyl
BODIPY	dipyrrromethene boron difluoride
C _{max}	peak blood concentrations
<i>C. trachomatis</i>	<i>Chlamydia trachomatis</i>
calc.	calculated
cAMP	cyclic adenosine monophosphate
Cbz	carboxybenzyl
Crp	cAMP receptor protein
CuAAC	Cu(I)-catalysed azide–alkyne cycloaddition
CUP	chaperone/usHER pathway
DCC	<i>N, N'</i> -dicyclohexyl carbodiimide
DCE	1,2-dichloroethane
DCM	dichloromethane
DIPEA	<i>N,N</i> -Diisopropylethyl amine or Hünig's base
DMAP	4-dimethylaminopyridine
DMF	<i>N,N</i> -dimethylformamide
DMSO	dimethyl sulfoxide
DPPA	diphenylphosphorylazide
EB	elementary body
<i>E. Coli</i>	<i>Escherichia coli</i>
Et	ethyl
Fnr	fumarate nitrate reductase regulator
HATU	1-[Bis(dimethylamino)methylene]-1 <i>H</i> -1,2,3-triazolo[4,5- <i>b</i>]pyridinium 3-oxid hexafluorophosphate
HGF	hepatocyte growth factor
HMBC	Heteronuclear Multiple-Bond Coherence
HPLC	High-Performance Liquid Chromatography
Hpt	hexose phosphate transporter
HTH	helix-turn-helix
InlA	internalin A
InlB	internalin B
ITC	isothermal titration calorimetry
<i>L. monocytogenes</i>	<i>Listeria monocytogenes</i>
LGV	lymphogranuloma venereum
LLO	listeriolysin O
<i>m</i>	meta

Me	methyl
MWI	microwave irradiation
NMR	nuclear magnetic resonance
NOE	nuclear Overhauser effect
<i>p</i>	para
PBS	phosphate-buffered saline
PID	pelvic inflammatory disease
PK	pharmacokinetic
PrfA	positive regulatory factor A
RB	reticulate body
ROESY	rotating frame Overhauser effect spectroscopy
SAR	structure-activity relationship
SPR	surface plasmon resonance
STI	Sexually transmitted infection
T ₃ P	1-propanephosphonic acid cyclic anhydride
TBTU	2-(1 <i>H</i> -Benzotriazole-1-yl)-1,1,3,3-tetramethyluronium tetrafluoroborate
TEA	triethylamine
TFA	trifluoroacetic acid
THF	tetrahydrofuran
WHO	World health organisation

List of publications

Within the text of this thesis, the papers are referred to by their Roman numerals.

- I. Martina Kulén*, Marie Lindgren*, Sabine Hansen, Andrew G. Cairns, Christin Grundström, Afshan Begum, Ingeborg van der Lingen, Kristoffer Brännström, Michael Hall, Uwe H. Sauer, Jörgen Johansson, A. Elisabeth Sauer-Eriksson, and Fredrik Almqvist. Structure-Based Design of Inhibitors Targeting PrfA, the Master Virulence Regulator of *Listeria monocytogenes*. *J. Med. Chem.* **2018**, 61, 4165–4175.
- II. James A. D. Good*, Martina Kulén*, Jim Silver, K. Syam Krishnan, Wael Bahnan, Carlos Nuñez-Otero, Ingela Nilsson, Emma Wede, Esmee de Groot, Åsa Gylfe, Sven Bergström, and Fredrik Almqvist. Thiazolino 2-Pyridone Amide Isosteres as Inhibitors of *Chlamydia trachomatis* Infectivity. *J. Med. Chem.* **2017**, 60, 9393–9399.
- III. Martina Kulén*, Carlos Núñez-Otero*, Andrew G. Cairns, Jim Silver, Anders E. G. Lindgren, Emma Wede, Pardeep Singh, Wael Bahnan, James A. D. Good, Richard Svensson, Sven Bergström, Åsa Gylfe, Fredrik Almqvist. Design, Synthesis, and Evaluation of *Chlamydia trachomatis* Infectivity Inhibitors with Improved Pharmacokinetic Properties. Manuscript.

*These authors contributed equally.

Papers have been reprinted with the permission from the publishers.

Other related published work:

Patent:

Good, James Arthur Dudley; Kulén, Anna Martina; Almqvist, Klas Fredrik; Cairns, Andrew Gerard; Pontén, John Fritiof. Ring-fused thiazolino 2-pyridones, methods for preparation thereof and their use in the treatment of bacterial infections; WO 2016075296 A1

Contributions to papers:

- I. Planned and performed synthesis, developed synthetic routes, analysed data, coordinated the writing of the manuscript, and major writing.
- II. Performed synthesis, analysed data, coordinated the writing of the manuscript, and medium writing.
- III. Planned and performed synthesis, developed synthetic routes, analysed data, coordinated the writing of the manuscript, and major writing.

Populärvetenskaplig sammanfattning

Antibiotikaresistens – ett globalt problem

Antibiotikaresistens hos bakterier är idag ett omfattande problem i hela världen. Då vi lever i en globaliserad värld, där vi har möjlighet att resa och förflytta oss över jorden i en mycket snabbare takt än tidigare och likaså är det för bakterier. Antibiotikaresistensen sitter i bakterien och därmed är det inte vi människor själva som är resistent mot antibiotikamedicinerna. Det är en naturlig del av bakteriens liv att genom förändringar, så kallade mutationer, förbättra sin chans till att överleva när det uppstår hot utifrån, som till exempel vid en antibiotikakur. Antibiotika verkar genom att döda eller stoppa bakteriens tillväxt. För att skydda sig mot detta så kan bakterien förändra sig själv eller ta upp förändringar från andra bakterier. Detta kan liknas med att den bygger en skyddsmur runt sig själv eller utrustar sig med bättre vapen för att antibiotikan inte ska kunna ta död på den. Att ha denna skyddsmur eller specialvapen är dock kostsamt för bakterien och därmed finns det inte så många av dessa. De andra bakterierna, som inte har något extraskydd, kan lättare konkurrera om de nödvändiga resurserna i omgivningen och kommer därmed föröka sig mer. Vid behandling med antibiotika så dör bakterierna utan extraskydd medan de med specialskydd överlever. Detta betyder att konkurrensen över resurserna kommer vara mycket lägre och de muterade bakterierna har fritt fram att ta för sig av det de behöver för att kunna föröka sig och sprida sig vidare.

Antibiotika används inte endast för att direkt bota sjukdomar orsakade av bakterier utan är även livsnödvändigt vid operationer, kejsarsnitt, neonatalvård, organdonationer och cancerbehandlingar för att förhindra eventuell bakterieinfektion. Dock är över- och felanvändning av antibiotika stor idag vilket har lett till att resistensutvecklingen hos bakterier har ökat och sker i en mycket snabbare takt än innan. Inom till exempel köttindustrin har antibiotika traditionellt använts för att behandla infektioner hos djuren men även som sjukdomsförebyggande och för att stimulera snabbare tillväxt av djuren. I Sverige är användningen av antibiotika som tillväxtstimulerande hos djur förbjudet sedan 1986 vilket har lett till en betydande minskning av antibiotikaanvändandet. Sverige är också ett av de västländer som har lägst förekomst av antibiotikaresistenta bakterier inom sjukvården. Konsekvenserna av att inte ha effektiva antibiotikaläkemedel är stora och år 2050 beräknas fler än 10 miljoner människor per år avlida till följd av resistent sjukdomar. Detta kommer att kosta samhället betydande summor, både genom produktionsbortfall och sjukhuskostnader.

2-pyridoner som avväpnare – en ny typ av antibiotika

För att minska trycket på bakterierna och deras utveckling av antibiotikaresistens samt för att kunna behandla bakteriella sjukdomar i framtiden så behövs nya läkemedel. Min forskning handlar om en ny typ av antibiotika, antivirulens-läkemedel, som inte dödar bakterier utan endast avväpnar dem. Några av sätten, som vi har valt, är att klippa av bakteriernas hår (som bakterierna använder sig av för att sätta sig fast på människoceller) eller genom att hindra bakterierna från att aktivera sin sjukdomsframkallande förmåga (virulens). Genom att skapa nya läkemedel som inte dödar bakterier men som avväpnar dem, hoppas vi på att minska risken för resistensutveckling hos bakterien. Dessa nya antivirulens-läkemedel fungerar genom att de stoppar bakterien från att kunna sprida sjukdomen i kroppen, men bakterierna kommer fortfarande att leva. Kroppens egna immunsystem kan då gå in och rensa bort de avväpnade bakterierna. Genom att inte döda bakterierna hindrar man skapandet av en miljö som gynnar tillväxten av bakterier med specialskydd och därmed gör man det svårare för dem att sprida sig.

I den här avhandlingen beskrivs min forskning för att hitta antivirulens-läkemedel mot två olika bakterier, *Listeria monocytogenes* (Listeria) och *Chlamydia trachomatis* (Klamydia). *L. monocytogenes* kan orsaka listerios, vilken kan leda till allvarlig blodförgiftning och hjärnhinneinflammation. Hos gravida kvinnor kan infektionen gå över till fostret och leda till missfall eller dödfödsel. *C. trachomatis* kan ge den sexuellt överförbara könssjukdomen klamydia och ögoninfektionen trakom. Klamydia kan spridas vidare och bland annat orsaka äggledarinflammation hos kvinnor och bitestikelinflammation hos män. I vår forskning har vi utvecklat molekyler (aktiva ämnet i läkemedel) som kallas 2-pyridoner. Inom Listeriaprojektet har vi utvecklat dessa 2-pyridoner till att hämma bakteriens sjukdomsframkallande förmåga genom att stänga bakteriens av/på-knapp som aktiverar detta. Inom Klamydia projektet så har vi utvecklat mycket effektiva 2-pyridoner som gör klamydiabakterierna infektionssterila. Vi har bevisat våra resultat genom studier i celler och i mer avancerade modeller.

1. Introduction

Antibiotic drugs

The revolutionary discovery of penicillin¹ during the first half of the 20th century and its introduction into the pharmaceutical market in the 1940's, was the starting point of a new era of therapeutic medicine.² During the following decades, called the 'Golden age' of antibiotic discovery, numerous new antibiotic classes were discovered. A rapid decline in the antibiotic drug pipeline began in the 1980's and only a few new antibiotic classes are under development today.^{3,4} During the last decades a majority of the new antibiotic drugs introduced into the market have been modifications of already existing antibiotic classes.³

Today, antibiotic drugs are extensively used as direct treatment or prevention of bacterial diseases, both in humans and food animal production. In US, over 70% of the sold antibiotics are used in animals.⁵ Antibiotic drugs usage is essential for neonatal care,⁶ caesarean sections, chemotherapy, and advanced surgery.^{5,7} However, antibiotic drugs are over- and misused in situations where they are not needed, both in humans and animals.^{5,8} Within the food production industry, antibiotics has been used as growth promoters in animals since the 1950's.⁹ This type of antibiotic management was banned in Sweden 1986.¹⁰ However, it took until 2006 for antibiotic growth promoters to be banned within the European Union.⁹ As a result of the ban, the quantity of antibiotics given to farmed animals has decreased. In Sweden the usage of antibiotics decreased with 65% by 2004, compared with before the ban.¹¹

Antibiotic resistance

The mode of action of antibiotic drugs are either bactericidal (by killing the bacteria) or bacteriostatic, where the latter hinders the bacterial growth cycle by disturbing central biochemical processes in the bacteria (*e.g.* protein synthesis).¹² This positions the treated bacteria under substantial stress and by eliminating sensitive strains of the pathogen, resistant strains will be able to grow without competition into large populations.^{13,14} Resistance development of antibiotics is a natural phenomenon in bacteria but the widespread use and misuse of these drugs has led to a comprehensive increase of antibacterial resistance, which has resulted in less effective or even ineffective drugs.^{7,15} The overuse of antibiotics has given rise to single as well as multidrug resistant bacteria.¹⁶ Antibiotics effectively kill or disturb growth of pathogenic bacteria, however, their lack of specificity, in particular for broad-spectrum antibiotics, results in disturbance of the host commensal microbiota.¹⁷ The level of disturbance depends on the antibiotic drug used, but can cause both long- and

short-term differences of the gut microbiota and favour resistant microorganism development.¹⁷⁻²⁰

Anti-virulence drug approach

An alternative infection treatment strategy is to inhibit the virulence of the pathogenic bacteria. Virulence is the pathogenic bacteria's ability to infect and cause disease in a host.²¹ After entering a host, the bacteria will recognise specific host signals and virulence factors will be activated, which empower the bacteria to invade cells, fight off host defence, and spread within the host.^{13,21} Examples of different virulence factors are invasion factors, endotoxins, exotoxins, siderophores, capsules, adherence factors, and quorum sensing.^{21,22}

An anti-virulence drug would target specific virulence factor(s) to disarm the bacteria, without disturbing bacterial growth or killing the bacteria.^{13,14} Inhibition of specific virulence factors could interfere and reduce the ability of the bacteria to colonise and recognise signals from the host, preventing further infection. These strategies would not directly damage the bacteria, instead only disarm them and allow the host immune system to clear any established infection.^{13,14} An anti-virulence drug approach requires comprehensive understanding of the virulence factors of the targeted pathogenic bacteria.²² Depending on the target, this type of drugs can be designed to be pathogen- or even strain-specific as well as be restricted to specific sites in the host where it is beneficial for the pathogen to express its virulence.^{23,24} By having a target-specific anti-virulence drug there is potential to minimise off-target effects, such as disturbance of the host gut microbiota.²³ Therefore, this approach might cause less selective pressure on bacteria and as a result repress the reproduction of resistant bacterial strains and hopefully lighten the burden of resistance development.^{13,14}

The anti-virulence treatment approach would especially be beneficial for non-emergency diseases (*e.g.* genital chlamydia infections), which do not have a fatal outcome and are today treated with broad-spectrum antibiotics.²⁵ Anti-virulence drugs can also be used in combination with antibiotic drugs, to obtain a synergetic effect between them.^{13,24} However, when considering extremely invasive diseases with rapid onset and high fatality rate, antibiotics with their rapid clearance of the infection are invaluable. Therefore, to be able to effectively treat these diseases in the future the antibiotic effectiveness needs to be preserved. There are several factors and areas which need to be considered, all from reduction of the over- and misuse of current drugs, infection prevention, vaccination programs, information campaigns about resistance, as well as obtaining new effective drugs. Both new antibiotics and virulence inhibitors could also help ease the resistance development pressure.⁵

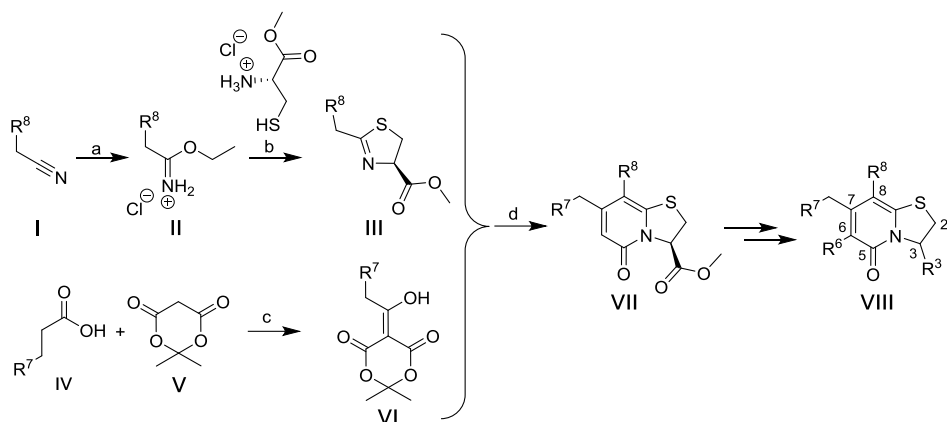
Design and development of ring-fused 2-pyridones

The compounds that have been developed in this thesis share a common heterocyclic central fragment, a ring-fused 2-pyridone. The development of the ring-fused 2-pyridones had its starting point in the search for substances that could prevent the formation of pili, virulence factors expressed in uropathogenic *Escherichia coli* (*E. coli*).²⁶ The target was the chaperone/usher pathway (CUP) that is essential for the formation of pili in *E. coli*.²⁷ Structure-based design was used to design peptidomimetic structures that could inhibit the chaperone, thus attenuating the following pili formation.^{26,28,29} Development of the structures resulted in the thiazolino ring-fused 2-pyridone scaffold (**VII**, Scheme 1.1), which is one of the core scaffolds the Almqvist research group is working with today. The expansion and development of the scaffold has opened doors for several new biological targets for future possible anti-virulence drug analogues.³⁰⁻³⁷ Although the core structure of the thiazolino ring-fused 2-pyridone is kept within several projects, the diverse substitution patterns distinguishes their specificity for different biological targets.

Over the years the synthetic route to thiazolino ring-fused 2-pyridones has been improved and is today well established.^{38,39} The core scaffold can readily be synthesised from commercially available nitriles (**I**) and carboxylic acids (**IV**). The nitrile (**I**) is transformed into an iminoether hydrochloride salt (**II**) *via* a Pinner reaction under acidic conditions (Scheme 1.1). The iminoether is, then converted to the corresponding thiazoline (**III**), through condensation with cysteine. Previously, the standard method in our research laboratory to obtain the iminoether hydrochloride salt analogues was by bubbling HCl gas through the reaction mixture, generated from sulfuric acid and ammonium chloride in a separate flask. However, the laboratory setup of this method is both time and space consuming. Therefore, a more convenient *in situ* method using acetyl chloride in ethanol was developed and is today the standard method in our laboratory. The acyl Meldrum's acid derivative (**VI**) is obtained *via* coupling of the substituted carboxylic acid (**III**) to Meldrum's acid (**V**). Thereafter, acyl Meldrum's acid derivative (**VI**) reacts through an acyl-ketene imine cycloaddition together with thiazoline (**III**) at elevated temperatures followed by an acid catalysed rearrangement and cyclocondensation to obtain the thiazolino ring-fused 2-pyridone scaffold (**VII**). The substituent (R^8) of the nitrile (**I**) is incorporated into the scaffold (**VII**) at C8-position and the R^7 substituent of C7-position is from the carboxylic acid (**IV**) (Scheme 1.1). Synthetic strategies to diversify the thiazolino ring-fused 2-pyridone scaffold have been developed in Almqvist's research group. An example of this is the introduction of halogens at R^7 *via* halogen-substituted Meldrum's acid, which enables diversification of this site using Suzuki-Miyaura cross-coupling.^{40,41}

Other examples of strategies are introduction of substituents at positions C2 and C6^{30,31,42,43} and expansion of the ring-system.^{36,41}

Scheme 1.1. The synthetic strategy developed to prepare the ring-fused 2-pyridone scaffold (**VII**) with the possibility of different substituents at R⁷ and R⁸.



Reagents and conditions: a) AcCl, EtOH, overnight; b) TEA, DCM, overnight; c) DCC, DMAP, DCM; d) TFA, DCE, heated at 65 °C in a sealed vessel overnight or 120 °C with MWI for 3 min.

Similarities and differences of the *Listeria monocytogenes* and the *Chlamydia trachomatis* projects

The common starting point of these two projects was the ring-fused 2-pyridone scaffold (**VII**, Scheme 1.1), which all compounds included in the projects are developed from. Analogue **1** (Figure 1.1) has served as a starting point with low potency in some projects, for example, in the Pilicide project²⁷ and *Chlamydia trachomatis* (*C. trachomatis*) project.⁴⁴ However, in the *Listeria monocytogenes* (*L. monocytogenes*) project the analogue **1** showed good potency in inhibiting *L. monocytogenes* cell infection.⁴⁵ The main structural difference between the compounds targeting *C. trachomatis* and the compounds targeting *L. monocytogenes* is the substituent at position C3. For the compounds to be potent against *C. trachomatis*, the C3-group should be a phenyl amide or amide isostere. While in the case for *L. monocytogenes*, the substituent at the C3-position should stay small and keep its hydrophilic character.

The *L. monocytogenes* and *C. trachomatis* are both intracellular bacteria and they replicate inside the host cell. The Gram-positive *L. monocytogenes* is a well-studied bacteria and we have identified the transcriptional virulence regulator PrfA (positive regulatory factor A) as the target of our ring-fuse 2-

pyridone analogues. With the crystal structure of PrfA at hand, structure-based design of new and improved structures has been performed. The Gram-negative bacteria *C. trachomatis* is difficult to study because of its strict intracellular lifestyle and we have no defined biological target of the ring-fused 2-pyridones yet. Therefore, the development of new compounds within this project is based on structure-activity relationship of the compounds and their effect in the cell-based assays.

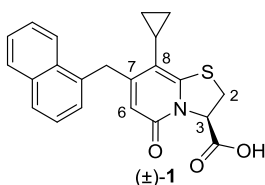


Figure 1.1. Chemical structure of the ring-fused 2-pyridone **1**, which has served as a starting point in the projects targeting *Listeria monocytogenes* and *Chlamydia trachomatis*.

Listeria monocytogenes

The natural environment of the Gram-positive bacteria *L. monocytogenes* is in soil, as a saprophyte living on decaying plant material. However, the bacterium has also been isolated from groundwater, sewage plants, silage, and a variety of food products.⁴⁶⁻⁴⁸ *L. monocytogenes* can cause the severe infectious disease listeriosis in humans and the bacterium is capable of crossing key protective barriers within the body, such as the intestinal, blood-brain and placenta barrier.⁴⁹ The most vulnerable groups towards infections by *L. monocytogenes* are pregnant women, elderly or immunocompromised individuals.⁴⁷ The infection can spread to the central nervous system and cause life-threatening encephalitis and meningitis.^{47,50} For pregnant women, the infection can cross the fetoplacental barrier to the developing fetus and lead to abortion, neonatal infections, or stillbirth.^{46,47} While the infection in healthy individuals commonly only occurs as a self-limiting gastroenteritis, the bacterial infection often take place as epidemic outbreaks but can also appear as sporadic infections.⁵¹ In 2016, a total of 2536 cases of listeriosis infections were reported from countries within the European union and 247 cases had fatal outcomes.⁴⁸ During the period 2008-2016, confirmed cases of listeriosis have been increasing in Europe and the most affected group is elderly people above the age of 64 years.⁴⁸ The infections are mainly caused by intake of *L. monocytogenes* contaminated food products, such as unpasteurised dairy products, soft cheeses, salads, fish, poultry, and refrigerated ready-to-eat products.^{48,52,53} This foodborne pathogen is a problematic contaminant in the food-processing industry due to its ability to

survive low pHs, high salt concentrations and is able to grow under refrigerated conditions.⁵²

Listeriosis in humans is generally treated with intravenous antibiotics, such as ampicillin or penicillin (Figure 1.2), usually as a combined treatment with gentamicin.^{54,55} Treatment combinations of vancomycin/teicoplanin or trimethoprim/sulfamethoxazole (Figure 1.2) can also be used, especially in cases where there is a known allergy to penicillins.⁵⁴ Antibiotic resistant strains of *L. monocytogenes* has been isolated from humans but with a low prevalence.^{55,56} However, strains isolated from food products and food processing environments have shown both single and multidrug resistance to several antibiotics.⁵⁷⁻⁵⁹

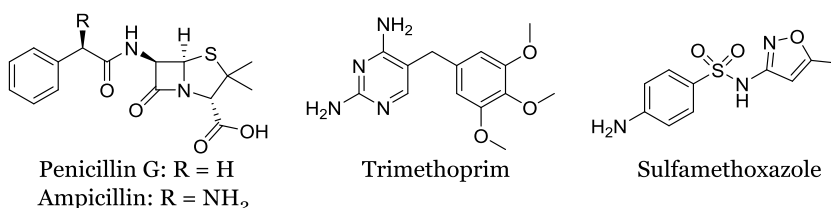


Figure 1.2. Chemical structures of four antibiotic drugs recommended for treatment of listeriosis, caused by *L. monocytogenes*.

Upon ingestion of contaminated food, *L. monocytogenes* will enter the blood stream *via* the intestines. The majority of bacteria will end up in the liver and spleen, where it will be cleared by the host immune system.⁴⁷ However, if the immune system is weakened, the bacteria can re-enter the blood stream and spread within the host. When *L. monocytogenes* has entered a host cell, it is able to avoid humoral immune responses by replicating within the cell and by cell-to-cell spread of the bacteria into adjacent cells (Figure 1.3).⁴⁷

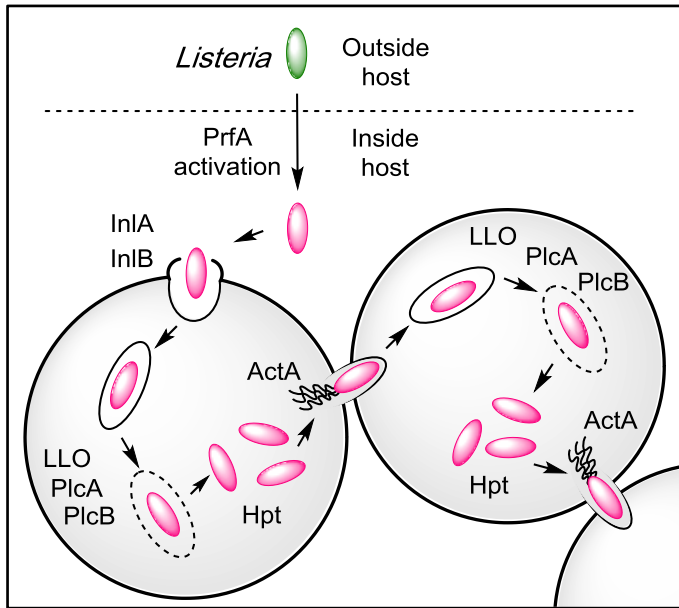


Figure 1.3. Activation of PrfA in the host transforms *L. monocytogenes* into an active pathogenic bacteria. The activated PrfA upregulates the virulence factors, which controls cell entry, replication, and cell-to-cell spread of the bacteria within the host. The figure is modified, with permission from ref. 60 ©1989 Tilney and Portnoy. Originally published in *The Journal of Cell Biology*, Rockefeller University Press.⁶⁰

The bacterial entry into the host cell is mediated by interaction with two bacterial surface proteins, the internalins InlA and InlB (Figure 1.3).^{47,61} The latter one binds to Met, a hepatocyte growth factor (HGF) receptor, while InlA bind to a host cell adhesion molecule, E-cadherin. After internalisation, two phospholipases (PlcA and PlcB) together with the pore-forming toxin listeriolysin O (LLO) facilitate the escape of *L. monocytogenes* from the membrane-bound vacuole into the cytosol. Intracellular replication of the bacteria is aided by host-cell hexose phosphate sugars transported through the bacterial hexose phosphate transporter Hpt.⁶¹ The actin-polymerising protein, ActA, will enable the cell-to-cell spread of the bacteria into neighbouring cells and the replication cycle will start again by secretion of LLO and the phospholipases to release bacteria inside the new cell (Figure 1.3).^{47,61} Almost all virulence factors, responsible for the spread and replication of *L. monocytogenes* within host cells, are positively regulated by the transcriptional regulator PrfA (positive regulatory factor A).⁶² This regulon is selectively activated during host cell infection and encodes gene products for each step of the listerial intracellular infection cycle.^{47,62}

Chlamydia trachomatis

C. trachomatis is a Gram-negative bacterial pathogen and is the causative agent behind the eye infection trachoma^{63,64} as well as counted as the most common sexually transmitted infection (STI).²⁵ Repeated trachoma infections are common in endemic areas and can lead to recurrent chronic inflammation, which can develop scar tissue in the eye and lead to lower vision and eventually blindness.⁶⁵ According to estimations, over 1 million people have lost their vision due to trachoma infection and it is the leading infectious cause of blindness globally.^{63,66} The four ocular serovars (A, B, Ba and C) of *C. trachomatis* are responsible for trachoma infection.⁶³

Infections caused by *C. trachomatis* are a global problem and a major concern for the public health system. During 2012, 131 million new cases of sexually transmitted Chlamydia infections were estimated by the World Health Organisation (WHO).^{25,67} In US, reported cases of Chlamydia infections have been doubled in 16 years, and in 2016, close to 1.6 million cases were reported.⁶⁸ While in Sweden, the number of cases has slightly decreased during the last years but still more than 33000 Chlamydia infections were reported to the Public Health Agency of Sweden during 2017.⁶⁹ The genital *C. trachomatis* infection is caused by serovars D to K.⁶⁴ Reinfections of sexually transmitted Chlamydia are common⁷⁰⁻⁷³ and can be due to reactivation of latent infections or re-exposure of bacteria by untreated or new sexual partners.⁷⁰ Whatever the cause, reinfections by pathogens are associated with more severe infections than initial exposure.⁷⁴ A *C. trachomatis* infection can be asymptomatic,⁷⁵ which is common with rectal Chlamydia infections.⁷⁶ Untreated genital infections in women can cause serious sequelae, such as pelvic inflammatory disease (PID), chronic pelvic pain, infertility, and ectopic pregnancy.⁷⁷ A less abundant infection, caused by serovars L1-L3 of *C. trachomatis*, is the sexually transmitted disease Lymphogranuloma venereum (LGV).⁷⁸ The recommended treatment of genital Chlamydial infection today is antibiotic treatment with azithromycin and doxycycline (Figure 1.4).²⁵ Treatment failure due to resistance has been reported⁷⁹ but it is not a significant clinical problem.

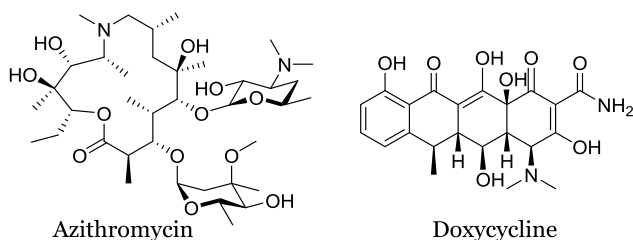


Figure 1.4. Chemical structures of azithromycin and doxycycline, today's recommended antibiotic treatment of genital *C. trachomatis* infection.

The strict intracellular bacterial pathogen *Chlamydia* is characterised by a biphasic lifecycle, where the bacteria shifts from its infectious elementary body (EB) to the replicative intracellular reticulate body (RB).^{64,80} The small elementary bodies are responsible for attachment and invasion of eukaryotic host cells.⁸⁰ Once inside the cell, the EBs form parasitophorous vacuoles known as inclusions. Two hours after internalisation into the host cell, the EBs start differentiating into the larger, less dense RBs.⁸¹ From 8 hours post-infection, this replicative form of *Chlamydia* will start to divide by binary fission and later they will differentiate back into progeny EBs. The re-formed infectious progeny EBs will be released from the host cell *via* lysis or reverse endocytosis (extrusion) around 24-72 hours after infection and are able to invade new host cells.^{64,81}

2. Objectives

The overall objective of the work in this thesis is to develop potent, nontoxic ring-fused 2-pyridone analogues, which target bacterial virulence without inhibiting the growth of or killing the concerned bacteria and the surrounding non-pathogenic bacteria. The scope of this thesis incorporates two different bacteria, *Listeria monocytogenes* and *Chlamydia trachomatis*, with the ring-fused 2-pyridone scaffold as the shared central character. The general long-term aim is to obtain potent ring-fused 2-pyridone compounds with favourable pharmacokinetic properties and specific activity towards certain bacteria.

Overall aims of both projects:

- Improve the anti-virulence activity by structural development of substituents on the ring-fused 2-pyridone scaffold, with focus on the C8-position.
- Develop efficient methodologies to decorate the ring-fused 2-pyridone scaffold.
- Long-term aims of the *Chlamydia trachomatis* project:
 - Develop analogues with properties useful for drug development, including improving the pharmacokinetic properties and specificity while maintaining the low toxicity of the compounds.
- Specific aims of the *Chlamydia trachomatis* project:
 - Utilise the structure-activity relationship to improve the design and activity of compounds.
- Specific aims of the *Listeria monocytogenes* project:
 - Via structure-based design in combination with crystal structure data of regulator PrfA - improve the hits generated within this project.

3. Structure-based design of ring-fused 2-pyridones targeting *Listeria monocytogenes* (Paper I)

*The first project in this thesis, is focused on L. monocytogenes. In this chapter and **paper I**, the design, synthesis, and evaluation of ring-fused 2-pyridone analogues with improved potency and selectivity towards L. monocytogenes are described. In addition, the specific binding events of the compounds are depicted by structural characterisation of the transcriptional regulator PrfA in complex with the compounds.*

The transcriptional regulator PrfA is a symmetrical homodimer and each monomer consists of an N-terminal domain that is linked *via* a long α -helix to a C-terminal domain.^{61,62,82} Two α -helices of the C-terminal domain construct a flexible helix-turn-helix (HTH) motif. The PrfA protein positively regulates virulence gene expression in *L. monocytogenes* by interaction of the HTH motif with the 'PrfA-box', a palindromic DNA-sequence. The flexible HTH motif must obtain a specific ordered conformation to be able to interact with DNA-sequence.^{82,83} In the constitutively active mutant PrfA_{G145S}, the HTH domain is stabilised due to structural rearrangement in the protein and binds with stronger affinity to DNA.⁸² The transcriptional regulator PrfA belongs to the family of cAMP receptor protein (Crp)/fumarate nitrate reductase regulators (Fnr) and a majority of the members of this family require a cofactor for activation.^{61,62,82} However, PrfA is capable of low affinity DNA binding even without a co-factor or small signal molecule.⁸² Upregulated activity of PrfA results from higher affinity DNA binding and it is proposed that this increase of activity is due to a co-factor.^{47,82} A recently suggested co-factor of PrfA is glutathione, which *via* allosteric binding to PrfA induces the correct DNA binding-structure of the HTH motifs and consequently increase the PrfA-DNA interaction (Figure 3.1).⁸⁴⁻⁸⁷

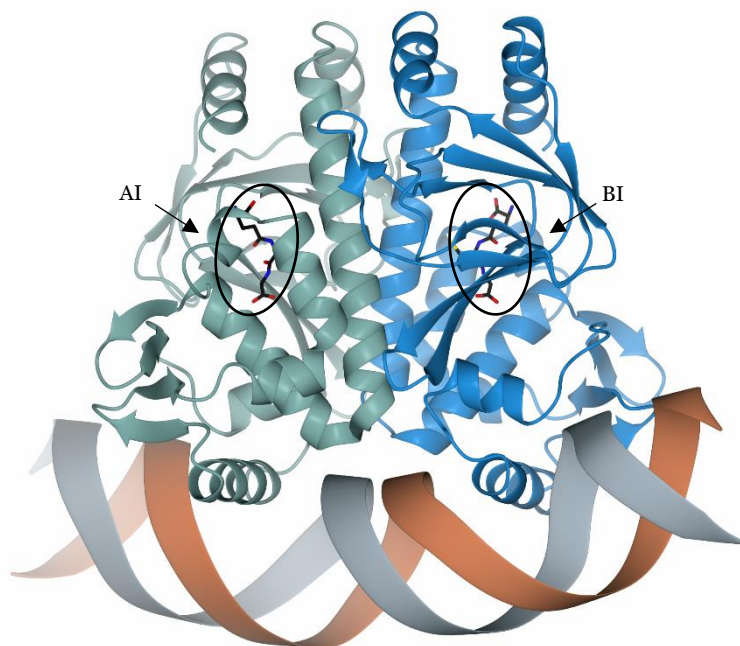


Figure 3.1. Co-crystal structure complex of PrfA binding to DNA with glutathione (black) that binds with one molecule in each monomer, at sites AI and BI. The monomeric units are coloured in sea green (A) and blue (B) and the DNA-sequence is coloured in grey and coral.

From the initial screening of ring-fused 2-pyridone analogues targeting *L. monocytogenes*, the two compounds **1** and **2** were identified as potent virulence inhibitors, while analogue **3** was less effective (Figure 3.2A).⁴⁵ The two potent analogues (**1** and **2**) inhibit uptake of *L. monocytogenes* into human cells and reduce the expression of the PrfA-regulated virulence factors ActA and LLO. The crystal structure of the PrfA:**1** complex was determined and carboxylic acid **1** binds to PrfA at two structurally different binding sites, referred to as AI and BII (Figure 3.2B).⁴⁵ Binding site BII is located close to the HTH motif, while site AI is in a hydrophobic pocket between the N- and C-terminal (Figure 3.2B).

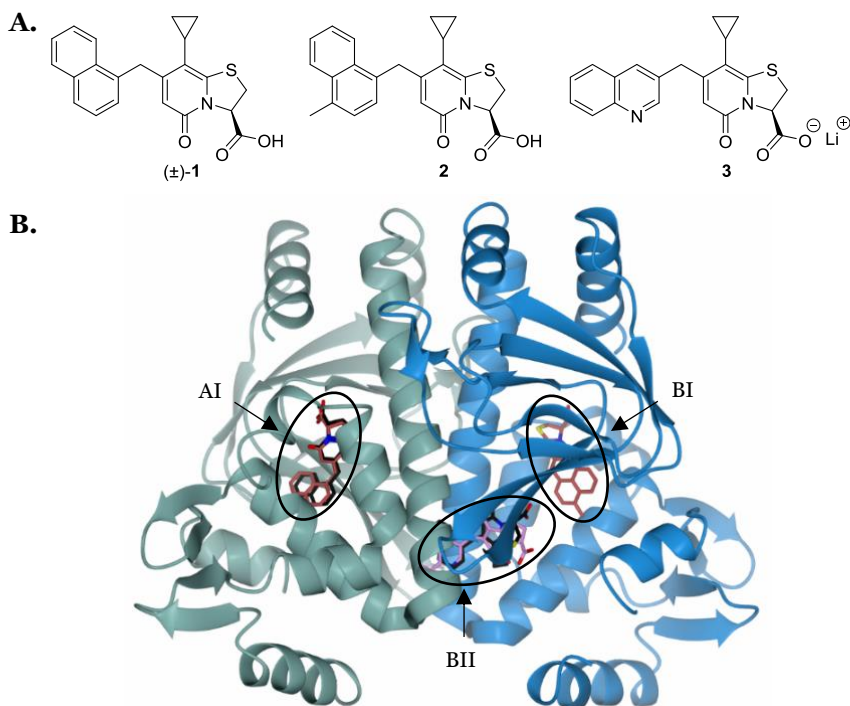


Figure 3.2. **A.** Chemical structure of analogues **1**, **2**, and **3**. **B.** Structural superposition of crystal structures of PrfA with analogues **1**, **2**, and **3** at their different interaction sites AI, BI, and BII. Compound **1** (black) interacts at sites AI and BII, compound **2** (coral) at sites AI and BI and compound **3** (pink) only at site BII. The monomeric units of PrfA are coloured in sea green (A) and blue (B).

From the previous study it was not clear if only one or both of the two binding sites AI and BII, were required to obtain the desired inhibitory effect on *L. monocytogenes*. To further evaluate this, the crystal structures of PrfA in complex with compound **2** and **3** respectively, were determined. The active analogue **2**⁴⁵ binds to site AI and BI (identical site to AI in monomer B) in the homodimer of PrfA, while the inactive compound **3** binds only to site BII (Figure 3.2B). With the BII site located close to the helix-turn-helix motif, we first believed that interaction at this site would affect the PrfA-DNA interaction. However, the results from the crystal structures show that site AI and BI seem to be more important for inhibition of PrfA, while site BII is unimportant in this context (Paper I).

At site AI and BI, the 4-methyl 1-naphthyl group of analogue **2** interacts through hydrophobic interaction and creates an extended hydrophobic cluster together with the involved amino acids from PrfA. This results in a rearrangement of the PrfA protein structure and positions the DNA binding HTH motif in an angle where it is unable to bind to DNA. However, compound **2** is unable to interact with the protein at site BII due to steric clashes of the 4-methyl-1-naphthyl substituent. Structural conclusions drawn based on the structure-activity relationship (SAR) of tested compounds together with the co-crystal structures of PrfA:compound, indicate that a large and hydrophobic substituent (*e.g.* naphthyl) at the benzylic position of C7 is advantageous for inhibitory activity. The part of the AI site where the cyclopropyl group is located, consists of a narrower region with several aromatic residues (Tyr, Phe, and Trp), suggesting that the C8-position should be occupied by small substituents. The carboxylic acid moiety at the C3-position is located in the vicinity of the charged amino acid residues Lys64 and Lys122.⁴⁵ The crystal structures of PrfA:**1** and PrfA:**2**, were used to inform the design of new molecules based on the ring-fused 2-pyridone core structure. We started to investigate heteroatom-based substituents at the C8-position, with the aim to obtain stronger interaction to site AI/BI and therefore increase the inhibitory effect. By introduction of heteroatoms, lipophilicity could be reduced and this was expected to increase solubility and in the end uptake and metabolic stability of the compounds.⁸⁸

Synthesis of the first compound set

The ring-fused 2-pyridone analogue **4**^{34,36} with a C8-methoxy substituent was envisaged to be a suitable intermediate to obtain different C8-oxygen substituents (Scheme 3.1A). Methyl ester **4** was synthesised from substituted Meldrum's acid **5** and methoxy substituted thiazoline **6**. Hydrolysis of the methyl ester using 1 M LiOH_(aq) in THF gave the carboxylic acid **7**. Demethylation of intermediate **4** with boron tribromide gave a mixture of the desired C8-hydroxy, C3-methyl ester **8** as well as the C8-hydroxy, C3-carboxylic acid analogue **9**, which were separable during the work up procedure. The C8-hydroxy substituent of either analogues **8** or **9** could readily be converted to different ethers with 2 molar equivalents of an alkyl halide together with a base in DMF. The formed esters were re-hydrolysed by aqueous 1 M LiOH, which generated the ethers **10**, **11**, and **13**, (Scheme 3.1A). Carboxylic acid **14** with a methane sulfonyl substituent at C8-position was obtained by reaction of methane sulfonyl thiazoline intermediate **15** with 1-naphthyl Meldrum's acid **5** and subsequent hydrolysis (Scheme 3.1B). For further discussion about the synthesis of analogue **14** see Chapter 7.

A

Reaction scheme A illustrates the synthesis of various 2,2-dimethyl-1,3-dioxane-5,6-dione derivatives. The scheme starts with 2-methoxyacetonitrile, which reacts via steps a and b to form intermediate 6. Intermediate 6 then reacts with 2-benzyl-4-methoxy-6-oxo-1,2,3,4-tetrahydro-1,2,4-triazine-5-carboxylic acid methyl ester (5) via step c to form intermediate 4. Intermediate 4 can be converted to (±)-7 via step d, or to (±)-9 and (±)-8 via step e. (±)-9 is converted to (±)-10 via step f, and (±)-9 is converted to (±)-11 via step g. (±)-8 is converted to (±)-12 (R' = CH₃) and (±)-13 (R' = H) via step h. A separate reaction shows the conversion of (±)-12 to (±)-13 via step i. A separate reaction shows the conversion of (±)-13 to (±)-14 via step j. A separate reaction shows the conversion of (±)-14 to (±)-15 via step k. A separate reaction shows the conversion of (±)-15 to (±)-16 via step l. A separate reaction shows the conversion of (±)-16 to (±)-17 via step m. A separate reaction shows the conversion of (±)-17 to (±)-18 via step n. A separate reaction shows the conversion of (±)-18 to (±)-19 via step o. A separate reaction shows the conversion of (±)-19 to (±)-20 via step p. A separate reaction shows the conversion of (±)-20 to (±)-21 via step q. A separate reaction shows the conversion of (±)-21 to (±)-22 via step r. A separate reaction shows the conversion of (±)-22 to (±)-23 via step s. A separate reaction shows the conversion of (±)-23 to (±)-24 via step t. A separate reaction shows the conversion of (±)-24 to (±)-25 via step u. A separate reaction shows the conversion of (±)-25 to (±)-26 via step v. A separate reaction shows the conversion of (±)-26 to (±)-27 via step w. A separate reaction shows the conversion of (±)-27 to (±)-28 via step x. A separate reaction shows the conversion of (±)-28 to (±)-29 via step y. A separate reaction shows the conversion of (±)-29 to (±)-30 via step z.

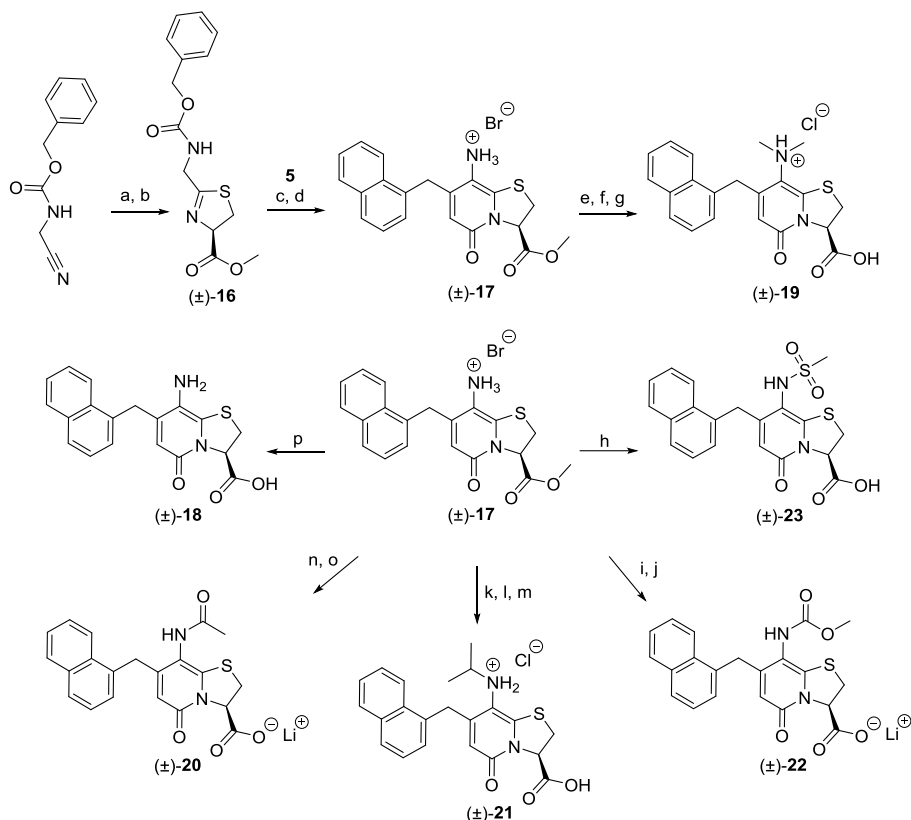
B

Reaction scheme B illustrates the synthesis of various 2,2-dimethyl-1,3-dioxane-5,6-dione derivatives. The scheme starts with 2-methyl-2-sulfonylacetonitrile, which reacts via steps i and j to form intermediate (±)-15. Intermediate (±)-15 then reacts with 2-benzyl-4-methyl-6-oxo-1,2,3,4-tetrahydro-1,2,4-triazine-5-carboxylic acid methyl ester (5) via step k to form intermediate (±)-14. Intermediate (±)-14 is then converted to (±)-16 via step l.

17

A synthetic method to obtain a free amine at the C8-position on the ring-fused 2-pyridone core structure was developed by Andrew G. Cairns. The free amine could serve as an intermediate to obtain different nitrogen containing substituents. The Cbz-protected amine substituted thiazoline **16** was obtained at 82% yield over two steps from *N*-(benzyloxycarbonyl)-2-aminoacetonitrile (Scheme 3.2). The Cbz-protected aminopyridone intermediate was formed *via* an acylketene-imine cycloaddition reaction of thiazoline **16** with 1-naphthyl Meldrum's acid **5**, followed by deprotection using hydrogen bromide in acetic acid, which resulted in the key intermediate **17** as a hydrobromide salt. Ester hydrolysis with aqueous 1 M LiOH of the hydrobromide salt **17** yielded the primary amine **18**. Methylation of the free amine, hydrolysis, and treatment with HCl gave the dimethyl analogue **19**. The two analogues **20** and **22** were obtained through substitution reaction using acetyl chloride and methyl chloroformate respectively, followed by hydrolysis. The methyl sulfonamide **23** was synthesised *via* a reaction with methanesulfonyl chloride and subsequent hydrolysis, while reductive amination of intermediate **17** resulted in the secondary amine **21** (Scheme 3.2).

Scheme 3.2. Synthesis of the nitrogen analogues **18-23**.



Reagents and conditions: a) acetyl chloride, EtOH, 0 °C – rt, 1 h; b) L-Cysteine methyl ester hydrochloride, TEA, DCM, rt, 2 days, 82% over two steps; c) **5**, TFA, DCM, 10 bar, 70 °C, 6 h; d) 33% HBr/AcOH, DCM, rt, 3 h, 69% over 2 steps; e) CH₃I, NaHCO₃, DMF, MWI, 70 °C, 10 h; f) 1 M LiOH_(aq), THF:MeOH (5:1), rt, overnight; g) suspended in DCM and dripped in to ethereal HCl, 46% over 3 steps; h) methanesulfonyl chloride, TEA, THF, rt, overnight; then: 1 M LiOH_(aq), MeOH, rt, 16 h, 49%; i) methyl chloroformate, pyridine, DCM, rt, 2 h; j) 1 M LiOH_(aq), THF:MeOH (5:1), rt, overnight, 35% over 2 steps; k) NaBH(OAc)₃, TFA, DCM, acetone, –15 °C – rt, overnight; l) 1 M LiOH_(aq), THF:MeOH (5:1), rt, 1 h; m) suspended in DCM and dripped in to ethereal HCl, 57% over 3 steps; n) acetyl chloride, pyridine, DCM, rt, overnight; o) 1 M LiOH_(aq), THF:MeOH (5:1), rt, 2 days, 34% over 2 steps; p) 1 M LiOH_(aq), THF:MeOH (6:1), rt, 16 h, 49%.

Biological screen of compounds

The small library of heteroatom C8-substituted ring-fused 2-pyridones (**7**, **9-11**, **13**, **14**, **18-22**) was evaluated in a cell-based assay, in order to measure the compounds ability to inhibit *L. monocytogenes* infection (Table 3.1). In summary, the compounds (**7**, **9-11**, **13**, **14**, **18-22**) at a concentration of 20 μ M were added to Caco-2 cells infected with green fluorescent protein expressing *L. monocytogenes*. The infected cells were incubated for one hour before external bacteria were removed by washing with phosphate-buffered saline (PBS) and cell medium containing antibiotics. After an additional three hours of incubation the bacterial uptake into the cells was measured by flow cytometry. DMSO-treated infected cells were used as a positive infection control (set to represent 100% infection) and untreated cells were used to establish background levels. The result is given as relative infection ratios between the tested compound **X** and compound **1**, a lower number indicates a more potent compound than compound **1**. In this initial screen the most active new compound was dimethylamine **19**. None of the compounds with a hydroxy or ether substituent at the C8-position were active, neither analogue **14** with a C8-methyl sulfonyl substituent.

Table 3.1. Initial biological screen of the compounds, relative infection ratio of the compound at a concentration of 20 μ M.

Compound	R ⁸	Relative infection ratio*
1		1
2[#]		0.5
3^{#,‡}		13
7		7
9		5
10		4
11		4
13		5
14		7
18		3
19[§]		0.7
20[¶]		5
21[§]		3
22[¶]		6
23		5

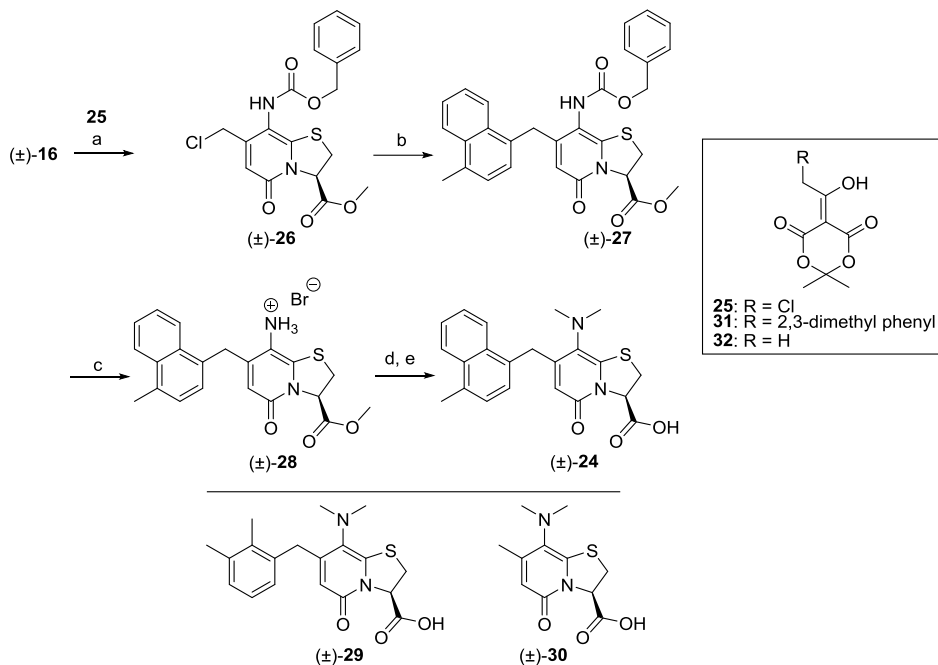
*The infection blocking capacity, at 20 μ M, as a ration of the compound (**X**) compared to compound **1**: (**1/X**). The data is from a representative set of experiments (median value). The value of compound **1** is set to 1 and a lower number, *e.g.* 0.5, indicates that this compound blocks bacterial uptake twice as efficiently as compound **1**.[#]Compound **2**: C7-4-methyl-1-naphthyl, compound **3**: C7-3-quinoline; see Figure 3.2. C3-R enantiomer from previous study.⁴⁵ [¶]Prepared as Li salt. [§]Prepared as HCl salt.

Design, synthesis, and evaluation of further analogues

With the results from the biological assays and the co-crystal structures of PrfA:1 and PrfA:2, we decided to use the most promising structural features from the different compounds and combine them. By combining the 4-methyl-1-naphthyl substituent at the C7-position from analogue **2** with the C8-dimethylamine substituent from compound **19**, analogue **24** was designed and synthesised (Scheme 3.3). The 4-methyl-1-naphthyl substituent at the C7-position was introduced *via* Suzuki–Miyaura cross-coupling to access analogue **27** from C7-chloro intermediate **26**, which in turn was synthesised *via* the acylketene-imine cycloaddition with chloro substituted Meldrum's acid **25** and thiazoline **16**. Deprotection of the Cbz-protection group using hydrogen bromide in acetic acid gave the hydrobromide salt **28** and then subsequent methylation and hydrolysis resulted in dimethylamine **24**. We were also interested to see if a smaller aromatic group or a methyl substituent at the C7-position would alter the *L. monocytogenes* virulence inhibiting effect. A smaller carbon-based substituent would reduce the hydrophobicity of the compound. The C8-dimethylamines **29** and **30** were synthesised in analogous fashion, however, the 2,3-dimethyl phenyl and methyl substituents were introduced from substituted Meldrum's acid intermediates **31** and **32**, respectively (Scheme 3.3).

The C8-dimethylamines **24** and **29** were highly effective at 20 μ M and inhibited *L. monocytogenes* uptake into human cells at a relative infection ratio of 0.7 and 0.6, respectively. While compound **30** had only a relative infection ratio of 10 and therefore accounted as inactive, which confirms our hypothesis that a relatively large substituent is required at the C7-position.

Scheme 3.3. Synthesis of dimethylamine **24** and the chemical structures of analogues **29** and **30**.



Reagents and conditions: a) **25**, TFA, DCM, 70 °C, 20 h, 68%; b) 4-Methyl-1-naphthaleneboronic acid, $\text{PdCl}_2(\text{PPh}_3)_2$, KF, MeOH, MWI, 120 °C, 10 min, 67%; c) 33% HBr/AcOH, DCM, rt, 100 min, 92%; d) CH_3I , NaHCO_3 , DMF, 70 °C, 19 h, sealed tube; e) 1 M $\text{LiOH}_{(\text{aq})}$, THF, rt, 17 h, 65% over 2 steps.

Further evaluation of inhibition candidates

Additional evaluation of the three most promising compounds, together with the inactive C8-methoxy analogue **7** as a negative control, was performed. The compounds were tested at lower concentrations and at 1 μM analogue **24** reduced the bacterial uptake by almost 90%, while compounds **19** and **29** were less effective (Figure 3.3). Additionally, none of the three compounds **19**, **24**, or **29** disturbed the growth of *L. monocytogenes* in brain heart infusion broth at 100 μM . This shows that the compounds only reduce the bacterial uptake into cells and that they are not bactericidal.

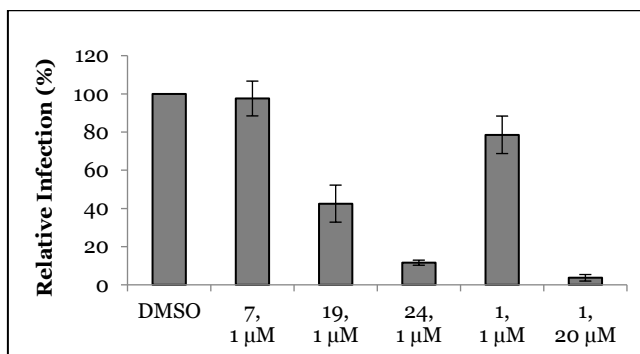


Figure 3.3. Relative infection of *L. monocytogenes* after treatment respective compound at a concentration of 1 μ M, compared to compound **1** at 20 μ M and DMSO-control. Error bars show standard deviations of biological triplicates.

The transcriptional regulator PrfA controls several virulence factors in *L. monocytogenes*, where two of them are ActA and LLO. The compounds effect on the expression of ActA, LLO, and PrfA were examined to determine if the reduced bacterial uptake in cells was due to reduced virulence factor expression. The expression of the virulence factors and PrfA were monitored at decreasing compound concentrations and as predicted, analogue **7** (at 10 μ M) did not affect either ActA or LLO to a significant level. Analogues **19** and **29** repressed virulence factor expression without affecting expression of PrfA, similar to compound **1**. While dimethylamine **24** did not show any effect of disturbing PrfA expression, however, it almost completely blocked the expression of ActA and LLO at 1 μ M. This shows that dimethylamine **24** does not affect the concentration of PrfA in the bacteria, but weakens its activity.

The encouraging results of analogue **24** as a virulence inhibitor inspired us to investigate the compound in a more advanced *in vivo* system, in a chicken embryo model. A chicken embryo lacks a developed immune system and the *in vivo* model has the advantages that it is an easy setup and can be performed in the laboratory.⁸⁹⁻⁹¹ In summary, 9-days old chicken embryos were injected on one side of the eggshell with *L. monocytogenes* suspended in PBS and directly after with a PBS solution of compound **24** or DMSO (as control substance) at a different site. The tiny holes from the needles where sealed and the eggs were screened for presence of blood vessels and movement regularly for 72 hours, before the chicken embryos were sacrificed by freezing. Uninfected embryos from the compound **24** treated group behaved as the untreated controls, which indicates that the compound displayed no toxicity towards the embryos. Compared to the DMSO-treated controls, analogue **24** prolonged the lifespan of the infected embryo by an average of 6 hours. By converting the compound **24** to an imidazole salt the solubility was slightly improved, which led to a longer

lifespan for the chicken embryo, by an average of 9 hours compared to controls. The chicken embryo study could not be performed with compound **1** due to the low solubility of the compound in the PBS solution.

To investigate the binding affinity of the compounds to PrfA, surface plasmon resonance (SPR) experiments were performed to measure how the compounds affect the binding of PrfA to the PrfA-regulated *hpt*-promoter DNA. The results show that the compounds **19**, **24**, and **29** reduce the PrfA binding to *hpt*-DNA with half maximal inhibitory concentrations [IC_{50}] in the low μ M range, while a higher concentration ($[IC_{50}] > 60 \mu$ M) is required for the inactive analogue **7** to reduce the binding. To evaluate the different sites and how the compounds bind, co-crystals of PrfA in complex with compounds **7**, **19**, **24**, or **29** were structurally characterized. The inactive control compound **7** binds only at site BII, in an analogous fashion to the inactive compound **3**. Compounds **24** (Figure 3.4A) and **29** bind to sites AI and BI in a similar way as analogue **2**, while compound **19** binds at all three sites, AI, BI, and BII. The matching binding of analogues **2** and **24** to PrfA follows our hypothesis that steric clashes of the methyl on the C7-4-methyl-1-naphthyl substituent makes the compound unable to interact with PrfA at site BII. At sites AI and BI, an interaction between the 4-methyl-1-naphthyl substituent and PrfA makes the hydrophobic residues Leu174 and Leu150 shift slightly and the C7-substituent becomes a part of a hydrophobic cluster (Figure 3.4B). Glutathione, a co-factor activator of PrfA, binds at the sites AI and BI and induces structural changes of the protein which enable DNA-binding.⁸⁴ The structural changes of the protein induced by dimethylamine **24** prevent PrfA from accessing the correct conformation for the HTH-motif to bind to DNA, resulting in the blocked PrfA activity caused by analogue **24**.

With almost identical interaction of the C8-dimethylamine substituent (compounds **19**, **24**, and **29**) at sites AI and BI, the substituent has a nonplanar geometry. The substituent is sandwiched between the phenyl rings of the amino acids Phe67 and Tyr126 and are in the vicinity of the aromatic amino acids Tyr63 and Trp224 (Figure 3.4C). This arrangement of the structure and the close distance of around 4Å to the aromatic amino acids, could allow interactions between the *N*-methyl hydrogens and the aromatic residues. Even though the C8-dimethylamine substituent is probably only weakly basic in solution, the dimethylamine might be protonated when bound to the protein. Such a protonation could give rise to non-classical hydrogen bonds⁹²⁻⁹⁵ between the compound and protein, and formation of this type of bond would increase the compound interactions with the protein.⁹⁶

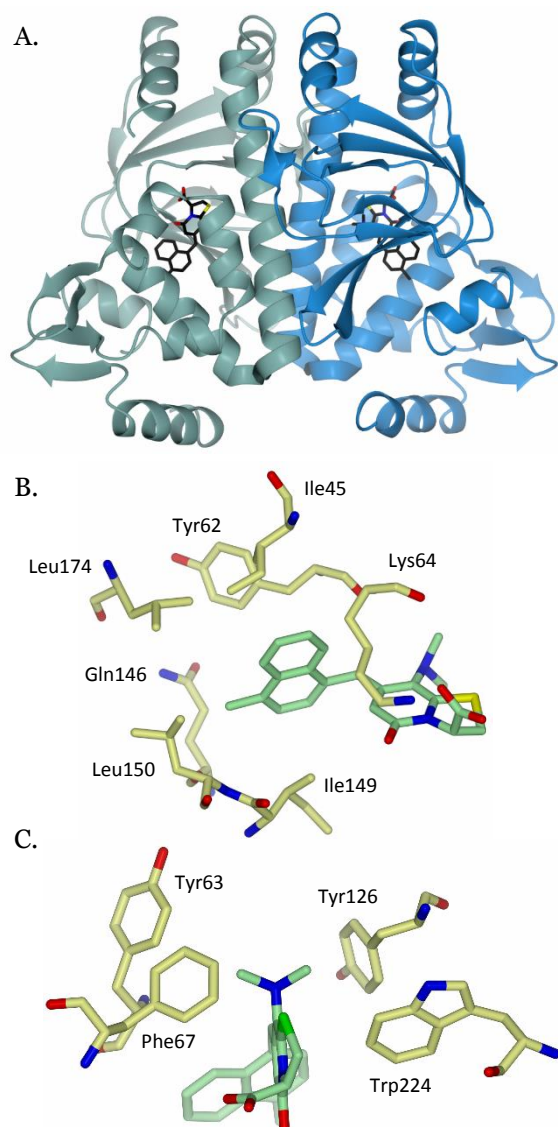


Figure 3.4. **A.** Crystal structure of PrfA with compound **24** (black) at site AI and BI. The monomeric units of PrfA are coloured in sea green (A) and blue (B). **B.** Interactions between the C7-4-methyl-1-naphthyl group of compound **24** (green) and the amino acid residues at the hydrophobic pocket in PrfA (yellow). **C.** Interaction of the C8-dimethylamine of compound **24** (green) with four aromatic residues of PrfA (yellow).

Summary and concluding remarks

This study describes the synthesis and evaluation of ring-fused 2-pyridone analogues that inhibit the transcriptional regulator PrfA. The compounds were designed from our previously characterised PrfA:1 crystal structure and with focus on structural changes at the C8-position by introduction of heteroatoms. The biological activity of the compounds were demonstrated by cell infection experiments and suppression of virulence factor expression, as well as chicken embryo survival. The interaction of the compounds with PrfA were elucidated by determination of the crystal structures of PrfA in complex with the compounds. The most potent analogue **24**, which almost completely blocked the expression of PrfA regulated virulence factors at 1 μ M, binds to sites AI and BI in PrfA. Due to steric clashes, the bulky C7-4-methyl-1-naphthyl substituent prevents compound **24** from interacting at site BII. At site AI (and BI), the sterically demanding 1-naphthyl group induce changes of the protein structure. These changes prevent appropriate folding of the HTH motif, requested for the DNA-binding of PrfA. This shows that ring-fused 2-pyridone compound interaction with sites AI and BI is important for PrfA inhibition.

4. Towards new ring-fused 2-pyridones targeting *Listeria monocytogenes* (Appendix 1)

In this chapter and appendix 1, ongoing investigations within the Listeria monocytogenes project are described. With the identified binding site AI (and BI) in the PrfA protein, further evaluation of possible structural changes of positions C3 and C7 are investigated.

During the previous investigation within the *L. monocytogenes* project, crystal structures of PrfA in complex with different compounds were characterised.³⁷ From these structures, it was concluded that the ring-fused 2-pyridone analogues can bind to three binding sites, referred to as AI, BI and BII, in the homodimer of PrfA (see Chapter 3, Figure 3.2). The two binding sites AI and BI are identical and located in one monomer each. It was determined that the most potent compounds (*e.g.* **24** and **29**) interacts with PrfA at binding sites AI and BI and their interactions with the protein are described in Chapter 3. The compounds adopt the same conformation as analogue **1** at binding site AI. In the co-crystal structure of PrfA:**1**, the carboxylic acid moiety is located near the charged amino acid residues Lys64 and Lys122⁴⁵ and the same can be seen in the crystal structures of PrfA in complex with compounds **19**, **24**, and **29**. To further investigate and optimise the ring-fused 2-pyridone scaffold, structure-based design of new analogues with the crystal structure of PrfA:**1** complex was performed. Two substitution sites of the ring-fused 2-pyridone scaffold, the C3-position and the 4'-position of the 1-naphthyl substituent at position C7, were analysed for possible interactions at site AI (Figure 4.1).

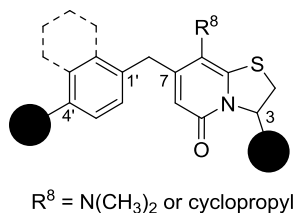


Figure 4.1. Structure of the ring-fused 2-pyridone core with marked sites for further interactions possibilities (black dots), with either a phenyl or 1-naphthyl substituent as base at the C7-position.

Upon interaction with site AI in PrfA, the C7-naphthyl ring of the ring-fused 2-pyridone becomes a part of a hydrophobic cluster. Going from a 1-naphthyl substituent to a 4-methyl-1-naphthyl substituent unable the ring-fused 2-pyridone analogues to fit at site BII and they interact only at site AI (and BI), this was shown for both compounds **1** and **2**, as well for compounds **19** and **24** (see Chapter 3 for structures).³⁷ We wanted to investigate if more hydrophilic substituents (*e.g.* primary alcohol) at the 4'-position of the 1-naphthyl group would be accepted. By introducing heteroatoms new possible interactions at the site could occur as well as reducing the lipophilicity, which could lead to improved pharmacokinetic properties of the compound.

An alcohol substituent can function as a hydrogen bond acceptor or donor. Docking of compound **33** at site AI in PrfA (AutoDock Vina,⁹⁷ see appendix 1 for details), showed possible interactions of the alcohol to the main chain amino group of Lys150 and to the main chain carboxyl group of Gln146 (Figure 4.2A & B, see appendix 1 for docking details). The primary alcohol **33** was synthesised *via* Suzuki–Miyaura cross-coupling from the C8-cyclopropyl, C7-chloro substituted ring-fused 2-pyridone intermediate **105**³⁵ with 4-methanol-1-naphthalene boronic acid pinacol ester (Appendix 1, Scheme A1). The analogous aldehyde **34**, with the starting materials in hand, was easily synthesised in a similar fashion (Figure 4.2A & Appendix 1, Scheme A1). The docking of compound **34** to PrfA showed a possible interaction of this hydrogen bond acceptor to Tyr154, which lie in the vicinity of the hydrophobic cluster surrounding the C7-substituent (Figure 4.2C). Additionally, an interaction between the C3-carboxylic acid and the amino acid residue Lys64 can be seen.

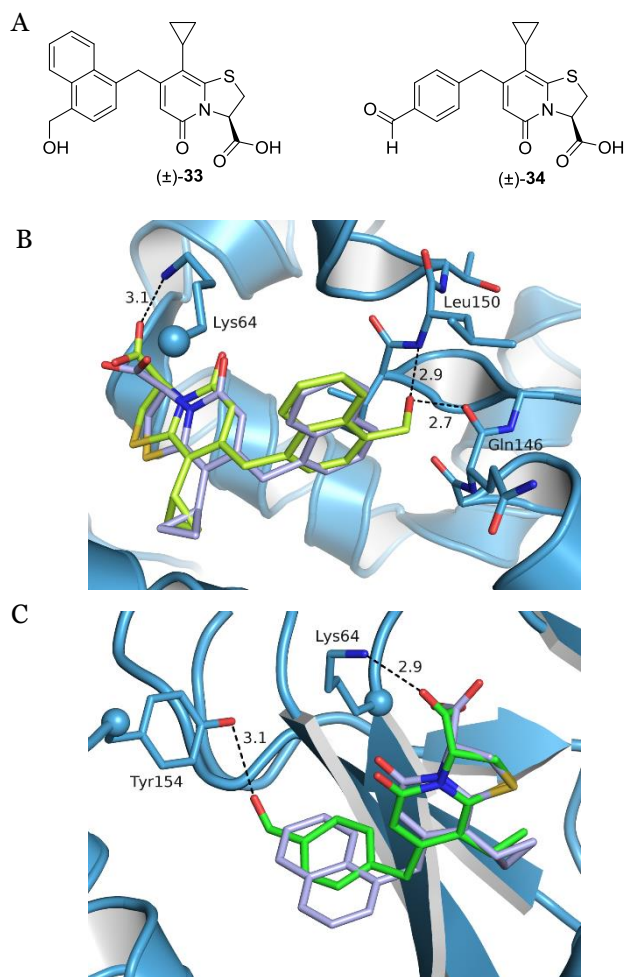


Figure 4.2. A. The chemical structures of analogues **33** and **34**. **B.** Docking of primary alcohol **33** (limon) to PrfA (skyblue) at site AI. Picture showing an overlay of compound **33** on compound **1** (light blue), with possible interactions to the main chains of Lys150 and Gln146, the residues are shown as sticks. **C.** Docking of aldehyde **34** (green) to PrfA (skyblue) at site AI. Picture showing an overlay of compound **34** on compound **1** (light blue), with possible interactions of the C7-aldehyde to Tyr154 and the C3-carboxylic acid to Lys64. The interactions are shown with black dashed lines and the distances are given in Å. See appendix 1 for reaction scheme (Scheme A1) and experimental details of the compounds.

The other site of interest was the C3-position and previously tested compounds within this project have a carboxylic acid moiety at this position. The distances between the C3-carboxylic acid and the amino acid residues Lys64 and Lys122 in PrfA are slightly too far for direct interactions. However, an indirect interaction *via* a water molecule is seen in the crystal structure of PrfA with the ring-fused 2-pyridone **1**.⁴⁵ Therefore, a prolongation of the carboxylic acid carbon chain can result in a closer position of the carboxylic acid to enable direct interaction, forming a salt-bridge, to the charged amino acid residues Lys64 and Lys122.

This motivated us to investigate extension of the C3-carboxylic acid carbon chain. Docking studies of the potential compound **35** show that the extended carboxylic acid could form direct interactions with Lys64 and Lys122 (Figure 4.3A & B). We had, from a previous project, a one-carbon extended C3-carboxylic acid analogue **36** (Figure 4.3A) in our hands.⁹⁸ Before we started to synthesise **35**, the ability of compounds **33**, **34**, and **36** to inhibit *L. monocytogenes* infection were evaluated in the earlier described cell-based assay at 20 μM ³⁷ (Chapter 3). None of the two C7-analogues **33** and **34** showed any promising inhibitory effect of infection at 20 μM . However, compound **36** inhibited *L. monocytogenes* infection at a relative infection ratio of 0.8, showing a comparable effectivity to analogue **24** (relative infection ratio: 0.7). These results spurred us to continue to investigate the possibilities of the C3-site.

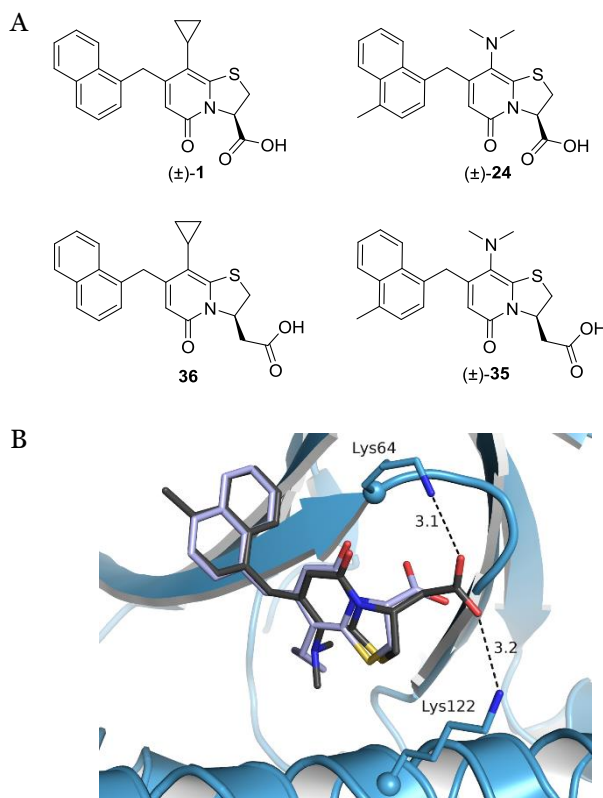
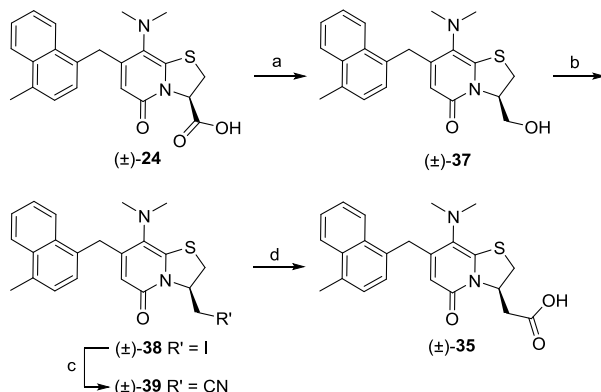


Figure 4.3. A. The chemical structures of compounds **1** and **24** with a carboxylic acid moiety, as well as compounds **35** and **36** with a one carbon extended carboxylic acid moiety at position C3. **B.** Docking of compound **35** (grey) to PrfA (skyblue) at site AI. Picture showing an overlay of compound **35** on compound **1** (light blue), with possible interactions of the C3-carboxylic acid to Lys64 and Lys122, the residues are shown as sticks. The interactions are shown with black dashed lines and the distances are given in Å.

To combine the features of the extended C3-chain and with the substituents of the most potent compound **24** from the previous study,³⁷ the carboxylic acid **35** was synthesised (Scheme 4.1). Starting from analogue **24**, reduction of the C3-carboxylic acid with borane dimethyl sulfide complex resulted in the primary alcohol **37**. The iodo intermediate **38** was obtained *via* an Appel reaction from **37** and followed by a substitution reaction with potassium cyanide to afford nitrile **39**. Through hydrolysis of the nitrile group, a CH₂-extended carboxylic acid was formed to give the carboxylic acid **35** (Scheme 4.1).

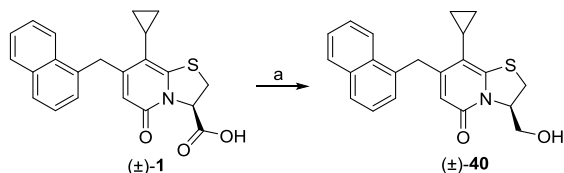
Scheme 4.1. Synthesis of C3-alcohol **37** and C3-CH₂-extended carboxylic acid **35**.



Reagents and conditions: a) 1 M BH₃·Me₂S, THF, rt, 22h, 45%; b) DCM, I₂, PPh₃, imidazole, rt, 19 h, 81%; c) KCN, MeCN, (see procedure in Appendix 1 for details), 71%; d) 2 M NaOH_(aq), EtOH, MWI, 130 °C, 5 min, 28%.

The primary alcohol **37**, with its character of being both a hydrogen bond donor and acceptor but without a potential negative charge, awakened our interest for the analogue. Therefore, we were also interested in testing the primary alcohol **40**, the corresponding analogue to **35** and **1**, which was easily synthesised over one step from **1** (Scheme 4.2).⁹⁸ The compounds **35**, **37**, and **40** were evaluated at 20 μM in the *L. monocytogenes* infection cell-based assay and resulted in a relative infection ratio at 1.1 for **35**, 0.9 for **37**, and 0.7 for **40**.

Scheme 4.2. Synthesis of C3-primary alcohol **40**.



Reagents and conditions: a) 1 M BH₃·Me₂S, THF, rt, 13h, 98%.⁹⁸

To determine if the activity of the compounds was due to reduced virulence factor expression, as with analogues **1** and **24**, the expression of the PrfA regulated virulence factor ActA was evaluated at 10 μM. The analogues **35**, **36**, and **37** fully repressed the virulence factor expression without affecting the expression of PrfA. While analogue **40** only slightly reduced the ActA expression at a concentration of 10 μM. To further evaluate the three potent compounds **35**, **36**, and **37**, their ability to inhibit the *L. monocytogenes*

infection were assessed at 2 μ M (Figure 4.4). The two compounds with an extended carboxylic acid at position C3, **35** and **36**, showed analogous results to the carboxylic acid **24** at 2 μ M.

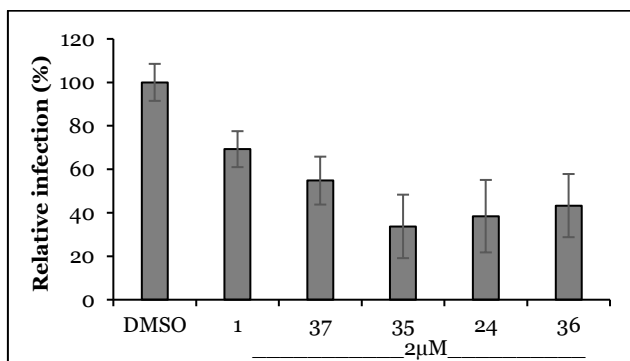


Figure 4.4. Relative infection of *L. monocytogenes* after treatment respective compound at a concentration of 2 μ M, compared to DMSO-control. All samples were made in triplicates and experiment was performed three times in a similar fashion as previously reported.³⁷ Error bars shows standard deviation.

These results encouraged us to determine how the four compounds **35**, **36**, **37**, and **40** interact with the PrfA protein. We have structurally characterised crystals of PrfA in complex with compound **35** (Figure 4.5). The refinement of the structure is not complete but the preliminary data show that the compound binds in a similar fashion as analogue **24** at site AI. However, the C3-moiety has the opposite configuration at position C3 and directs the extended carboxylic acid in a different direction compared to previously characterised compounds. The C3-carboxylic acid of **35** creates an interaction with the amino acid residue Cys229. The co-crystallisation of the compounds **36**, **37**, and **40** with PrfA is performed and the structural characterisation of the crystals are under investigation.

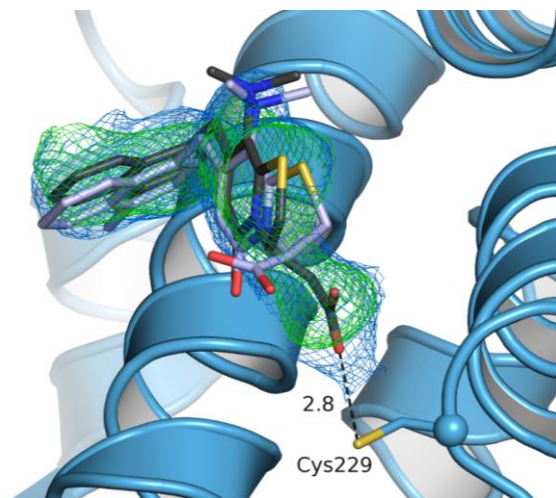


Figure 4.5. Crystal structure of PrfA (skyblue) in complex with compound **35** (grey) at a resolution of 2.6 Å (R_{work} : 24.0%; R_{free} : 30.7%). Showing an overlay with compound **24** (light blue) and the interaction between the C3-extended carboxylic acid of compound **35** and Cys229. The interaction is shown with a black dashed line and the distance is given in Å. The electron density maps are shown with a radius of 1.6 Å around the compound and are coloured in marine ($2F(\text{obs})-F(\text{calc})$ map) and green ($F(\text{obs})-F(\text{calc})$ omit map). The crystallisation and structural refinement of the PrfA:**35** crystal structure was performed in a similar way as previously described.³⁷

Summary and future plans

The compounds **35**, **36**, and **37** showed a similar biological activity as analogue **24** at 2 μM and they repressed the expression of virulence factor ActA, without affecting the expression of PrfA. The different orientation of the extended C3-carboxylic acid of compound **35** in the co-crystal structure with PrfA gives an interaction to Cys229. This interaction has not been seen with the ring-fused 2-pyridone analogues before. The structural characterisation of the crystal structures of the analogues **36**, **37**, and **40** in complex with PrfA is under investigation. The biological results of compound **35** has motivated us to continue with this compound and it will be evaluated in the chicken embryo model in a similar way as was shown for analogue **24**.

The potential extension of the C3-carboxylic acid has opened up new possibilities for the ring-fused 2-pyridones. By addition of a sp^3 -carbon between the 5-membered ring and the carboxylic acid, the molecule becomes less planar and increases the flexibility of the substituent. These changes could result in new interactions with the target protein PrfA and that the molecule is less

ordered in crystal lattice. This new sp^3 -carbon with its two α -protons could also give rise to a new possible substitution site, which further can be explored. The carbon chain could as well be extended with one or two more carbons, following the same synthetic route as analogue **35**. However, there is always a balance between the flexibility of the compound and the entropy loss which would occur when the compound binds to the protein.

5. Ring-fused 2-pyridone amide isosteres inhibiting *Chlamydia trachomatis* infection (Paper II)

The second project in this thesis is targeting *Chlamydia trachomatis*. In this chapter and **paper II**, the structural changes at position C3 of the ring-fused 2-pyridone are investigated. The aims of this study were to improve the potency of the compounds as well as investigate the possible prodrug effect of the C3-phenyl amide.

The first investigation of *C. trachomatis* inhibitors was performed with a small library of ring-fused 2-pyridone analogues. They were evaluated in a phenotypic screen to detect their ability to affect intracellular *C. trachomatis* infection.⁴⁴ The lead compound was the C3-phenyl amide **41** (Figure 5.1). At a concentration of 10 μM , it almost completely blocked *C. trachomatis* infectivity of the three tested *C. trachomatis* serovars A, D, and L2, without showing bactericidal effect or affecting the host cell viability. Treatment with amide **41** resulted in a change of the Chlamydia progeny, which were unable to infect new HeLa cells.⁴⁴ Further development of the amide **41** scaffold with focus on positions C3 and C7 and saturation of the C2/C3 double bond resulted in compounds with improved activity.³⁵ In addition, no activity difference could be seen between the corresponding (*R*)- and (*S*)-enantiomers of phenyl amide **42**. As an extension of the peptidomimetic backbone of the ring-fused 2-pyridone, an amine group was introduced at position C6 and this afforded amine **43** (Figure 5.1), which attenuated $\geq 95\%$ Chlamydial infectivity at 0.25 μM .³⁵

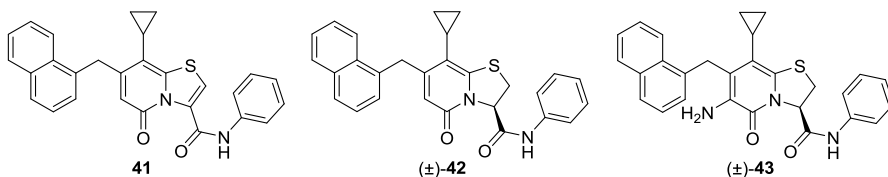


Figure 5.1. Chemical structures of analogues **41**,⁴⁴ **42**,³⁵ and **43**.³⁵

In this study, one of the aims was to investigate if the C3-positioned phenyl amide is the active molecule or if it functions as a pro-drug, with its possible carboxylate metabolite as the active substance.⁹⁹ In the initial screening of possible anti-chlamydial compounds, a variety of substituted ring-fused 2-pyridones with a C3-carboxylic acid were evaluated and some of them weakly inhibited *C. trachomatis* at high concentrations (50-100 μM).⁴⁴ We started to

investigate non-hydrolysable biocompatible amide isosteres at position C3. Amide isosteres have shown potency as peptide surrogates¹⁰⁰⁻¹⁰³ and do not undergo *in vivo* hydrolysis. This would circumvent the possible release of the potentially toxic metabolite aniline *in situ*.¹⁰⁴

Synthesis of compounds

The focus of the study was on changes in the C3-position as well as addition of an amine substituent at the C6-position of promising candidates, while preserving the 1-naphthyl at the C7-position. With this in mind, we envisioned that a variety of amide isosteres could be synthesised from carboxylic acid **1**. Imidazole **45**, oxazole **46**, and thiazole **47** were generated from intermediate **1** *via* the C3- β -keto amide **44**, while acyl sulfonamide **48** was obtained over one step directly from carboxylic acid **1** (Scheme 5.1). The two oxadiazole regioisomers **49** and **50** were also synthesised from intermediate **1** over one and two steps, respectively (Scheme 5.1). 1,2,4-triazole analogues **51** and **52** were obtained from carboxylic acid **1** *via* a one-pot method¹⁰⁵ including amide coupling, ring closure, and deprotection, while C6-amine **53** was synthesised from 1,2,4-triazole **51** through nitration and reduction (Scheme 5.2).

Chemical reaction scheme showing the synthesis of various thiazolidine derivatives from intermediate **1**.

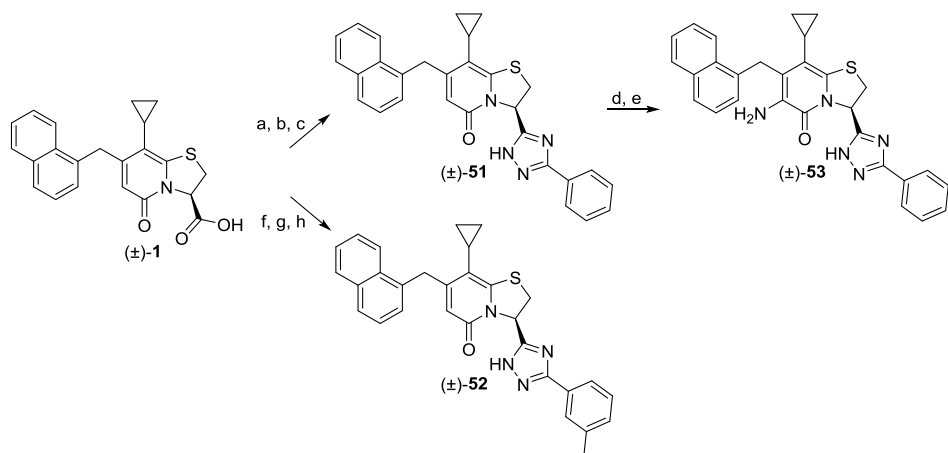
Intermediate **1** ((\pm) -**1**) is a thiazolidine ring substituted with a 2-(cyclopropylmethyl)-6-(naphthalen-1-ylmethyl)-4-oxo-1,2,3,4-tetrahydropyrimidin-5-yl group and a carboxylic acid group.

Reactions and products:

- a**: Reaction of **1** yields **49** ((\pm) -**49**), a thiazolidine ring substituted with a 2-(cyclopropylmethyl)-6-(naphthalen-1-ylmethyl)-4-oxo-1,2,3,4-tetrahydropyrimidin-5-yl group and a 1-phenyl-1,2,4-oxadiazol-5-yl group.
- b**: Reaction of **1** yields **48** ((\pm) -**48**), a thiazolidine ring substituted with a 2-(cyclopropylmethyl)-6-(naphthalen-1-ylmethyl)-4-oxo-1,2,3,4-tetrahydropyrimidin-5-yl group and a 1-phenyl-1,2,4-oxadiazol-5-yl group.
- c, d**: Reaction of **1** yields **50** ((\pm) -**50**), a thiazolidine ring substituted with a 2-(cyclopropylmethyl)-6-(naphthalen-1-ylmethyl)-4-oxo-1,2,3,4-tetrahydropyrimidin-5-yl group and a 1-phenyl-1,2,4-oxadiazol-5-yl group.
- e**: Reaction of **1** yields **44** ((\pm) -**44**), a thiazolidine ring substituted with a 2-(cyclopropylmethyl)-6-(naphthalen-1-ylmethyl)-4-oxo-1,2,3,4-tetrahydropyrimidin-5-yl group and a 1-phenyl-1,2,4-oxadiazol-5-yl group.
- f**: Reaction of **1** yields **47** ((\pm) -**47**), a thiazolidine ring substituted with a 2-(cyclopropylmethyl)-6-(naphthalen-1-ylmethyl)-4-oxo-1,2,3,4-tetrahydropyrimidin-5-yl group and a 1-phenyl-1,2,4-oxadiazol-5-yl group.
- g**: Reaction of **1** yields **46** ((\pm) -**46**), a thiazolidine ring substituted with a 2-(cyclopropylmethyl)-6-(naphthalen-1-ylmethyl)-4-oxo-1,2,3,4-tetrahydropyrimidin-5-yl group and a 1-phenyl-1,2,4-oxadiazol-5-yl group.
- h**: Reaction of **1** yields **45** ((\pm) -**45**), a thiazolidine ring substituted with a 2-(cyclopropylmethyl)-6-(naphthalen-1-ylmethyl)-4-oxo-1,2,3,4-tetrahydropyrimidin-5-yl group and a 1-phenyl-1,2,4-oxadiazol-5-yl group.

39

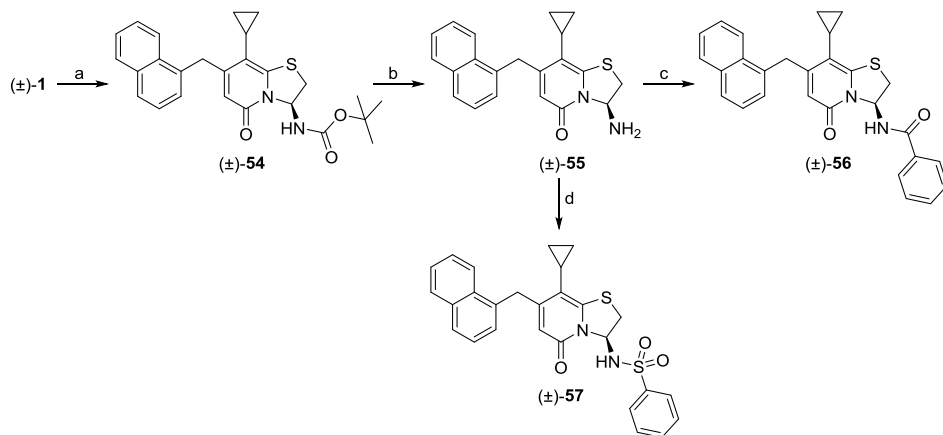
Scheme 5.2. Synthesis of 1,2,4-triazole analogues **51**, **52**, and **53**.



Reagents and conditions: a) benzamidine·HCl, HATU, DIPEA, DMF, 3.5 h; b) (4-methoxybenzyl) hydrazine·HCl, AcOH, 80 °C, 20 h; c) TFA, DCM, 50 °C, 22 h, 43%; d) NaNO₂, TFA, DCM, O₂ atmosphere, rt, 17 h; e) activated Zn dust, DCM:AcOH (2:1), rt, 27 h, 28% over 2 steps; f) 3-methylbenzamidine·HCl, HATU, DIPEA, DMF, 3.5 h; g) (4-methoxybenzyl) hydrazine·HCl, AcOH, 80 °C, 18 h; h) TFA, DCM, 50 °C, 22 h, 44%.

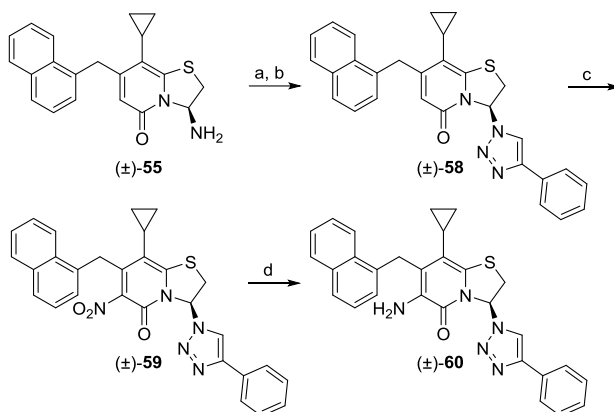
The BOC-protected amine **54** was obtained *via* Curtius rearrangement of carboxylic acid **1**, by heating it in a mixture of diphenylphosphoryl azide (DPPA) and trimethylamine (TEA) in anhydrous *tert*-butyl alcohol (Scheme 5.3). Deprotection of analogue **54** under acidic conditions resulted in amine **55**, which after amide coupling using benzoic acid and HATU yielded the reversed phenyl amide **56**. The sulfonamide **57** was synthesised from C3-amine **55** and benzenesulfonyl chloride (Scheme 5.3). Diazo transfer with imidazole-1-sulfonyl-azide of amide **55** and Cu(I)-catalysed azide-alkyne cycloaddition (CuAAC)^{106,107} resulted in 1,2,3-triazole **58** (Scheme 5.4). The C6-nitro substituted intermediate **59** was obtained *via* nitration of analogue **58** with NaNO₂ in dichloromethane under O₂ atmosphere³⁰ and subsequent reduction with Pd/C (10%) under H₂ atmosphere resulted in amine **60**. Several of the reaction steps to obtain 1,2,3-triazole analogues **58** and **60** were low yielding. In scale up, the limiting step was the Curtius rearrangement of carboxylic acid **1** to yield BOC-protected amine **54**. For the final reduction of the C6-nitro substituent into an amine group, zinc in acetic acid was first examined. The zinc in acetic acid system used for reduction of C6-nitro on ring-fused 2-pyridones^{30,35} proved slow in reducing the analogue **59** to the amine **60**, giving incomplete conversion and problematic purification. Palladium on carbon with hydrogen atmosphere was therefore chosen instead and resulted in full conversion and less troublesome purification, which contributed to a higher yield of the amine **60**.

Scheme 5.3. Synthesis of sulfonamide **57** and reversed phenylamide **56** via amine **55**.



Reagents and conditions: a) DPPA, TEA, *t*-BuOH, 5 h, 85 °C, 75%; b) TFA, DCM, 5 h, rt, 87%; c) benzoic acid, DIPEA, HATU, DCM, 2 h, rt, 64%; d) benzenesulfonyl chloride, pyridine, -10 °C to rt, 18 h, rt, 57%.

Scheme 5.4. Synthesis of 1,2,3-triazole analogues **58** and **60**.

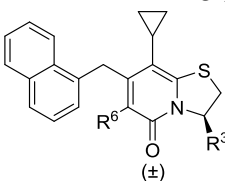


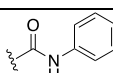
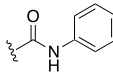
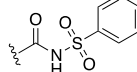
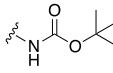
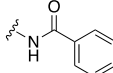
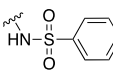
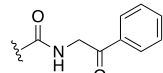
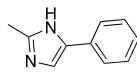
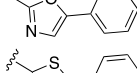
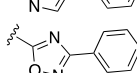
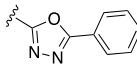
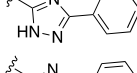
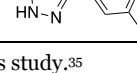

Reagents and conditions: a) imidazole-1-sulfonyl azide- H_2SO_4 , CuSO_4 , K_2CO_3 , MeOH, 72 h, rt; b) phenylacetylene, CuSO_4 , sodium ascorbate, DMF/ H_2O (1:1), rt, 22 h, 26% over 2 steps; c) NaNO_2 , TFA, DCM, O_2 atmosphere, rt, 30 h, 37%; d) Pd/C (10%), H_2 , THF/MeOH (1:1), rt, 19 h, 79%.

Evaluation of biological activity

To evaluate the anti-infective activity of the compounds towards *C. trachomatis* infectivity, a re-infection assay (referred to as the Reinfect₉₅ assay)³⁵ was performed to measure the minimum concentration of compound required to reduce the relative infection level by 95%. The compounds were evaluated at fixed concentrations of 2.5 μ M, as well as at 1, 0.5, 0.25 or 0.1 μ M, depending on observed activity. Briefly, serovar LGV-L2 infected HeLa cells were treated with compound and incubated. The infected cells were lysed 48 h post-infection and the collected bacteria were used to re-infect fresh HeLa cells. After 48 h of incubation of the re-infected cells, the HeLa cells were fixed, stained, and analysed by ArrayScan to count the number of new inclusions formed during the re-infection. The number of new inclusion forming units corresponds to the number of viable infectious bacteria in treated cells and these were compared to untreated DMSO controls. To check that the effect of the compounds not was due to non-specific toxicity, the cytotoxicity of the compounds was tested in a resazurin cell toxicity assay at a concentration of 10 μ M. In summary, the compounds were added to uninfected HeLa cells and incubated for 48 h. Resazurin reagent was added and the cells were incubated in the dark before fluorometry analysis.³⁵

In this study, lead compound **43** from the previous investigation and its precursor the phenyl amide **42** served as benchmark compounds (Table 5.1). A majority of the 1,3-heterocycles, oxadiazoles and amide analogues were either inactive at tested concentrations or showed equivalent effect as **42** (Table 5.1). However, 1,3,4-oxadiazole **50** attenuated $\geq 95\%$ infectivity at 1 μ M and the 1,2,4-triazole analogues **51** and **52** ablated the infection by $\geq 95\%$ at 0.5 μ M. None of the active compounds showed any cell toxicity in the resazurin assay at 10 μ M (HeLa viability, Table 5.1). The 1,2,3-triazole **58** attenuated $\geq 95\%$ infectivity down at 0.25 μ M (Table 5.2). To further explore the structure-activity relationship, a C6-amine substituent was added to the analogues **51** and **58**, resulting in amines **53** and **60**, respectively. Both these compounds reduced the infection by $\geq 95\%$ at 0.25 μ M without showing any cytotoxicity towards HeLa cells (Table 5.2).

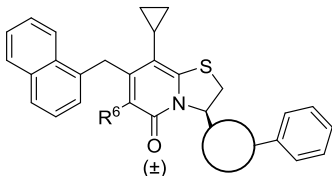
Table 5.1. Investigation of amide isosteres at C3-position.


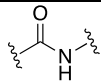
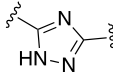
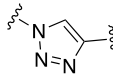
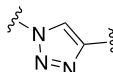
ID	R ³	R ⁶	HeLa Viability 10 μM (%)	Reinfect ₉₅ (μM)
42*		H	100 ± 4	2.5
43*		NH ₂	101 ± 3	0.25
48		H	105 ± 4	>2.5
54		H	105 ± 3	>2.5
56		H	114 ± 6	2.5
57		H	114 ± 3	>2.5
44		H	107 ± 4	2.5
45		H	106 ± 7	2.5
46		H	83 ± 5	2.5
47		H	97 ± 4	>2.5
49		H	99 ± 5	>2.5
50		H	103 ± 2	1
51		H	98 ± 4	0.5
52		H	95 ± 6	0.5

*Data from previous study.³⁵

To further evaluate the compounds, their EC₅₀ values were determined against serovars D and LGV-L2. Against serovar LGV-L2, the 1,2,3-triazoles **58** and **60** (EC₅₀ ≈ 18 and 13 nM respectively) were both more potent than the lead compound **43**, while the 1,2,4-triazole **53** was less potent (Table 5.2). The difference between the phenyl amide **43** and the 1,2,3-triazoles **58** and **60** were less significant with serovar D (Table 5.2). None of the two most active compounds, **58** and **60**, inhibited the growth of selected bacteria or fungi from the commensal flora¹⁰⁸ and neither showed mutagenic potential (at 10 µg/spot) according to Ames test spot-based screening procedure.¹⁰⁹

Table 5.2. Further evaluation of C3-isosteres analogues.



ID	Amide isostere	R ⁶	HeLa Viability 10 µM (%)	Reinfect ₉₅ (µM)	Serovar D EC ₅₀ (nM)*	Serovar LGV-L2 EC ₅₀ (nM)*
43 [#]		NH ₂	101 ± 3	0.25	58 (45-76)	59 (38-93)
53		NH ₂	100 ± 4	0.25	not determined	107 (74-153)
58		H	96 ± 4	0.25	37 (30-45)	18 (10-31)
60		NH ₂	105 ± 4	0.25	35 (27-44)	13 (9-18)

*95% confidence intervals in parentheses; [#]Data from previous study.³⁵

In the previous study,³⁵ the BODIPY fluorophore substituted analogue **61** was developed (Figure 5.2A). This fluorescent analogue accumulates in *C. trachomatis* bacterial inclusions and co-treatments were performed with the 1,2,3-triazoles **58** and **60**. The co-treatment experiment resulted in a reduced accumulation of fluorescent analogue **61**, which suggest that the fluorescent analogue is out-competed at its target by the 1,2,3-triazoles **58** and **60** (Figure 5.2B and C). The results are similar to the result of co-treatment with phenyl amide **43**³⁵ and this points toward that the compounds show an analogous mode of action.

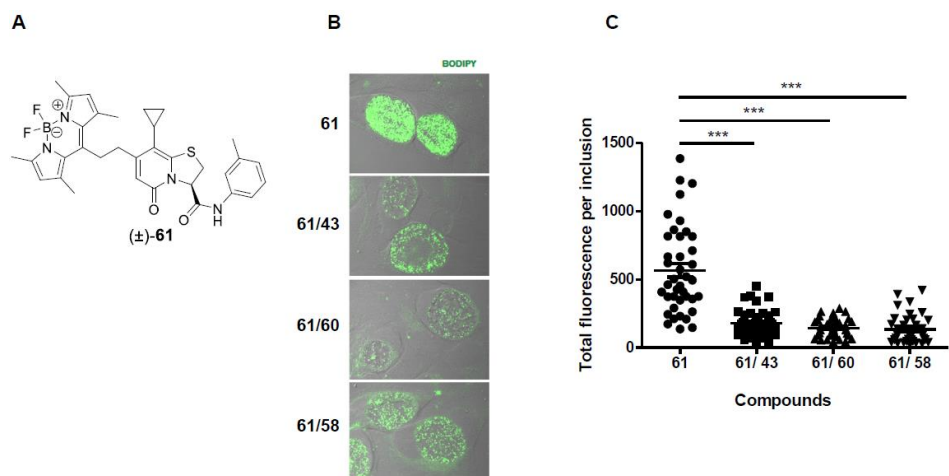


Figure 5.2. Co-treatment with compounds **43**, **58**, or **60** with fluorescent analogue **61**. **A.** Chemical structure of fluorescent analogue **61**. **B.** *C. trachomatis* infected HeLa cells were incubated with 0.5 μM of **61** alone or with **61** alongside with analogues **43**, **58**, or **60** at the same concentration. After 48 h of incubation, the cells were fixed and imaged by confocal microscopy and the images were processed using identical parameters. **C.** The fluorescent intensity of each inclusion was analysed with ImageJ software¹¹⁰ and was plotted into a graph. The data shown is representative from at least two independent experiments and for each experiment 40 inclusions were analysed. ***indicates $p < 0.05$ and statistical significance using a nonparametric one-way ANOVA test.

Summary and concluding remarks

In this study, potent and non-hydrolysable ring-fused 2-pyridone amide isosteres that inhibit *C. trachomatis* infectivity were synthesised and evaluated. The biological results of the non-hydrolysable amide isosteres show that the C3-phenyl amide compounds are not prodrugs, they are the active substances that gives the anti-infective effect. The 1,2,3-triazoles **58** and **60** reduced *C. trachomatis* infection by $\geq 95\%$ at nanomolar concentrations without showing host cell toxicity. Additionally, neither of them show mutagenic potential nor inhibited the growth of tested bacteria in the microbiota. These findings show that the ring-fused 2-pyridone amide isostere analogues are potent inhibitors of *C. trachomatis* infectivity without non-target toxicity and show an analogous mode of action to phenyl amide **43**.

6. C8-substituted ring-fused 2-pyridone amide analogues targeting *Chlamydia trachomatis* infectivity (Paper III)

Beyond improving the potency of the compounds designed for the *Chlamydia trachomatis* project, other factors such as reducing lipophilicity and improve pharmacokinetic properties were targeted to improve the usefulness of the compounds *in vivo*. In this chapter and **paper III**, various C8-heteroatom substituted analogues were synthesised and evaluated against *C. trachomatis* infectivity and their pharmacokinetic properties were measured.

From the previous investigation of ring-fused 2-pyridone analogues targeting *C. trachomatis* by Engström *et. al.*,⁴⁴ it was discovered that a small substituent (*e.g.* cyclopropyl) at the C8-position was beneficial for activity. While compounds with larger substituents (*e.g.* phenyl) were not as effective in blocking chlamydial infectivity.⁴⁴ The C3-, C6-, and C7-positions of the ring-fused 2-pyridone scaffold have been examined earlier within the project,³⁵ as well as investigation of non-hydrolysable C3-amide isostere analogues¹⁰⁸ (Chapter 5). In the previous studies, 1,2,3-triazoles **58** and **60** were highly potent with an anti-infective activity at low nanomolar concentrations, matching the potent amide analogue **43** (Figure 6.1). These results motivated an *in vivo* pharmacokinetic (PK) study (orally and intravenously in mice) of the two compounds **43** and **60**. The concentration of compound **43** in the blood samples was unfortunately too low to properly calculate the pharmacokinetic parameters. The exposure of the 1,2,3-triazole **60** in mice was better than for amide **43**, although the uptake and area under curve (AUC) was very low (data shown in Paper III).

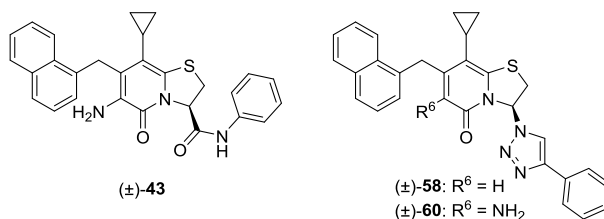


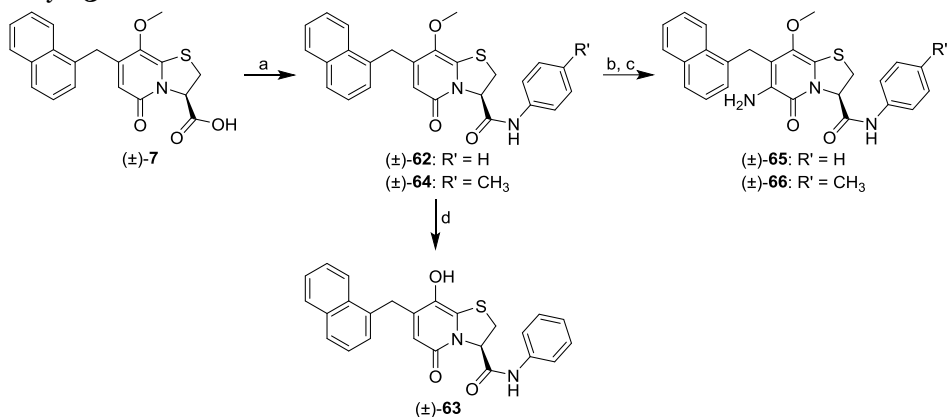
Figure 6.1. Chemical structures of ring-fused 2-pyridone analogues **43**, **58**, and **60**.

In this study, we wanted to further explore the C8-position of the ring-fused 2-pyridone and how small heteroatom-based substituents would affect the anti-infective activity and the pharmacokinetic properties of the compound. Introduction of heteroatoms at the C8-position has proven to be beneficial for the activity of compounds targeting *L. monocytogenes* (Chapter 3).³⁷ Reduced lipophilicity of the compound would potentially lead to improved pharmacokinetic properties.⁸⁸ The aim was to design compounds with preserved reasonable activity levels towards *C. trachomatis* infectivity and reduced lipophilicity that could improve the oral availability of the compounds.

Synthesis of the first set of inhibitor candidates

This study started with exchanging the C8-cyclopropyl group to a hydroxy or methoxy substituent and a set of fourteen analogues were designed and synthesised. The carboxylic acid **7** has previously been synthesised within the *L. monocytogenes* project³⁷ and served as the key intermediate in the synthesis of the C3-amide analogues. The C8-methoxy, C3-phenyl amide analogue **62** was obtained *via* amide coupling with coupling reagent propylphosphonic anhydride and aniline from the carboxylic acid **7** (Scheme 6.1). An initial trial attempted to obtain the corresponding C8-hydroxy analogue **63** through amide coupling of C8-hydroxy, C3-carboxylic acid **9** (for structure see Chapter 3, Scheme 3.1). However, no conversion to amide **63** could be detected and the compound was instead generated by demethylation of the C8-methoxy analogue **62** with boron tribromide. Replacing the C3-phenyl amide with a *p*-methyl phenyl amide as well as different amide isosteres gave successful results in earlier investigations.^{35,108} To investigate if the C3-substituent would have a similar effect in combination with C8-methoxy, *p*-methyl phenyl amide analogue **64** was synthesized *via* amide coupling of carboxylic acid **7** with *p*-methylaniline. A key substituent for increasing potency and reducing lipophilicity has been an amine at the C6-position.^{35,108} Therefore a C6-amine was introduced through nitration and then reduction with zinc in acetic acid, which gave the two amines **65** and **66** (Scheme 6.1).³⁰

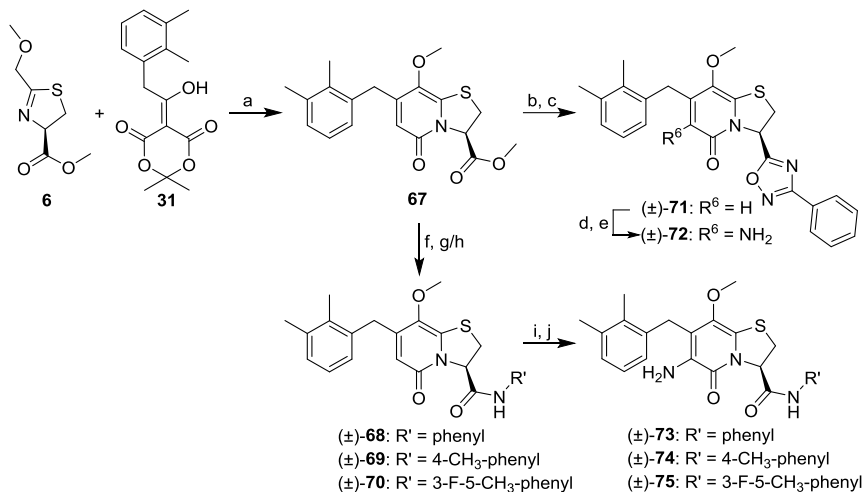
Scheme 6.1. Synthesis of C8-methoxy analogues **62**, **64**, **65**, and **66** and C8-hydroxy **63**.



Reagents and conditions: a) R-aniline, propylphosphonic anhydride (50% in EtOAc), pyridine, MeCN/EtOAc (1:1), -10 °C to rt, 24-43 h, **62**: 58%, **64**: 38%; b) NaNO₂, TFA, DCM, O₂ atmosphere, rt, 1-7 h; c) activated Zn dust, AcOH, rt, 31-48 h, **65**: 30% over two steps; **66**: 35% over two steps; d) BBr₃, DCM, -40 °C to rt, 6 h, 10%.

Exchanging the relatively large and hydrophobic C7-1-naphthyl group to a smaller 2,3-dimethyl phenyl, would slightly decrease the lipophilicity of the compounds (*e.g.* 1-naphthyl **62** (5.0) to 2,3-dimethyl phenyl **68** (4.4), see Table 6.1). This change of substituent has previously shown to preserve the anti-infective activity of the analogues.³⁵ The 2,3-dimethyl phenyl substituent was first introduced *via* Suzuki–Miyaura cross-coupling with a C7-chloro substituted ring-fused 2-pyridone intermediate. On subsequent scale up, the C7-substituent was instead introduced *via* 2,3-dimethyl phenyl substituted Meldrum’s acid **31** to obtain the intermediate **67** in one less reaction step as well as avoiding palladium coupling reactions (Scheme 6.2). Hydrolysis of intermediate **67** and then subsequent amide coupling with aniline or *p*-methylaniline resulted in amide **68** and **69**, respectively. In the previous study,³⁵ only mono-substituted amides were investigated and to study if di-substituted amides would be tolerated, 3-fluoro-5-methylaniline was incorporated at the C3-position, resulting in amide **70**. The amide isostere 1,2,4-oxadiazole **71** was obtained by first hydrolysing the methyl ester **67** from which the 1,2,4-oxadiazole moiety was acquired by amide coupling with benzamideoxime and TBTU followed by cyclisation.¹¹¹ These four amide and amide isostere compounds (**68-71**) were converted to the C6-amine analogues **72**, **73**, **74**, and **75** *via* nitration and then reduction of the formed C6-nitro group (Scheme 6.2).³⁰

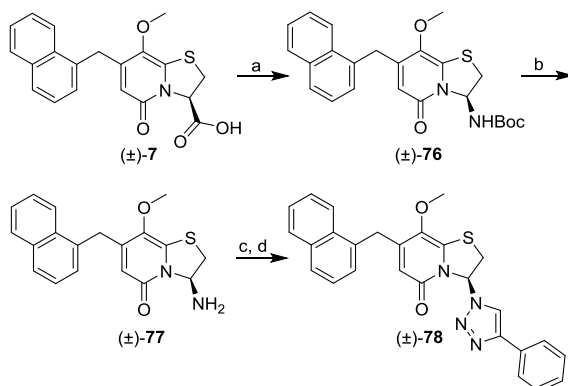
Scheme 6.2. Synthesis of C8-methoxy analogues with C3-phenyl amides **68-70**, **73-75** and 1,2,4-oxadiazoles **71** and **72**.



Reagents and conditions: a) TFA, DCE, MWI, 120 °C, 3 min, 80%; b) 1 M LiOH_(aq), THF, rt, 15 h; c) Benzamidoxime, TBTU, DIPEA, DMF, MWI, 170 °C, 12 min, 46%; d) NaNO₂, TFA, DCM, O₂ atmosphere, rt, 1 h; e) activated Zn dust, AcOH, rt, 19 h, 60%; f) 1 M LiOH_(aq), THF, rt, 15 h; g) For **68** and **69**: R-aniline, propylphosphonic anhydride (50% in EtOAc), pyridine, MeCN/EtOAc (1:1), -10 °C to rt, 24 h, **68**: 82% **69**: 39%; h) For **70**: 3-Fluoro-5-methylaniline, HATU, DIPEA, DCM, 2 h, see procedure; i) NaNO₂, TFA, DCM, O₂ atmosphere, rt, 2.5-6 h; j) activated Zn dust, AcOH, rt, 20-23 h, **73**: 30%, **74**: 17%, **75**: 38% over two steps.

The most potent amide isostere substituent in the previous screen was a 1,2,3-triazole (analogues **58** and **60**) and this motivated us to further explore this substituent in combination with the C8-methoxy group. The BOC-protected amine **76** was obtained through Curtius rearrangement of intermediate **7**, using DPPA in *tert*-butyl alcohol (Scheme 6.3). Subsequent acidic deprotection, using TFA, resulted in the primary amine **77**, which was converted by diazo transfer followed by Cu(I)-catalysed azide-alkyne cycloaddition (CuAAC), to give the 1,2,3-triazole **78**.

Scheme 6.3. Synthesis of 1,2,3-triazole analogue **78**.



Reagents and conditions: a) DPPA, TEA, *t*-BuOH, 2 h, 85 °C, 60%; b) TFA, DCM, 2 h, rt, 32%; c) imidazole-1-sulfonyl azide·H₂SO₄, CuSO₄, K₂CO₃, MeOH, 40 h, 50 °C; d) phenyl acetylene, CuSO₄, sodium ascorbate, DMF, H₂O, rt, 4 h, 4% from **77**.

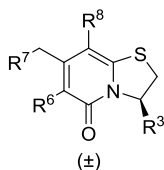
Evaluation of biological effectivity of the first set of inhibitor candidates

The anti-infective *C. trachomatis* activity of the C8-methoxy and hydroxy compounds were evaluated with a Reinfest assay, previously described in Chapter 5.^{35,108} The assay measures how much the compound reduces the relative infection level (give in percentage) of *C. trachomatis* after reinfection in new cells, at fixed compound concentrations (2.5 and 1 μM). The cytotoxicity of the compounds was tested in resazurin cell toxicity assay, at a concentration of 10 μM.^{35,108}

In this study, the phenyl amide **42** served as benchmark compound along with the lead compounds **43** and **60** from previous studies^{35,108} (Table 6.1). Overall, the result of the evaluation showed a drop in efficacy of the C8-hydroxy and methoxy analogues compared to the benchmark compounds. However, the two phenyl amides **64** and **69** showed a decent potency at 2.5 μM, while the 3-fluoro-5-methylaniline **70** was more potent than the benchmark compound **42** at 1 μM. All the tested compounds showed low cytotoxicity towards HeLa cells (Table 6.1). The analogue **70** seemed to be a potent candidate and was resynthesised in larger scale (> 5 g). The scale up of the synthesis worked well and the final product was recrystallised to obtain amide **70** as a crystalline product. To evaluate if the methoxy analogue **70** could improve the oral uptake and the compound distribution in blood compared to the 1,2,3-triazole **60**, an *in vivo* pharmacokinetic study was performed. In the *in vivo* study with analogues **60** and **70** a lipid emulsion formulation was used for the oral administration (for details about the vehicle see Paper III). Unfortunately, the gastrointestinal

uptake of these compounds was so low that the pharmacokinetic parameters of the oral administration could not be calculated. However, the AUC and the peak blood concentrations (C_{\max}) after intravenous administration of the methoxy analogue **70** showed a 10-fold improvement compared to 1,2,3-triazole **60** (data shown in Paper III).

Table 6.1. Ring-fused 2-pyridone analogues with C8-methoxy and -hydroxy substituents.



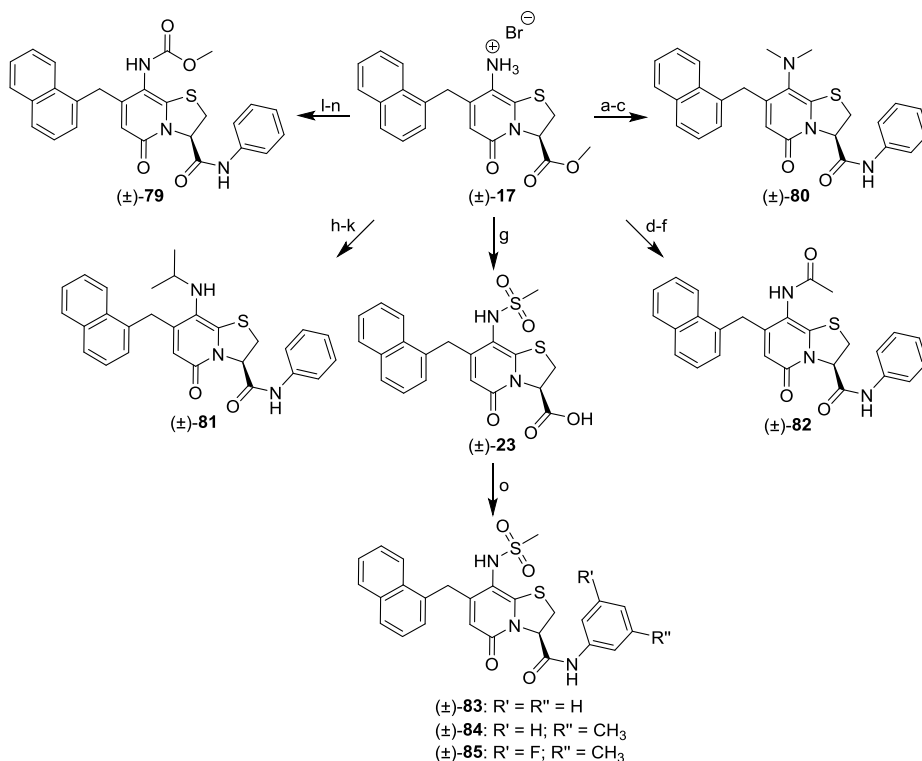
ID	R ³	R ⁶	R ⁷	R ⁸	Calcd. Log P ¹¹²	HeLa Viability (10 μM)	Reinfect 2.5 μM (%)	Reinfect 1 μM (%)
42		H			5.1	100 ± 4*	97 ± 2	49 ± 6
43		NH ₂			5.1	100 ± 3*	97 ± 2	98 ± 1
60		NH ₂			5.1	105 ± 4 [#]	99 ± 0 [±]	99 ± 0
63		H		OH	4.8	87 ± 3	21 ± 14	n.d.
62		H		OCH ₃	5.0	91 ± 6	24 ± 8	n.d.
65		NH ₂		OCH ₃	4.5	94 ± 2	25 ± 14	n.d.
64		H		OCH ₃	5.3	89 ± 4	94 ± 0	62 ± 1
66		NH ₂		OCH ₃	4.8	91 ± 2	51 ± 16	n.d.
68		H		OCH ₃	4.4	89 ± 2	32 ± 8	n.d.
73		NH ₂		OCH ₃	3.9	94 ± 1	25 ± 14	n.d.
69		H		OCH ₃	4.7	88 ± 3	98 ± 1	71 ± 4
74		NH ₂		OCH ₃	4.2	93 ± 1	56 ± 13	n.d.
70		H		OCH ₃	5.0	90 ± 2	99 ± 0	95 ± 8
75		NH ₂		OCH ₃	4.4	92 ± 2	47 ± 16	n.d.
71		H		OCH ₃	4.8	91 ± 3	1 ± 4	n.d.
72		NH ₂		OCH ₃	4.3	94 ± 2	17 ± 8	n.d.
78		H		OCH ₃	5.2	87 ± 3	81 ± 9	n.d.

*;# Data provided from previous study. [±]35 [#]108 [±]Tested at 2 μM.

Synthesis and biological evaluation of the second set of inhibitor candidates

As an alternative to the C8-hydroxy and -methoxy analogues we wanted to investigate C8-nitrogen substituents. Introduction of nitrogen based C8-substituents would possibly reduce the overall lipophilicity and give rise to new possible interactions of the ring-fused 2-pyridone with possible target(s) in *C. trachomatis*. A set of five C8-amine analogues **79-83**, were synthesised from the intermediate **17**³⁷ (Scheme 6.4). The C8-amine analogues were synthesised by first formation of the respective C8-substituent, then hydrolysis of the C3-methyl ester, and subsequent amide coupling with aniline as the last reaction step to obtain analogues **79-83**. The calculated Log P¹¹² values of these compounds were lower than for the cyclopropyl analogues, especially the methyl sulfonamide **83** (Table 6.2). Although the anti-infective activity of the compounds in the reinfection assay was lower (Table 6.2). Analogue **83** inhibited reinfection by 89% at 2.5 μ M and in an attempt to improve the potency, two C3-amide analogues **84** and **85** were synthesised. The two C8-methyl sulfonamides **84** and **85** were obtained from intermediate **17** via carboxylic acid **23** (Scheme 6.4). Unfortunately, none of these two phenyl amide derivatives showed any improvement of the anti-infective activity towards *C. trachomatis* (Table 6.2).

Scheme 6.4. Synthesis of C8-nitrogen analogues **79-83**, **84** and **85**.

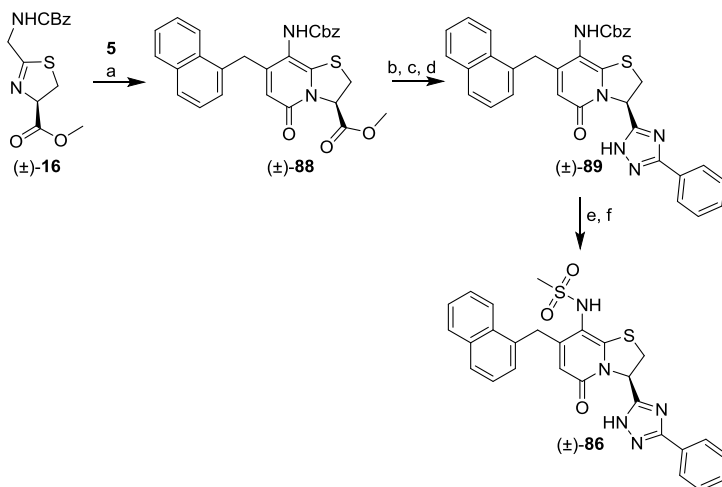


Reagents and conditions: a) CH₃I, NaHCO₃, DMF, 70 °C, 10 h; b) 1 M LiOH_(aq), THF:MeOH (5:1), rt; c) aniline, HATU, DIPEA, DMF, 1 h, 55% from **17**; d) acetyl chloride, pyridine, DCM, rt, overnight; e) 1 M LiOH_(aq), THF:MeOH (5:1), rt, 2 h; f) aniline, HATU, DIPEA, DMF, 1 h, 50% from **17**; g) methanesulfonyl chloride, TEA, THF, rt, overnight; then: 1 M LiOH_(aq), MeOH, rt, 16 h, 49%; h) NaBH(OAc)₃, TFA, DCM, acetone, -15 °C to rt, overnight; i) 1 M LiOH_(aq), THF:MeOH (4:1), rt, 1 h; j) suspended in DCM and dripped in to ethereal HCl, -20 °C, overnight; k) aniline, HATU, DIPEA, DMF, 1 h, 43% from **17**; l) methyl chloroformate, pyridine, DCM, rt, 2 h; m) 1 M LiOH_(aq), THF:MeOH (5:1), rt; n) aniline, HATU, DIPEA, DMF, 1 h, 38% from **17**; o) R-aniline, HATU, DIPEA, DMF, 1-4 h, **83**: 52% from **17**, **85**: 49% and **84**: 78% from **23**.

The anti-infective activity of the C8-cyclopropyl analogues was improved by introduction of C3-amide isosteres (*e.g.* analogue **60**). To investigate if a similar boost in effectivity would occur with the C8-methyl sulfonamide, two amide isosteres 1,2,4-triazole **86** (Scheme 6.5) and 1,2,3-triazole **87** (Scheme 6.6) were designed and synthesized. The *N*-carboxybenzyl protected methyl ester **88** was obtained from the Cbz-protected amine substituted thiazoline **16** and 1-naphthyl Meldrum's acid derivative **5** (Scheme 6.5). Intermediate **88** was hydrolysed and *via* a one pot reaction¹⁰⁵ including amide coupling, ring closure, and deprotection of the 4-methoxybenzyl by TFA, the 1,2,4-triazole intermediate **89** was obtained. The C8-Cbz-protected intermediate **89** was

deprotected and the obtained C8-amine was treated with methanesulfonyl chloride to yield the methyl sulfonamide **86** (Scheme 6.5).

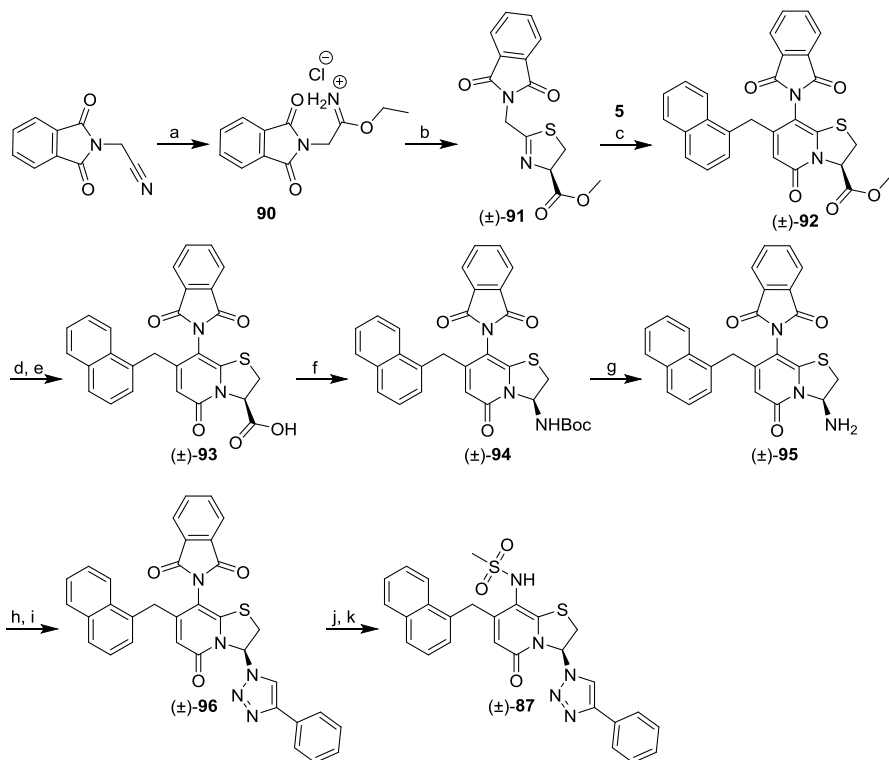
Scheme 6.5. Synthesis of 1,2,4-triazole **86**.



Reagents and conditions: a) a) **5**, TFA, DCM, 70 °C, 20 h, 85%; b) 1 M LiOH_(aq), THF, rt, 2 h; c) benzamidine·HCl, HATU, DIPEA, DMF, 3.5 h; then (4-methoxybenzyl) hydrazine·HCl, AcOH, 80 °C, 20 h; d) TFA, DCM, 50 °C, 22 h, 39% from **88**; e) 33% HBr/AcOH, DCM, rt, 2 h; f) methanesulfonyl chloride, pyridine, rt, 18 h; then: 1 M LiOH_(aq), THF:MeOH (3:1), rt 53% from **89**.

With a cyclopropyl¹⁰⁸ or a methoxy substituent at the C8-position, the C3-1,2,3-triazole moiety was obtained *via* diazo transfer with imidazole-1-sulfonyl-azide of the corresponding C3-primary amine. However, with the C8-*N*-carboxybenzyl protecting group, the diazo transfer reaction from a C3-primary amine to azide was unsuccessful due to dimerization of the ring-fused 2-pyridone. An alternative route using a phthalimide protecting group, developed by Anders E. G. Lindgren, was used instead and substituted thiazoline **91** was obtained from 2-(1,3-dioxoisindolin-2-yl) acetonitrile *via* intermediate **90** (Scheme 6.6). After 4 days of stirring at 80 °C, the ring-fused 2-pyridone methyl ester **92** was obtained from thiazoline **91** and acyl Meldrum's acid **5**. Hydrolysis of the methyl ester **92** using aqueous LiOH and following re-closure of the phthalimide resulted in carboxylic acid **93**. Curtius rearrangement in *tert*-butyl alcohol of carboxylic acid **93** gave the BOC-protected amine **94**, which was deprotected by TFA to yield primary amine **95**. Diazo transfer with imidazole-1-sulfonyl-azide of amine **95** and following Cu(I)-catalysed azide-alkyne cycloaddition with phenyl acetylene resulted in 1,2,3-triazole **96**. Deprotection of the C8-position and following reaction with methanesulfonyl chloride generated the final 1,2,3-triazole **87** (Scheme 6.6).

Scheme 6.6. Synthesis of 1,2,3-triazole analogue **87** with a C8-methyl sulfonamide substituent.



Reagents and conditions: a) AcCl, EtOH/EtOAc (1:1), 0 °C to rt, 17 h, (see procedure); b) L-Cysteine methyl ester-HCl, TEA, DCM, rt, 3 days, 64%; c) **5**, TFA, DCM, 80 °C, 4 days, 62%; d) 1 M LiOH_(aq), THF, rt, 4 h; e) AcOH, DMF, 150 °C, 20 h, 78% from **92**; f) DPPA, TEA, t-BuOH, 2 h, 85 °C, 57%; g) TFA, DCM, rt, 2 h, 88%; h) imidazole-1-sulfonyl azide·H₂SO₄, CuSO₄, K₂CO₃, MeOH, 24 h, 50 °C; i) phenyl acetylene, CuSO₄, sodium ascorbate, DMF, H₂O, rt, 3.5 h, 1% from **95**; j) methyl amine, EtOH, rt, 20 h; k) methanesulfonyl chloride, pyridine, rt, 26 h; then: 1 M LiOH_(aq), THF:MeOH (3:1), rt, 2 h, 99% from **96**.

Table 6.2. Ring-fused 2-pyridone analogues with C8-nitrogen substituents.

ID	R ³	R ⁸	Calcd. Log P ₁₁₂	HeLa Viability (10 μM)	Reinfect 2.5 μM (%)	Reinfect 1 μM (%)
79			4.6	88 ± 3	12 ± 15	-19 ± 21
80			5.0	92 ± 3	94 ± 0	78 ± 20
81			5.5	91 ± 4	79 ± 9	25 ± 4
82			4.4	90 ± 5	3 ± 9	44 ± 47
83			4.2	94 ± 2	89 ± 4	23 ± 12
84			4.5	92 ± 2	-2 ± 5	n.d.
85			4.7	91 ± 2	6 ± 17	6 ± 6
86			4.7	93 ± 1	20 ± 4	n.d.
87			4.3	91 ± 0	88 ± 7	n.d.

Although neither the 1,2,4-triazole **86** nor the 1,2,3-triazole **87** showed any improvement of activity in the Reinfect assay, compared to phenyl amide **83**. Even though compound **83** was less potent than the analogues **43** and **60**, it had a fair activity at low micromolar concentrations, showed no toxicity at tested concentrations and in comparison to the other compounds, a relatively low Log P value. In addition, the Caco-2 permeability of compound **83** was

improved compared to the previous candidates, showing a value corresponding to a high permeability compound¹¹³ (details shown in Paper III). Therefore we chose to evaluate the pharmacokinetic properties of the methyl sulfonamide **83** *in vivo*. Rewardingly, in good correlation with the *in vitro* data, the methyl sulfonamide **83** had significantly improved PK properties with an oral bioavailability of 41% (data shown in Paper III). This encouraged further evaluation of the analogue and an *in vivo* study with oral treatment of pre-infected mice was conducted. Unfortunately, no significant effect on the *C. trachomatis* infection was seen after treatment with compound **83**, however, no negative signs of the treatment was detected on the mice (data shown in Paper III).

Summary and concluding remarks

In summary, the introduction of heteroatoms at the C8-position showed a drop of potency compared to previous potent ring-fused 2-pyridone analogues, however, the pharmacokinetic properties were improved. The analogues **43** and **60** from the previous screens were very potent in the Reinfect assay, although their oral bioavailability *in vivo* was very low. To find a suitable compound for further studies in higher models, there must be a balance between high activity and good bioavailability *in vivo*. The C8-methyl sulfonamide ring-fused 2-pyridone **83** showed a lower anti-infective activity but a remarkable increase in the oral bioavailability. These findings, that the C8-methyl sulfonamide ring-fused 2-pyridone could improve oral bioavailability is a great step towards a proof of concept for an orally available drug to treat *C. trachomatis* infection. Low toxicity of the compounds enables higher treatment dose and with improved vehicles, studies with a higher dose could be possible.

7. Formation of ring-fused 4-pyridones (Appendix 2)

During the synthesis of ring-fused 2-pyridone analogues with electron-withdrawing or sterically hindered substituents at C8-position, another compound with the same mass was observed for some substituents. In this chapter and appendix 2, the parallel formation of ring-fused 4-pyridone analogues will be discussed.

In the beginning of the project changing substituents at the C8-position, the initial attention was on small carbon-based substituents. Within both the *L. monocytogenes* and *C. trachomatis* projects, a majority of the previously investigated compounds have been equipped with a cyclopropyl at the C8-position, like compound **1** (see Chapter 1 and Figure 1.2 for structure). A close analogue to a cyclopropyl group, although more sterically demanding, is an isopropyl substituent. In the attempt to obtain the C8-isopropyl analogue **98** (Figure 7.1), by heating isopropyl thiazoline **97** and acyl Meldrum's acid **5** to 120 °C for 3 min (MWI), two compounds with identical mass were observed. They had different retention time on LC-MS (reversed phase 18-column) but were not separable on silica. The ratio between the two compounds was close to 1:1 according to crude ¹³C-NMR. The aim was to obtain the carboxylic acid analogue **100** and the mixture of the compounds was hydrolysed with aqueous LiOH. The subsequent separation by high-performance liquid chromatography (HPLC) resulted in the expected ring-fused 2-pyridone (**100**) and the ring-fused 4-pyridone analogue (**101**) (Figure 7.1).

Two-dimensional nuclear magnetic resonance (2D-NMR) techniques were used to distinguish between the two compounds and specific heteronuclear multiple-bond coherence (HMBC) and nuclear Overhauser effect (NOE) correlations confirmed the correct structures of the two molecules. The HMBC spectrum of 2-pyridone **100** reveals a three-bond coupling between the H1' proton and the C7 carbon (153.6 ppm). While, the HMBC spectrum of 4-pyridone **101** show the same type of three-bond range coupling from the H1' proton to a carbon peak at 175.0 ppm, which indicates a different structure. In the HMBC spectrum of 2-pyridone **100**, couplings can be seen between the C9 carbon and the H1' proton, the H3 proton and one of the protons on C2 (not shown in the figure). Neither the H3 proton nor any of the protons on C2 show coupling to the C7 carbon and this differentiates the C9 carbon from the C7 carbon in the structure of the 2-pyridone **100**. In the rotating frame Overhauser effect spectroscopy (ROESY) spectrum of the 4-pyridone **101**, the structure gives rise to a NOE coupling between the protons on C3 and C10, which cannot be seen in the ROESY

spectrum of 2-pyridone **100**. However, the ROESY spectrum of the ring-fused 2-pyridone **100** reveals two NOE couplings between the protons on C1' and C10 respectively C2' and C12.

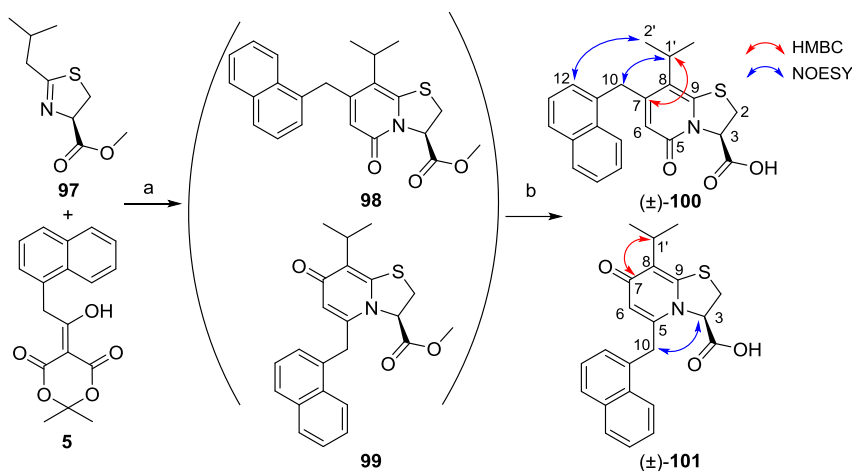


Figure 7.1. Synthesis of the C8-isopropyl analogues, resulting in the ring-fused 2-pyridone analogue **100** and the ring-fused 4-pyridone analogue **101**. The key HMBC and NOE correlations to distinguish between the two compounds are marked in each structure. Reaction and conditions: a) TFA, DCE, 120 °C (MWI), 3 min; b) 1 M LiOH_(aq), THF, rt, overnight (for details see Appendix 2).

A similar problem, with observing two compounds with identical mass, was encountered in the reaction between methanesulfonyl substituted thiazoline **15** and 1-naphthyl Meldrum's acid **5** (see Scheme 3.1B in Chapter 3). These two methyl ester analogues were separable on silica but it was difficult to obtain pure material of the methyl esters. Therefore the two crude methyl ester intermediates were separately hydrolysed and purified by HPLC to obtain the ring-fused 4-pyridone **102** and the ring-fused 2-pyridone **14** (Figure 7.2). The correct structures of the compounds were determined with 2D NMR techniques.

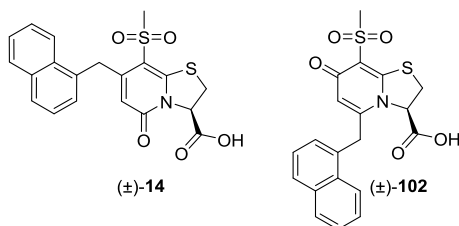


Figure 7.2. Chemical structures of ring-fused 2-pyridone **14** and ring-fused 4-pyridone **102**.

The problem of obtaining ring-fused 4-pyridones seems to occur when having a strong electron withdrawing substituent or by steric effects of the R⁸-substituent at the thiazoline. However, this has not been encountered with flat aromatic substituents such as phenyl or *m*-trifluoro phenyl. Zahedifar *et. al.* encountered the same problem of ring-fused 4-pyridones when they aimed for obtaining ring-fused 2-pyridones from acyl Meldrum's acid derivatives and 2-(1,3-benzothiazole-2-yl)acetonitrile.¹¹⁴ In their case they obtained only the ring-fused 4-pyridone analogue and not a mixture of the compounds. This supports our findings with obtaining the ring-fused 4-pyridone analogue when having an electron withdrawing R⁸-substituent at the thiazoline moiety. The formation of the ring-fused 4-pyridone scaffold could possibly be explained by the following tentative mechanism (Figure 7.3). An attack of the thiazoline enamine tautomer **A2** on the acylketene intermediate **C**, generated from thermolysis of the acyl-Meldrum's acid derivative **B**, could give intermediate **D**. The possible following cyclocondensation, *via* imine attack on the carbonyl carbon (**D**), loss of water (**E**) and aromatisation of the molecule could result in the ring-fused 4-pyridone (**H**). A similar mechanism with addition and cyclocondensation has been suggested for the formation of ring-fused 2-pyridones from heterocyclic ketene N,S-acetals and methyl propiolate.¹¹⁵

The biological effect of the ring-fused 4-pyridone analogues **101** and **102** were evaluated within the *L. monocytogenes* project. However, neither of them inhibit *L. monocytogenes* infection in cells and no further investigation of the compounds were pursued within this project.

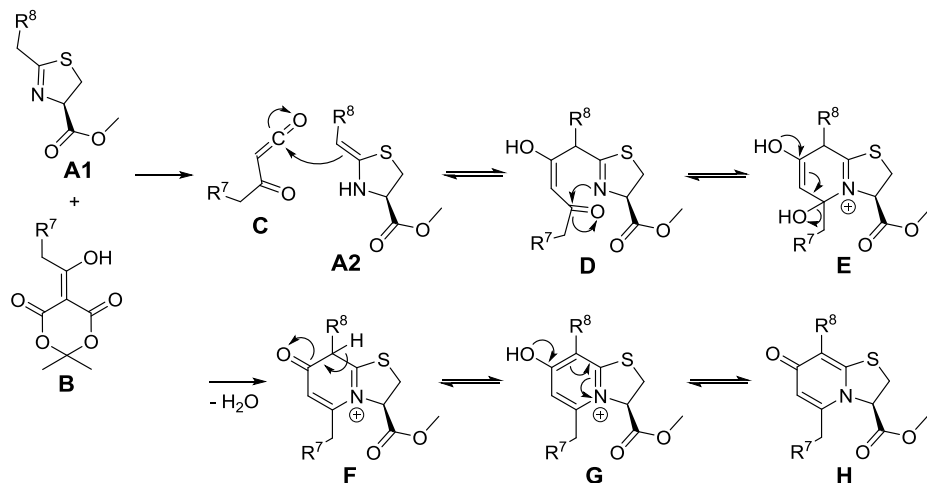


Figure 7.3. Tentative mechanism of the formation of the ring-fused 4-pyridone scaffold.

Summary and concluding remarks

The parallel formation of the ring-fused 4-pyridone analogues has mainly been an unwanted side-track, resulting in low yields of the desired ring-fused 2-pyridone analogues. The tested compounds, **101** and **102**, showed no effect on *L. monocytogenes* infection and no further investigation or development of this scaffold has been pursued at the moment. However, this heterocycle is interesting and could be further explored for its biological value and be evaluated towards other biological targets.

8. Summary and future directions

The global problem of antibiotic resistance is increasing and the need for action is urgent. An alternative treatment strategy to antibiotics is the anti-virulence treatment approach, where the virulence of the bacteria is inhibited. The research described in this thesis has been focused on ring-fused 2-pyridone analogues targeting *Listeria monocytogenes* and *Chlamydia trachomatis*. These two bacteria are both human pathogens with intracellular infection lifestyles, however, they give rise to very diverse diseases and their routes of infection are different.

The central character in this thesis is the ring-fused 2-pyridone scaffold, which constitutes the basis of the two projects. The overall aim in the two projects was to develop nontoxic compounds which target virulence of the specified bacteria. The bacterial virulence should be blocked without inhibiting the growth of or killing the pathogenic bacteria and surrounding non-pathogenic bacteria. By different substitution patterns of the ring-fused 2-pyridone scaffold, the activity of the compounds can be directed. The main structural difference between the compounds targeting *L. monocytogenes* versus *C. trachomatis* is the substituent at the C3-position. A phenyl amide or amide isostere is required for the compound to show good activity towards *C. trachomatis*, while a carboxylic acid is preferred to attenuate *L. monocytogenes* infection.

Within the *Listeria monocytogenes* project, the target of the ring-fused 2-pyridone analogues is the transcriptional regulator PrfA, which controls most of the virulence factors in *L. monocytogenes*. By structure-based design with the co-crystal structure of PrfA:1, we synthesised new improved ring-fused 2-pyridone analogues (Chapter 3, Paper I). As a result of our efforts, we obtained compounds that enabled us to confirm the specific interaction sites in PrfA as well as improve the life-span of *L. monocytogenes* infected chicken embryos. Introduction of imidazole salt as a counter ion to the carboxylic acid of analogue **24** improved the solubility of the compound and consequently resulted in better activity. These results triggered us to further investigate the potency of these compounds. The ongoing research within this project focuses on the C3-position, where our hypothesis is that a prolongation of the carboxylic acid moiety would be beneficial for drug-target protein interaction. The analogue **35**, with an extended carboxylic acid at the C3-position, showed similar activity as compound **24** at low concentrations. The preliminary co-crystal structure of PrfA:**35** showed that the carboxylic acid of analogue **35** is located in the opposite direction, compared to the carboxylic acid of compound **24**, and interacts with amino acid residue Cys229. This finding opens up for new interactions of the ring-fused 2-pyridones to PrfA. These possible interactions

can be studied by extending the carbon chain further as well as introducing new substituents along the carbon chain. Along with this, the interactions of the primary alcohol **37** to PrfA will be evaluated.

The *L. monocytogenes* project is a proof of concept project where we have proved that our ring-fused 2-pyridone analogues block the virulence transcriptional regulator PrfA, a Crp/Fnr family member. This concept could be used for other biological targets within the Crp/Fnr family. Due to the invasive character of listeriosis, caused by *L. monocytogenes*, perhaps an anti-virulence treatment option alone would not be able to clear the infection fast enough. However, the anti-virulence compound could be administrated as part of a combinatorial treatment option, in combination with an antibiotic drug, to obtain a synergetic effect between them. By having one drug targeting virulence factor(s) of the pathogenic bacteria in combination with an antibiotic drug could boost the overall effect. These possible combinatorial treatment options would hopefully decrease the pressure on the pathogen to develop resistance towards the drugs and hence prolong the life-time of the drugs.

In the project targeting the virulence of *Chlamydia trachomatis*, very potent compounds have been developed, such as compounds **43** and **60**. They inhibit *C. trachomatis* infectivity at low nanomolar concentrations, without showing host cell toxicity or affecting the viability of commensal microbiota. The development from the C3-phenyl amide **43** to the non-hydrolysable 1,2,3-triazole **60** confirmed that the C3-phenyl amide moiety does not work as a prodrug. The possible hydrolysis of the C3-phenyl amide would result in aniline, with possible toxic effects. Therefore, an interesting compound from the same screen is the analogue **56**, with a reversed phenyl amide at the C3-position, which showed equal potency as compound **42** in the Reinfect₉₅ screen. Upon *in vivo* hydrolysis, this compound would give rise to benzoic acid, a less toxic metabolite. Different amide analogues to the phenyl amide **42** were obtained from the accessible intermediate **1**. Amide analogues to the reversed phenyl amide **56** would require Curtius rearrangement of carboxylic acid **1**, with following deprotection to acquire the precursor C3-amine **55**. However, further investigations of the reversed phenyl amide **56** analogues has not been investigated at the moment, but is a very interesting path to explore.

One key attribute to obtain an efficient drug agent is a balanced hydrophilicity. Advancements of reaching less lipophilic compounds have been investigated within the *C. trachomatis* project. By exchanging the C8-cyclopropyl group (*e.g.* analogues **43** and **60**) to a methyl sulfonamide (analogue **83**), the calculated log P value was reduced, however the potency was unfortunately not conserved. On the other hand, the pharmacokinetic properties of the compound were dramatically improved both *in vitro* and *in vivo*. From almost no *in vivo* uptake

of analogue **60** to an oral bioavailability of 41% of compound **83** in mice. A site of interest on the ring-fused 2-pyridone scaffold for further exploration could be the C6-position. By introduction of a primary amine substituent at the C6-position, the anti-Chlamydial activity was improved (analogues **42** vs. **43** and **58** vs. **60**). Introduction of methyl sulfonamide at the C8-position improved the pharmacokinetic properties of the compound **83** but the anti-Chlamydial activity was reduced. The loss of activity when removing the C8-cyclopropyl shows that this substituent is important for the activity. Studies to improve the overall compound properties could be directed to other substituents and alternative substitution patterns might increase the potency of the compounds. Besides improving the compounds, efforts to find more efficient vehicles are needed. With new vehicles that can dissolve higher doses of the compounds, the desired proof of concept of a treatment for *C. trachomatis* infection *via* oral delivery could be within reach.

Genital infection caused by *C. trachomatis* is a non-emergency disease that today is treated with broad-spectrum antibiotics such as azithromycin or doxycycline. By estimations of WHO, there are more than 130 million cases of sexually transmitted *C. trachomatis* in a year. This can be recalculated into 130 million doses of broad-spectrum antibiotics used in a year to treat sexually transmitted *Chlamydia* infections. The resistance selection pressure on both the *C. trachomatis* bacteria, the surrounding bacteria in the host as well as the environment is increased by this. These broad-spectrum antibiotics could be replaced by an anti-virulence treatment option. This would reduce the amount of antibiotics produced and used world-wide and as a result this could reduce the resistance selection pressure on bacteria.

With the high abundance of the genital *C. trachomatis* infection, the optimal treatment option is an orally distributed drug due to the simplicity of administration. To be able to use ring-fused 2-pyridones in an oral drug the pharmacokinetic properties must be improved, while retaining or improving the potency of the compound. However, for the eye infection trachoma, a topical administration could be suitable. A topical administered drug for trachoma could be locally applied directly around or in the eye. By this, a more lipophilic drug could potentially be used and the concerns around the oral availability and distribution could be dismissed.

A key to finding a proper small molecule drug is to identify the biological target of the biologically active compound. Therefore, in parallel with our project targeting *C. trachomatis* infectivity, we are searching for the target(s) of the potent ring-fused 2-pyridone analogues in *C. trachomatis*. By knowing the target, a more elucidative and precise design of new ring-fused 2-pyridone analogues can be performed. Design, synthesis, and optimisation of ring-fused

2-pyridone analogues with photoreactive groups (e.g. diazirines) are ongoing. These will be used in identifying the target and thus enable the determination of the exact mode of action.

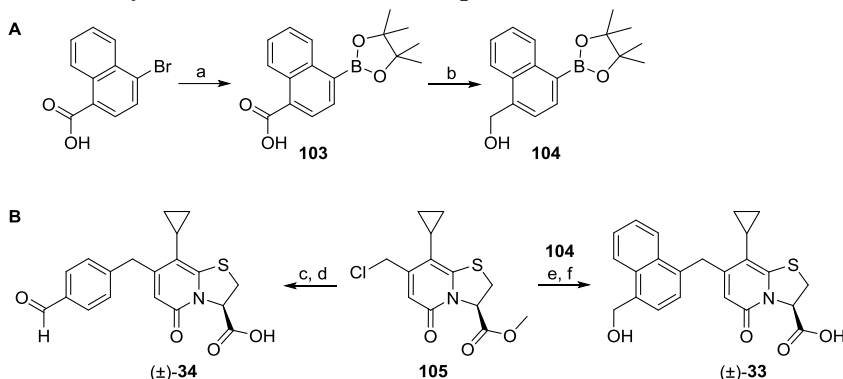
Antibiotic resistance is a problem that affects every country around the world. This means that collaborations between countries, organisations, industries, and research groups are needed to solve the increasing problem of resistance. It is not only new effective drugs that are required to solve this, but several other aspects must also be considered. One step towards using fewer drugs is to prevent infection and this involves different ways of action depending on the disease. Access to clean water is a basic need but still a rare thing in several countries. By ensuring access to clean water would increase the standard of hygiene and reduce the spread of infections. Another step would be to stop overusing antibiotics when they are not necessary, both in animal and humans. To reduce this, better and faster diagnostic tools and better health care in all the areas in the world would be needed. A part of the strategy of halting the spread of antibiotic resistance could be to run information campaigns about how to avoid getting infections and the problems with overusing antibiotics. Resistance is a natural phenomenon and therefore it will continue to arise, however, the speed of resistance development can be halted if we find ways to avoid feeding it.

Conclusion

The discovery of new therapeutic agents to battle bacterial infections is complex and many different aspects need to be considered. The two projects in this thesis have resulted in potent ring-fused 2-pyridone analogues with anti-virulent activity towards *L. monocytogenes* or *C. trachomatis*. With the known target in *L. monocytogenes*, structure-based design was performed and resulted in a potent analogue that block virulence factor expression without stopping the growth of the bacteria. This compound was also effective *in vivo* and improved the life-span of *L. monocytogenes* infected chicken embryos. Further structural development has resulted in new potent compounds and the evaluation of them is ongoing. Within the project targeting *C. trachomatis*, the most potent compounds inhibit *C. trachomatis* infectivity at low nanomolar concentrations. The compounds are non-mutagenic, have low toxicity and do not inhibit growth of commensal bacteria. Further development of these compounds resulted in an analogue with improved pharmacokinetic properties and remarkable increased oral bioavailability. All together, these finding have resulted in several important steps forward towards our goal of finding suitable anti-virulence compounds useful for drug development.

Appendix 1

Scheme A1. Synthesis of **33** and **34** from published intermediate **105**.⁴¹



Reagents and conditions: a) bis(pinacolato)diboron, 1,1'-bis(diphenylphosphino)ferrocene]-dichloropalladium(II) complex with DCM KOAc, dioxane, 100 °C, 23 h, 88%; b) 2 M borane dimethyl sulfide complex in THF, THF, rt, 20 h; 96%; c) 4-formylbenzeneboronic acid, bis(triphenylphosphine)palladium(II) dichloride, KF, MeOH, MWI, 100 °C, 10 min, %; d) 1 M LiOH_(aq), THF, rt, 23 h, 13% over 2 steps; e) bis(triphenylphosphine)palladium(II) chloride, KF, MeOH, MWI, 120 °C, 10 min; f) 1 M LiOH_(aq), THF, rt, 38 h, 22% over 2 steps.

Experimental data:

4-(4,4,5,5-tetramethyl-1,3,2-dioxaborolan-2-yl)-1-naphthoic acid **103**

Bis(pinacolato)diboron (439 mg, 1.73 mmol), KOAc (499 mg, 5.09 mmol) and 1,1'-bis(diphenylphosphino)ferrocene]-dichloropalladium(II) complex with DCM (58 mg, 0.071 mmol) were added to a solution of 4-bromo-1-naphthalenecarboxylic acid (362 mg, 1.44 mmol) in dioxane (1.2 mL) and the reaction mixture was heated at 100 °C for 23 h. The mixture was filtered through Celite, washed with EtOAc and DCM. The organic layer was washed with brine, dried (Na₂SO₄) and concentrated under reduced pressure. Purification by flash chromatography (SiO₂, 0-50% EtOAc in heptane) gave the product as a white solid (378 mg, 88%). ¹H NMR (400 MHz, CDCl₃): δ 9.03-8.99 (m, 1H), 8.84-8.79 (m, 1H), 8.31-8.27 (m, 1H), 8.12-8.08 (m, 1H), 7.68-7.54 (m, 2H), 1.44 (s, 12H). ¹³C NMR (100 MHz, CDCl₃): δ 171.4, 137.5, 133.9, 131.1, 130.0, 129.1, 128.3, 127.6, 126.8, 126.0, 84.4, 25.1.

[4-(4,4,5,5-tetramethyl-1,3,2-dioxaborolan-2-yl)naphthalen-1-yl]methanol **104**

2 M borane dimethyl sulfide complex (2.4 mL, 4.8 mmol) was added dropwise to a stirred solution of **103** (361 mg, 1.21 mmol) in anhydrous THF (15 mL) and was stirred at rt for 19 h. The reaction mixture was cooled on ice, quenched slowly with MeOH (5 mL) and the mixture was stirred for 30 min and then concentrated under reduced pressure. Purification by flash chromatography (SiO₂, 0-50% EtOAc in heptane) obtained the product as a white solid (284 mg, 83%). ¹H NMR (400 MHz, CDCl₃): δ 8.85-8.78 (m, 1H), 8.17-8.02 (m, 2H), 7.59-7.50 (m, 3H), 5.20-5.15 (m, 2H), 1.77-1.69 (m, 1H), 1.42 (s, 12H). ¹³C NMR (100 MHz, CDCl₃): δ 139.7, 137.3, 135.5, 130.9, 129.3, 126.4, 126.1, 124.2, 123.7, 83.9, 63.9, 25.1.

8-cyclopropyl-7-[(4-(hydroxymethyl)naphthalen-1-yl)methyl]-5-oxo-2,3-dihydrothiazolo[3,2-*a*]pyridine-3-carboxylic acid (±)-**33**

Compound **104** (139 mg, 0.490 mmol), compound **105** (98 mg, 0.33 mmol), KF (32 mg, 0.55 mmol) and bis(triphenylphosphine)palladium(II) chloride (21 mg, 0.030 mmol) were suspended in dry MeOH (3 mL). The suspension was heated in MWI at 120 °C for 10 min, cooled to rt, quenched with sat. NaHCO_{3(aq)}, diluted with EtOAc and filtered. The organic layer was washed with H₂O:brine (1:1) and the aqueous layer was extracted with EtOAc. The combined organic layers were washed with brine, dried (Na₂SO₄), and concentrated under reduced pressure. The crude was semi-purified by flash chromatography (SiO₂, 70-100% EtOAc in heptane) to obtain a mixture of the product and the dehalogenated analogue as a white foam (91 mg). The crude (80 mg) was dissolved in dry THF (5 mL). 1 M LiOH_(aq) (0.38 mL) was added and the mixture was stirred at rt for 38 h, cooled on ice, and quenched with 1 M HCl_(aq) (1 mL). The aqueous layer was extracted with EtOAc (×4) and the combined organic layers were washed with brine, dried (Na₂SO₄), and concentrated under reduced pressure. Purification by HPLC (MeCN/H₂O with 0.75% formic acid, 30–100% for 30 min, at 214 nm) and subsequent freeze drying gave the product as an off-white powder (39 mg, 22%).

¹H NMR (400 MHz, DMSO-*d*₆): δ 13.33 (br s, 1H), 8.17-8.11 (m, 1H), 7.90-7.84 (m, 1H), 7.58-7.49 (m, 3H), 7.34 (d, *J* = 7.2 Hz, 1H), 5.35-5.25 (m, 2H), 5.21 (s, 1H), 4.97 (d, *J* = 5.1 Hz, 2H), 4.48, 4.37 (ABq, *J*_{AB} = 17.4 Hz, 1H), 3.78 (dd, *J* = 9.1, 11.9 Hz, 1H), 3.50 (dd, *J* = 1.8, 11.9 Hz, 1H), 1.68-1.79 (m, 1H), 0.99-0.84 (m, 2H), 0.80-0.72 (m, 1H), 0.69-0.59 (m, 1H). ¹³C NMR (100 MHz, DMSO-*d*₆): δ 169.6, 159.9, 156.5, 147.9, 137.1, 133.7, 131.6, 131.2, 127.2, 125.9, 125.7, 124.6*, 124.1, 113.4, 111.9, 62.4, 61.3, 35.4, 31.2, 10.7, 7.4, 7.2. HRMS (ESI⁺) (*m/z*): [M +

$\text{Na}]^+$ calcd for $\text{C}_{23}\text{H}_{21}\text{NNaO}_4\text{S}$, 430.1082 found: 430.1084. *Note: Overlap of two aromatic carbons, seen in HSQC-spectra.

8-cyclopropyl-7-(4-formylbenzyl)-5-oxo-2,3-dihydrothiazolo[3,2-*a*]pyridine-3-carboxylic acid (\pm)-**34**

Compound **105** (200 mg, 0.667 mmol), 4-formylbenzeneboronic acid (202 mg, 1.35 mmol), KF (78 mg, 1.3 mmol) and bis(triphenylphosphine)palladium(II) dichloride (23 mg, 0.033 mmol) were suspended in anhydrous MeOH (10 mL). The suspension was heated in MWI at 100 °C for 10 min, cooled to rt, diluted with EtOAc, quenched with sat. $\text{NaHCO}_3(\text{aq})$ and filtered. The organic layer was washed with H_2O /brine (1:1) and the aqueous layer was extracted with EtOAc. The combined organic layers were washed with brine, dried (Na_2SO_4) and concentrated under reduced pressure. Purification by flash chromatography (SiO_2 , 70-100% EtOAc in heptane) resulted in a mixture of the product and the dehalogenated analogue of the starting material, as a green oil (118 mg), which was used without further purification in the next step. The crude mixture (61 mg) was dissolved in dry THF (3 mL) and 1 M $\text{LiOH}(\text{aq})$ (0.33 mL) was added. The mixture was stirred at rt for 23 h, cooled on ice, and quenched with 1 M $\text{HCl}(\text{aq})$ (2 mL). The aqueous layer was extracted with EtOAc ($\times 4$). The combined organic layers were washed with brine, dried (Na_2SO_4), and concentrated under reduced pressure. Purification by HPLC (MeCN/ H_2O with 0.75% formic acid, 10–100% for 30 min, at 214 nm) and subsequent freeze drying gave the product as a white powder (16 mg, 13%). ^1H NMR (600 MHz, $\text{DMSO}-d_6$): δ 13.30 (br s, 1H), 9.98 (s, 1H), 7.88 (d, $J = 7.9$ Hz, 2H), 7.47 (d, $J = 7.9$ Hz, 2H), 5.80 (s, 1H), 5.41-5.37 (m, 1H), 4.12, 4.06 (ABq, $J_{AB} = 15.6$ Hz, 2H), 3.78 (dd, $J = 9.3, 11.6$ Hz, 1H), 3.53-3.47 (m, 1H), 1.40-1.31 (m, 1H), 0.93-0.80 (m, 2H), 0.66-0.58 (m, 1H), 0.55-0.48 (m, 1H). ^{13}C NMR (151 MHz, $\text{DMSO}-d_6$): δ 192.7, 169.6, 159.9, 155.4, 148.6, 146.0, 134.7, 129.81, 129.79, 114.4, 111.7, 62.6, 38.3, 31.3, 10.9, 7.7, 7.5. HRMS (ESI $^+$) (m/z): $[\text{M} + \text{H}]^+$ calcd for $\text{C}_{19}\text{H}_{18}\text{NO}_4\text{S}$, 356.0951 found: 356.0954.

Compound (\pm)-**40** was resynthesized according to published procedures from racemic (\pm)-**1** and NMR-data was in agreement with published compound.⁹⁸

8-(dimethylamino)-3-(hydroxymethyl)-7-[(4-methylnaphthalen-1-yl)methyl]-2,3-dihydro-5H-thiazolo[3,2-*a*]pyridin-5-one (\pm)-**37**

The experiment was run in two vials, with half amount in each. 1 M $\text{BH}_3\cdot\text{Me}_2\text{S}$ in DCM (1.6 mL, 1.6 mmol) was slowly added to a suspension of (\pm)-**24** (154 mg, 0.390 mmol) in dry THF (8 mL) at rt and the vials were capped. The suspension turned transparent upon addition of $\text{BH}_3\cdot\text{Me}_2\text{S}$ and after 10 min it turned into a milky-like solution/suspension. After stirring the reaction mixture at rt for 22 h,

it had turned transparent again. The solution was cooled on ice and MeOH (5 mL in each vial) was added very slowly and the solution was stirred for 30 minutes before being transferred and combined in a round bottom flask and concentrated under reduced pressure. Purification by flash chromatography (SiO₂, heptane/EtOAc/MeOH, 0.5:9:0.5) gave the crude product (136 mg). A portion of the crude (27 mg) was further purified by flash chromatography (SiO₂, heptane/EtOAc/MeOH 0.5:9:0.5 in heptane, 50-100%) and afforded the product as a yellow powder (13 mg). The impure fractions (8 mg) was combined with crude product (20 mg) and was purified by flash chromatography (SiO₂, heptane/EtOAc/MeOH 0.5:9:0.5 in heptane, 50-100%) which afforded more of the yellow product (10 mg). The yield of the pure product was 23 mg (45%). ¹H NMR (600 MHz, CDCl₃) δ 8.02 (d, *J* = 8.4 Hz, 1H), 7.80 (d, *J* = 8.3 Hz, 1H), 7.53-7.48 (m, 1H), 7.48-7.43 (m, 1H), 7.27-7.24 (m, 1H), 7.17 (d, *J* = 7.1 Hz, 1H), 5.71 (s, 1H), 5.22-5.16 (m, 1H), 4.31-4.23 (m, 2H), 4.00 (dd, *J* = 6.9, 11.2 Hz, 1H), 3.78 (dd, *J* = 5.5, 11.2 Hz, 1H), 3.54 (dd, *J* = 8.1, 11.6 Hz, 1H), 3.22 (dd, *J* = 2.5, 11.6 Hz, 1H), 2.78 (s, 6H), 2.69 (s, 3H). ¹³C NMR (151 MHz, CDCl₃) δ 162.1, 157.1, 146.5, 134.0, 133.3, 132.3, 132.1, 127.9, 127.7, 126.4, 125.9, 125.7, 125.1, 124.6, 114.9, 65.4, 63.1, 43.0, 42.1, 34.7, 31.0, 19.6. HRMS (ESI⁺) (*m/z*): [M+H]⁺ calcd. for C₂₂H₂₅N₂O₂S, 381.1631; found, 381.1633.

8-(dimethylamino)-3-(iodomethyl)-7-[(4-methylnaphthalen-1-yl)methyl]-2,3-dihydro-5H-thiazolo[3,2-a]pyridin-5-one (±)-**38**

(±)-**37** (72 mg, 0.19 mmol) was dissolved in anhydrous DCM (5 mL). I₂ (65 mg, 0.26 mmol), PPh₃ (114 mg, 0.435 mmol) and imidazole (34 mg, 0.50 mmol) were added, formed a turbid yellow mixture and was stirred at room temperature for 19 h. The reaction mixture was diluted with DCM and washed with 5% Na₂S₂O₃ (aq) (×2). The combined aqueous layers were extracted with DCM and the organic layers were combined, dried (Na₂SO₄) and concentrated under reduced pressure. Purification by flash chromatography (SiO₂, 20-100% EtOAc in heptane) afforded the product as a yellow foam (75 mg, 80%). ¹H NMR (400 MHz, CDCl₃) δ 8.05-8.00 (m, 1H), 7.83-7.78 (m, 1H), 7.54-7.42 (m, 2H), 7.28-7.23 (m, 1H), 7.18 (d, *J* = 7.1 Hz, 1H), 5.64 (s, 1H), 5.29-5.20 (m, 1H), 4.29-4.18 (m, 2H), 3.64-3.53 (m, 2H), 3.52-3.44 (m, 2H), 2.76 (s, 6H), 2.69 (s, 3H). ¹³C NMR (100 MHz, CDCl₃) δ 160.5, 157.0, 144.4, 133.8, 133.3, 132.5, 132.1, 127.7, 127.0, 126.4, 125.8, 125.6, 125.0, 124.6, 115.2, 63.2, 43.1, 42.0, 34.7, 33.3, 19.6, 2.7. HRMS (ESI⁺) (*m/z*): [M+H]⁺ calcd. for C₂₂H₂₄IN₂OS, 491.0649; found, 491.0653.

2-(8-(dimethylamino)-7-[(4-methylnaphthalen-1-yl)methyl]-5-oxo-2,3-dihydro-5H-thiazolo[3,2-a]pyridin-3-yl)acetonitrile (±)-**39**

KCN (12 mg, 0.18 mmol) was added to a stirred suspension of (±)-**38** (43 mg, 0.088 mmol) in MeCN (1 mL) at rt. In a capped microwave vial the reaction

mixture was heated at 50 °C for 5.5 h, the solution was allowed to reach rt and stirred for 16 h. The reaction mixture was re-heated at 60 °C for 8 h, and the heated at 65 °C for 4.5 h. The temperature was reduced to 40 °C and the solution was stirred for 16.5 h. The mixture was again re-heated to 60 °C for 3 h and was allowed to return to rt and was diluted with EtOAc and washed with successively with saturated aqueous NaHCO₃ solution, H₂O, and brine. The aqueous layers were combined and extracted with EtOAc (× 2). The combined organic layers were dried (Na₂SO₄) and concentrated under reduced pressure. Purification by flash chromatography (SiO₂, 70-100% EtOAc in heptane) gave the nitrile as a yellow powder (24 mg, 70%). ¹H NMR (400 MHz, CDCl₃) δ 8.05-8.00 (m, 1H), 7.81-7.75 (m, 1H), 7.54-7.42 (m, 2H), 7.28-7.23 (m, 1H), 7.18 (d, *J* = 7.1 Hz, 1H), 5.64 (s, 1H), 5.31-5.23 (m, 1H), 4.30-4.20 (m, 2H), 3.71 (dd, *J* = 7.7, 12.1 Hz, 1H), 3.32 (d, *J* = 12.1 Hz, 1H), 3.02 (dd, *J* = 3.7, 16.5 Hz, 1H), 2.92 (dd, *J* = 9.5, 16.5 Hz, 1H), 2.78 (s, 6H), 2.69 (s, 3H). ¹³C NMR (100 MHz, CDCl₃) δ 160.4, 157.6, 144.0, 134.0, 133.3, 132.2, 132.0, 127.7, 127.4, 126.4, 125.9, 125.6, 125.1, 124.5, 116.5, 115.3, 58.2, 43.2, 42.0, 34.7, 32.6, 19.6, 19.1. HRMS (ESI⁺) (*m/z*): [M+H]⁺ calcd. for C₂₃H₂₄N₃OS, 390.1635; found, 390.1636.

2-(8-(dimethylamino)-7-[(4-methylnaphthalen-1-yl)methyl]-5-oxo-2,3-dihydro-5H-thiazolo[3,2-a]pyridin-3-yl)acetic acid (±)-**35**

2 M NaOH_(aq) (460 μL, 0.920 mmol) was added to a stirred solution of (±)-**39** (30 mg, 0.077 mmol) in EtOH (1.2 mL) at rt. The reaction vessel was capped and heated in microwave at 130 °C for 5 min. The mixture was allowed to reach rt and was acidified with 2 M HCl_(aq) and concentrated under reduced pressure. The residue was dissolved in DCM, the organic layer was washed with H₂O and the combined aqueous layers were extracted with DCM. The combined organic layers were dried (Na₂SO₄) and concentrated under reduced pressure and lyophilized from MeCN:H₂O (1:5) to afford the crude product (22.9 mg). The crude (10.3 mg) was partly recrystallized from CH₃OH (not all was dissolved) and lyophilized from MeCN:H₂O to afford the product as a white powder (4 mg, 28%#) ¹H NMR (600 MHz, DMSO-*d*₆) δ 12.68 (br s, 1H), 8.07-8.03 (m, 1H), 7.87-7.84 (m, 1H), 7.59-7.51 (m, 2H), 7.33 (d, *J* = 7.1 Hz, 1H), 7.26 (d, *J* = 7.1 Hz, 1H), 5.26 (s, 1H), 5.14-5.08 (m, 1H), 4.26, 4.22 (ABq, *J*_{AB} = 16.9 Hz, 2H), 3.76-3.70 (m, 1H), 3.26 (d, *J* = 11.8 Hz, 1H), 2.71 (s, 6H), 2.68-2.60 (m, 5H). ¹³C NMR (151 MHz, DMSO-*d*₆) δ 171.6, 158.9, 155.8, 145.5, 133.1, 132.8, 132.5, 131.5, 127.4, 126.2, 126.0, 125.7, 124.8, 124.5, 113.3, 58.3, 42.8, 41.6, 34.0, 33.7, 33.0, 19.1. HRMS (ESI⁺) (*m/z*): [M+H]⁺ calcd. for C₂₃H₂₅N₂O₃S, 409.1580; found, 409.1587. #Calculation based on that only 45% of the crude was recrystallized.

Docking: Docking of compounds was performed with AutoDock Vina.⁹⁷ Compound **1** in complex with PrfA (PDB code: 5F1R) was used as the receptor. The whole protein was treated rigid except for the docking of compound **34**,

where Tyr154 was allowed to be flexible. All water molecules were removed except for water 412. The 3-dimensional structures/coordinates of the ligands (**33**, **34**, and **35**) were obtained by the ligand builder implemented in COOT.¹¹⁶ The search space was chosen to cover the tunnel site of monomer A (site AI) of the PrfA protein and default values were used for the other parameters.

Appendix 2

methyl (*R*)-2-isobutyl-4,5-dihydrothiazole-4-carboxylate **97**

Isovaleronitrile (3.77 mL, 36.05 mmol) was added to ethanol (50 mL) at 0 °C, followed by dropwise addition of acetyl chloride (28.2 mL, 398 mmol). The reaction mixture was stirred at 0 °C for 24 h and concentrated under reduced pressure. The reaction mixture was evaporated from EtOAc to obtain the crude amino ether (5.9 g). L-Cysteine methyl ester hydrochloride (7.947 g, 46.30 mmol) and the crude amino ether (5.9 g) were suspended in DCM (50 mL), cooled to 0 °C and triethyl amine (6.70 mL, 48.1 mmol) was added. The reaction mixture was stirred at 0 °C for 2.5 h and then allowed to return to rt and stirred overnight. The reaction mixture was diluted with DCM, washed with sat. NaHCO_{3(aq)} (×2), and the combined aqueous layers were extracted with DCM. The combined organic layers were washed with brine, dried (Na₂SO₄), and concentrated under reduced pressure. Purification by flash chromatography (SiO₂, 0–100% EtOAc in heptane) afforded the product as a colourless oil (4.7 g, 65%). ¹H-NMR, 600 MHz, (CDCl₃) δ 5.07 (t, *J* = 9.0 Hz, 1H), 3.79 (s, 3H), 3.59–3.54 (m, 1H), 3.52–3.47 (m, 1H), 2.43 (d, *J* = 7.3 Hz, 2H), 2.07–1.96 (m, 1H), 0.96 (dd, *J* = 6.6, 2.6 Hz, 6H). ¹³C-NMR, 151 MHz, (CDCl₃) δ 174.7, 171.5, 77.8, 52.8, 43.4, 35.6, 27.9, 22.4. Optical rotation: [α]_D²⁰ = 34 (c 0.003, CHCl₃). HRMS (ESI⁺) (*m/z*): [M+H]⁺ calcd. for C₉H₁₆NO₂S, 202.0896; found, 202.0897

8-isopropyl-7-[(naphthalen-1-yl)methyl]-5-oxo-2,3-dihydrothiazolo[3,2-a]pyridine-3-carboxylic acid (±)-**100** and 8-isopropyl-5-[(naphthalen-1-yl)methyl]-7-oxo-2,3-dihydrothiazolo[3,2-a]pyridine-3-carboxylic acid (±)-**101**

TFA (0.12 mL, 1.6 mmol) was added dropwise to a mixture of naphthyl meldrum's acid **5** (1.3 g, 4.2 mmol) and **97** (303 mg, 1.51 mmol) in DCE (7 mL) and heated in MWI at 120 °C for 3 min. The reaction mixture was allowed to cool to rt, then diluted with DCM and quenched with sat. NaHCO_{3(aq)}. The aqueous layer was extracted with DCM (×2) and the combined organic layers were washed successively with H₂O (added sat. NaHCO_{3(aq)} to aid separation) and brine, dried (Na₂SO₄) and concentrated under reduced pressure. Partially purified by flash chromatography twice, (first time: SiO₂, EtOAc in heptane, 20–100%; second time: SiO₂, EtOAc in heptane, 30–100%) and to obtain a crude mixture of the ring-fused 2-pyridone and the ring-fused 4-pyridone (118 mg).

Parts of the crude mixture (50 mg) was dissolved in THF (5.1 mL) and 1 M LiOH_(aq) (0.254 mL, 0.254 mmol) was added and stirred at rt overnight. The

reaction mixture was quenched with 1 M HCl_(aq) and diluted with EtOAc. The aqueous layer was extracted with EtOAc (×3) and the combined organic layers were successively washed with H₂O and brine, then dried (Na₂SO₄) and concentrated under reduced pressure. Purification and separation by HPLC (MeCN/H₂O with 0.75% formic acid, 10–100% for 30 min, at 254 nm) subsequent freeze drying gave the two compounds; ring-fused 2-pyridone (±)-**100** (off-white powder, 13 mg, 5%) and ring-fused 4-pyridone (±)-**101** (white powder, 11 mg, 5%).

(±)-**100**: ¹H-NMR, 400 MHz, (DMSO-*d*₆) δ 8.00–7.92 (m, 2H), 7.86 (d, *J* = 8.2 Hz, 1H), 7.60–7.52 (m, 2H), 7.51–7.45 (m, 1H), 7.21 (d, *J* = 7.0 Hz, 1H), 5.54 (s, 1H), 5.39–5.32 (m, 1H), 4.36, 4.29 (ABq, *J*_{AB} = 17.1 Hz, 2H), 3.82 (dd, *J* = 11.8, 9.1 Hz, 1H), 3.55 (dd, *J* = 11.8, 1.2 Hz, 1H), 3.07–2.96 (m, 1H), 1.20 (dd, *J* = 6.5 Hz, 6H). ¹³C-NMR, 100 MHz, (DMSO-*d*₆) δ 169.6, 159.7, 153.6, 144.7, 134.6, 133.4, 131.4, 128.7, 127.3, 126.7, 126.4, 125.9, 125.6, 123.7, 117.8, 115.0, 61.9, 35.7, 31.5, 20.6, 19.4. HRMS (ESI⁺) (*m/z*): [M+H]⁺ calcd. for C₂₂H₂₂NO₃S, 380.1315; found, 380.1313. *NOTE: The peak of the tertiary carbon on the isopropyl substituent is not shown in C-NMR or in HSQC.

(±)-**101**: ¹H-NMR, 400 MHz, (DMSO-*d*₆) δ 8.00–7.90 (m, 3H), 7.56–7.46 (m, 3H), 7.37 (d, *J* = 6.9 Hz, 1H), 5.87 (d, *J* = 7.0 Hz, 1H), 4.98 (s, 1H), 4.45, 4.24 (ABq, *J*_{AB} = 17.2 Hz, 2H), 3.87–3.74 (m, 2H), 2.81–2.70 (m, 1H), 1.20–1.13 (m, 6H). ¹³C-NMR, 100 MHz, (DMSO-*d*₆) δ 175.0, 169.9, 149.8, 149.5, 133.5, 131.8, 131.6, 128.6, 128.4, 128.1, 126.5, 126.0, 125.8, 125.4, 124.2, 114.1, 65.6, 35.6, 32.3, 30.6, 19.4, 19.2. LRMS (*m/z*): [M+H]⁺ calcd. for C₂₂H₂₂NO₃S, 380.1; found, 380.1.

8-(methylsulfonyl)-5-[(naphthalen-1-yl)methyl]-7-oxo-2,3-dihydrothiazolo[3,2-*a*]pyridine-3-carboxylic acid (±)-**102**

The hydrolysis procedure was prepared by adaptation of the procedure reported by Mattsson *et. al.*¹¹⁷

Methyl (R)-2-[(methylsulfonyl)methyl]-4,5-dihydrothiazole-4-carboxylate³⁷ (445 mg, 1.88 mmol) and **5** (1.478 g, 4.732 mmol) were mixed with DCM (5 mL) and TFA (151 μL, 1.97 mmol) was added dropwise. Heated at 64 °C for 22 h. Reaction mixture was quenched with sat. NaHCO_{3(aq)} and diluted with DCM. Aqueous layer was extracted with DCM (× 3), combined organic layers were successively washed with H₂O and brine, then dried (Na₂SO₄) and concentrated under reduced pressure. Partially purified by flash chromatography (SiO₂, EtOAc in heptane, 40–100%) to obtain the crude (70 mg), which was purified by flash chromatography (SiO₂, MeOH in DCM, 5%) to obtain the crude ring-fused

4-pyridone (39 mg). The crude ring-fused 4-pyridone was dissolved in MeCN with 2% H₂O (3 mL, v/v), triethylamine (45 μ L, 0.32 mmol) and lithium bromide (80 mg, 0.91 mmol) were added and stirred at rt for 2.5 h. Additional lithium bromide (50 mg, 0.58 mmol) was added and stirred overnight. Additional lithium bromide (50 mg, 0.58 mmol) was added and stirred for 30 h, then cooled on ice and quenched with 1 M HCl_(aq) (5 mL). The mixture was extracted with EtOAc (\times 4) and the combined organic layers were washed with brine, dried (Na₂SO₄) and concentrated under reduced pressure. Purification by HPLC (MeCN/H₂O with 0.75% formic acid, 30–100% for 20 min, at 214 nm) and subsequent freeze drying gave the ring-fused 4-pyridone carboxylic acid (17 mg, 2%). ¹H-NMR, 400 MHz, (DMSO-*d*₆) δ 8.03–7.94 (m, 2H), 7.93–7.88 (m, 1H), 7.59–7.51 (m, 3H), 7.43–7.38 (m, 1H), 6.10–6.02 (m, 1H), 5.06 (s, 1H), 4.56, 4.25 (ABq, J_{AB} = 17.6 Hz, 2H), 3.80–3.72 (m, 2H), 3.21 (s, 3H). ¹³C-NMR, 100 MHz, (DMSO-*d*₆) δ 172.7, 170.0, 158.0, 152.3, 133.5, 131.5, 130.9, 128.8, 128.5, 128.4, 126.7, 126.2, 125.9, 123.9, 120.6, 116.7, 64.6, 42.6, 35.8, 32.0. HRMS (ESI⁺) (m/z): [M+H]⁺ calcd. for C₂₀H₁₈NO₅S₂, 416.0620; found, 416.0631.

Acknowledgement

Suddenly the time is here, five years has passed since I for the first time entered the land of 2-pyridones. These years have been interesting, challenging, and wonderful. There are so many colleagues and friends I would like to thank for their contribution to my research and the time here in Umeå and at the 4th floor in the Chemistry building at Umeå University – Thank all you very, very much!

I would especially like to thank:

Fredrik Almquist, för att du gav mig möjligheten att arbeta som doktorand i din grupp och för all din positiva energi under åren. Du har en unik förmåga att se möjligheter i allt och du är en aldrig sinande källa av nya idéer. Tack så mycket för alla peppande möten och samtal vi har haft under åren och för att du har stöttat och visat uppskattning för mina lyckosamma och kanske inte fullt så lyckosamma resultat i labbet.

Mina två co-supervisors:

Anna Linusson, tack så mycket för dina råd och din hjälp under åren samt alla intressanta samtal vi har haft om allt från kemi till löpning.

Fritiof Pontén, två år in i min doktorandtid så klev du in på scenen och jag är mycket glad för detta. Tack så mycket för all kunskap du har delat med dig av om livet på labb, i industrin och livet i allmänhet. Stort tack för att du alltid har tagit dig tid till att hjälpa mig med både stora och små saker.

The Almquist group: **Pardeep**, for everything and anything you have helped me with during the years. **Andrew**, for still answering all my endless questions. **Mari**, för alla våra härliga fredagssamtal. **Anders**, för att du kan allt. **Souvik**, for always being so positive and helpful. **Dan**, för all pepp, dina sköna kommentarer och för att du är en fantastisk kollega.

All the past members and project workers: especially **Daniel**, **Mette**, **Torbjörn**, **Deepak**, **Duanting**, **Syam**, **Dang**, **Christina**, and **Ingeborg**.

James, for welcoming me into the ‘Listeria’ and ‘Chlamydia’ projects and for introducing me to the lab when I first arrived.

Erik and all the present and past members of the Chorell group and **Paz**.

I would like to thank Swedish Research Council (VR), the Knut and Alice Wallenberg Foundation, the Göran Gustafsson Foundation, Swedish Foundation for Strategic Research (SSF), the Kempe Foundation, Umeå Center for Microbial Research (UCMR), and Umeå University for funding, which made our research possible. I would also like to thank Apotekarsocieteten and Helge Ax:sons Johnsons stiftelse for scholarships, which gave me the opportunity to attend several international conferences abroad.

There are so many people I would like to thank for their work within the ‘Listeria’ and ‘Chlamydia’ projects, for the great work they have done over the years, all interesting discussions, and everything they have helped me with.

All the involved members of the 'Listeria' project: especially **Elisabeth "Liz", Marie, Jörgen, Melanie, Christin, Michael, and Katarina.**

All the involved members of the 'Chlamydia' project: especially **Carlos, Jim, Wael, Sven, Åsa, Emma, Ingela, Esmee and Richard (UDOPP).**

Thank you, **Liz and Melanie**, for providing docking and crystal structure figures, and **Carlos**, for the fluorescent study figure in this thesis.

Henrik och Karina för ert engagemang och stöd under doktoranduppföljningsmötena.

Many hours have been spent teaching in the course lab and I would like to thank **Michael S, Tomas K, Dan A, Bertil, and Dan J** for great teamwork.

Tomas K, för alla tips och trix på labb, cykelkunskap och sköna diskussioner.

Everyone in the corridor on the 3rd and the 4th floor for great discussions and creating a good working environment during these years!

Jag vill tacka alla i kemihuset som har hjälpt mig och förgyllt tiden här, speciellt vill jag tacka:

Marcus för HPLC support, **Mattias** och **Tobias** för att ni har svarat på mina miljoner frågor om NMR, **Irena** och **Pelle** för ovärderlig assistans på kurslabb, **L-G** och **Jonas** för all hjälp med krånglande datorer, alla lokalvårdare som håller rent på våra labb/kontor, alla på Kemiförrådet och alla administratörer/ekonomiansvariga för all hjälp ni bistått med. Framförallt vill jag tacka **Maria J** för att du alltid tar dig tid för mina frågor och för allt administrativt som du har fixat med.

Livet består av så många delar och det är flera personer som jag vill tacka utanför UmUs väggar. Jag vill verkligen tacka alla i "Barbrogympa"-gänget på IKSU för fem härliga år, svettandes och kämpandes tillsammans. Framförallt vill jag tacka **Barbro** för hennes engagemang och energi!

Jag vill visa min djupaste tacksamhet till alla mina vänner i Umeå och Göteborg, för att ni är helt underbara och alltid finns där. Speciellt vill jag tacka **Kicki, Sarah, Linda, Erika** och **Amanda**. Och **L**, tack för att du läste hela, flera gånger.

Lazarus, asante sana kwa kila kitu katika maisha.

Jag är oerhört tacksamt för min familj, mamma **Anne-Marie**, bror **Fredrik**, pappa **Jan, Morgan** and **Connie**. Tack så mycket för att ni alltid stöttar mig och peppar mig på ert egna speciella sätt. Jag vill också tacka familjen **Svensson** för ert stöd.

Robert, för att du helt enkelt är absolut bäst, i alla kategorier!

References

1. Fleming, A. On the antibacterial action of cultures of a penicillium, with special reference to their use in the isolation of *B. influenzae*. *Br. J. Exp. Pathol.* **1929**, *10*, 226-236.
2. Aminov, R. I. A brief history of the antibiotic era: Lessons learned and challenges for the future. *Front. Microbiol.* **2010**, *1*, 134.
3. Silver, L. L. Challenges of antibacterial discovery. *Clin. Microbiol. Rev.* **2011**, *24*, 71-109.
4. Antibacterial agents in clinical development: An analysis of the antibacterial clinical development pipeline, including tuberculosis; World Health Organization: Geneva, Switzerland, **2017**.
5. O'Neill, J. The review on antimicrobial resistance. Tackling drug-resistant infections globally: Final report and recommendations; **2016**.
6. Hsieh, E. M.; Hornik, C. P.; Clark, R. H.; Laughon, M. M.; Benjamin, D. K.; Smith, P. B. Medication use in the neonatal intensive care unit. *Am. J. Perinatol.* **2014**, *31*, 811-822.
7. Blair, J. M.; Webber, M. A.; Baylay, A. J.; Ogbolu, D. O.; Piddock, L. J. Molecular mechanisms of antibiotic resistance. *Nat. Rev. Microbiol.* **2015**, *13*, 42-51.
8. Worldwide country situation analysis: response to antimicrobial resistance; World Health Organization: Geneva, Switzerland, **2015**.
9. Castanon, J. I. R. History of the use of antibiotic as growth promoters in european poultry feeds. *Poult. Sci.* **2007**, *86*, 2466-2471.
10. Grave, K.; Jensen, V. F.; Odensvik, K.; Wierup, M.; Bangen, M. Usage of veterinary therapeutic antimicrobials in Denmark, Norway and Sweden following termination of antimicrobial growth promoter use. *Prev. Vet. Med.* **2006**, *75*, 123-132.
11. Bengtsson, B.; Wierup, M. Antimicrobial resistance in scandinavia after a ban of antimicrobial growth promoters. *Anim. Biotechnol.* **2006**, *17*, 147-156.
12. Brown, E. D.; Wright, G. D. Antibacterial drug discovery in the resistance era. *Nature* **2016**, *529*, 336.
13. Rasko, D. A.; Sperandio, V. Anti-virulence strategies to combat bacteria-mediated disease. *Nat. Rev. Drug Discov.* **2010**, *9*, 117-128.
14. Allen, R. C.; Popat, R.; Diggle, S. P.; Brown, S. P. Targeting virulence: can we make evolution-proof drugs? *Nat. Rev. Micro.* **2014**, *12*, 300-308.
15. Antimicrobial resistance: global report on surveillance 2014; World Health Organization: WHO Press, Geneva, Switzerland, **2014**.
16. Davies, J.; Davies, D. Origins and evolution of antibiotic resistance. *Microbiol. Mol. Biol. Rev.* **2010**, *74*, 417-433.
17. Jernberg, C.; Löfmark, S.; Edlund, C.; Jansson, J. K. Long-term impacts of antibiotic exposure on the human intestinal microbiota. *Microbiology* **2010**, *156*, 3216-3223.
18. Dethlefsen, L.; Relman, D. A. Incomplete recovery and individualized responses of the human distal gut microbiota to repeated

antibiotic perturbation. *Proc. Natl. Acad. Sci. U. S. A.* **2011**, *108 Suppl 1*, 4554-4561.

19. De La Cochetière, M. F.; Durand, T.; Lepage, P.; Bourreille, A.; Galmiche, J. P.; Doré, J. Resilience of the dominant human fecal microbiota upon short-course antibiotic challenge. *J. Clin. Microbiol.* **2005**, *43*, 5588-5592.

20. Vincent, C.; Manges, A. R. Antimicrobial use, human gut microbiota and *Clostridium difficile* colonization and infection. *Antibiotics* **2015**, *4*, 230-253.

21. Peterson, J. W. Bacterial Pathogenesis, Chapter 7. In *Medical Microbiology*, 4th ed.; Baron, S., Ed. University of Texas medical branch at Galveston: Galveston, 1996.

22. Totsika, M. Disarming pathogens: benefits and challenges of antimicrobials that target bacterial virulence instead of growth and viability. *Future Med. Chem.* **2017**, *9*, 267-269.

23. Totsika, M. Benefits and challenges of antivirulence antimicrobials at the dawn of the post-antibiotic era. *Curr. Med. Chem.* **2016**, *6*, 30-37.

24. Cegelski, L.; Marshall, G. R.; Eldridge, G. R.; Hultgren, S. J. The biology and future prospects of antivirulence therapies. *Nat. Rev. Microbiol.* **2008**, *6*, 17-27.

25. WHO guidelines for the treatment of *Chlamydia trachomatis*; 978 92 4 154971 4; World Health Organization: WHO Document Production Services, Geneva, Switzerland, **2016**.

26. Svensson, A.; Larsson, A.; Emtenäs, H.; Hedenström, M.; Fex, T.; Hultgren, S. J.; Pinkner, J. S.; Almqvist, F.; Kihlberg, J. Design and evaluation of pilicides: Potential novel antibacterial agents directed against uropathogenic *Escherichia coli*. *ChemBioChem* **2001**, *2*, 915-918.

27. Pinkner, J. S.; Remaut, H.; Buelens, F.; Miller, E.; Åberg, V.; Pemberton, N.; Hedenström, M.; Larsson, A.; Seed, P.; Waksman, G.; Hultgren, S. J.; Almqvist, F. Rationally designed small compounds inhibit pilus biogenesis in uropathogenic bacteria. *Proc. Natl. Acad. Sci. U. S. A.* **2006**, *103*, 17897-17902.

28. Emtenäs, H.; Carlsson, M.; Pinkner, J. S.; Hultgren, S. J.; Almqvist, F. Stereoselective synthesis of optically active bicyclic β -lactam carboxylic acids that target pilus biogenesis in pathogenic bacteria. *Org. Biomol. Chem.* **2003**, *1*, 1308-1314.

29. Pemberton, N.; Emtenäs, H.; Boström, D.; Domaille, P. J.; Greenberg, W. A.; Levin, M. D.; Zhu, Z.; Almqvist, F. Cycloaddition of Δ^2 -thiazolines and acyl ketenes under acidic conditions results in bicyclic 1,3-oxazinones and not 6-acylpenams as earlier reported. *Org. Lett.* **2005**, *7*, 1019-1021.

30. Åberg, V.; Sellstedt, M.; Hedenström, M.; Pinkner, J. S.; Hultgren, S. J.; Almqvist, F. Design, synthesis and evaluation of peptidomimetics based on substituted bicyclic 2-pyridones-targeting virulence of uropathogenic *E. coli*. *Bioorg. Med. Chem.* **2006**, *14*, 7563-7581.

31. Chorell, E.; Das, P.; Almqvist, F. Diverse functionalization of thiazolo ring-fused 2-pyridones. *J. Org. Chem.* **2007**, *72*, 4917-4924.

32. Åberg, V.; Das, P.; Chorell, E.; Hedenström, M.; Pinkner, J. S.; Hultgren, S. J.; Almqvist, F. Carboxylic acid isosteres improve the activity of ring-fused 2-pyridones that inhibit pilus biogenesis in *E. coli*. *Bioorg. Med. Chem. Lett.* **2008**, *18*, 3536-3540.
33. Bengtsson, C.; Almqvist, F. Regioselective halogenations and subsequent Suzuki–Miyaura coupling onto bicyclic 2-pyridones. *J. Org. Chem.* **2010**, *75*, 972-975.
34. Chorell, E.; Pinkner, J. S.; Bengtsson, C.; Banchelin, T. S.-L.; Edvinsson, S.; Linusson, A.; Hultgren, S. J.; Almqvist, F. Mapping pilicide anti-virulence effect in *Escherichia coli*, a comprehensive structure–activity study. *Bioorg. Med. Chem.* **2012**, *20*, 3128-3142.
35. Good, J. A.; Silver, J.; Nunez-Otero, C.; Bahnan, W.; Krishnan, K. S.; Salin, O.; Engstrom, P.; Svensson, R.; Artursson, P.; Gylfe, A.; Bergstrom, S.; Almqvist, F. Thiazolino 2-pyridone amide inhibitors of *Chlamydia trachomatis* infectivity. *J. Med. Chem.* **2016**, *59*, 2094-2108.
36. Singh, P.; Chorell, E.; Krishnan, K. S.; Kindahl, T.; Åden, J.; Wittung-Stafshede, P.; Almqvist, F. Synthesis of multiring fused 2-pyridones via a nitrene insertion reaction: Fluorescent modulators of α -synuclein amyloid formation. *Org. Lett.* **2015**, *17*, 6194-6197.
37. Kulén, M.; Lindgren, M.; Hansen, S.; Cairns, A. G.; Grundström, C.; Begum, A.; van der Lingen, I.; Brännström, K.; Hall, M.; Sauer, U. H.; Johansson, J.; Sauer-Eriksson, A. E.; Almqvist, F. Structure-based design of inhibitors targeting PrfA, the master virulence regulator of *Listeria monocytogenes*. *J. Med. Chem.* **2018**.
38. Emtenäs, H.; Alderin, L.; Almqvist, F. An enantioselective ketene–imine cycloaddition method for synthesis of substituted ring-fused 2-pyridinones. *J. Org. Chem.* **2001**, *66*, 6756-6761.
39. Emtenäs, H.; Taflin, C.; Almqvist, F. Efficient microwave assisted synthesis of optically active bicyclic 2-pyridinones via Δ^2 -thiazolines. *Mol. Diversity* **2003**, *7*, 165-169.
40. Chorell, E.; Bengtsson, C.; Sainte-Luce Banchelin, T.; Das, P.; Uvell, H.; Sinha, A. K.; Pinkner, J. S.; Hultgren, S. J.; Almqvist, F. Synthesis and application of a bromomethyl substituted scaffold to be used for efficient optimization of anti-virulence activity. *Eur. J. Med. Chem.* **2011**, *46*, 1103-1116.
41. Sellstedt, M.; Krishna Prasad, G.; Syam Krishnan, K.; Almqvist, F. Directed diversity-oriented synthesis. Ring-fused 5- to 10-membered rings from a common peptidomimetic 2-pyridone precursor. *Tetrahedron Lett.* **2012**, *53*, 6022-6024.
42. Pemberton, N.; Åberg, V.; Almstedt, H.; Westermarck, A.; Almqvist, F. Microwave-assisted synthesis of highly substituted aminomethylated 2-pyridones. *J. Org. Chem.* **2004**, *69*, 7830-7835.
43. Chorell, E.; Pinkner, J. S.; Phan, G.; Edvinsson, S.; Buelens, F.; Remaut, H.; Waksman, G.; Hultgren, S. J.; Almqvist, F. Design and synthesis of C-2 substituted thiazolo and dihydrothiazolo ring-fused 2-pyridones: pilicides with increased antivirulence activity. *J. Med. Chem.* **2010**, *53*, 5690-5695.
44. Engström, P.; Krishnan, K. S.; Ngyuen, B. D.; Chorell, E.; Normark, J.; Silver, J.; Bastidas, R. J.; Welch, M. D.; Hultgren, S. J.; Wolf-Watz, H.; Valdivia, R. H.; Almqvist, F.; Bergström, S. A 2-pyridone-amide inhibitor

targets the glucose metabolism pathway of *Chlamydia trachomatis*. *mBio* **2014**, 6, e02304-14.

45. Good, J. A.; Andersson, C.; Hansen, S.; Wall, J.; Krishnan, K. S.; Begum, A.; Grundström, C.; Niemiec, M. S.; Vaitkevicius, K.; Chorell, E.; Wittung-Stafshede, P.; Sauer, U. H.; Sauer-Eriksson, A. E.; Almqvist, F.; Johansson, J. Attenuating *Listeria monocytogenes* virulence by targeting the regulatory protein prfA. *Cell. Chem. Biol.* **2016**, 23, 404-414.

46. Vázquez-Boland, J. A.; Kuhn, M.; Berche, P.; Chakraborty, T.; Domínguez-Bernal, G.; Goebel, W.; González-Zorn, B.; Wehland, J.; Kreft, J. *Listeria* pathogenesis and molecular virulence determinants. *Clin. Microbiol. Rev.* **2001**, 14, 584-640.

47. Freitag, N. E.; Port, G. C.; Miner, M. D. *Listeria monocytogenes* – from saprophyte to intracellular pathogen. *Nat. Rev. Microbiol.* **2009**, 7, 623-628.

48. European Food Safety Authority. The European Union summary report on trends and sources of zoonoses, zoonotic agents and food-borne outbreaks in 2016. *EFSA Journal* **2017**, 15, e05077.

49. Lecuit, M. Understanding how *Listeria monocytogenes* targets and crosses host barriers. *Clin. Microbiol. Infect.* **2005**, 11, 430-436.

50. Doganay, M. Listeriosis: clinical presentation. *FEMS Immunol. Med. Microbiol.* **2003**, 35, 173-175.

51. Drevets, D. A.; Bronze, M. S. *Listeria monocytogenes*: epidemiology, human disease, and mechanisms of brain invasion. *FEMS Immunol. Med. Microbiol.* **2008**, 53, 151-165.

52. Thévenot, D.; Dernburg, A.; Vernozy-Rozand, C. An updated review of *Listeria monocytogenes* in the pork meat industry and its products. *J. Appl. Microbiol.* **2006**, 101, 7-17.

53. Cabedo, L.; Barrot, L. P. i.; Canelles, A. T. i. Prevalence of *Listeria monocytogenes* and *Salmonella* in ready-to-eat food in Catalonia, Spain. *J. Food Prot.* **2008**, Vol. 71, 855-859.

54. Swaminathan, B.; Gerner-Smidt, P. The epidemiology of human listeriosis. *Microbes Infect.* **2007**, 9, 1236-1243.

55. Madeo, M.; Musumeci, R.; Careddu, A. M. L.; Amato, E.; Pontello, M. M.; Cocuzza, C. E. Antimicrobial susceptibility of *Listeria monocytogenes* isolates from human cases in northern Italy, 2008–2010: MIC determination according to EUCAST broth microdilution method. *J. Chemother.* **2015**, 27, 201-206.

56. Hansen, J. M.; Gerner-Smidt, P.; Bruun, B. Antibiotic susceptibility of *Listeria monocytogenes* in Denmark 1958–2001. *APMIS* **2005**, 113, 31-36.

57. Doménech, E.; Jimenez -Belenguer, A.; Amoros, J. A.; Ferrus, M. A.; Escriche, I. Prevalence and antimicrobial resistance of *Listeria monocytogenes* and *Salmonella* strains isolated in ready-to-eat foods in Eastern Spain. *Food Control* **2015**, 47, 120-125.

58. Gómez, D.; Azón, E.; Marco, N.; Carramiñana, J. J.; Rota, C.; Ariño, A.; Yangüela, J. Antimicrobial resistance of *Listeria monocytogenes* and *Listeria innocua* from meat products and meat-processing environment. *Food Microbiol.* **2014**, 42, 61-65.

59. Conter, M.; Paludi, D.; Zanardi, E.; Ghidini, S.; Vergara, A.; Ianieri, A. Characterization of antimicrobial resistance of foodborne *Listeria monocytogenes*. *Int. J. Food Microbiol.* **2009**, *128*, 497-500.
60. Tilney, L. G.; Portnoy, D. A. Actin filaments and the growth, movement, and spread of the intracellular bacterial parasite, *Listeria monocytogenes*. *J. Cell Biol.* **1989**, *109*, 1597-1608.
61. de las Heras, A.; Cain, R. J.; Bielecka, M. K.; Vázquez-Boland, J. A. Regulation of *Listeria* virulence: PrfA master and commander. *Curr. Opin. Microbiol.* **2011**, *14*, 118-127.
62. Scotti, M.; Monzó, H. J.; Lacharme-Lora, L.; Lewis, D. A.; Vázquez-Boland, J. A. The PrfA virulence regulon. *Microbes Infect.* **2007**, *9*, 1196-1207.
63. Burton, M. J.; Mabey, D. C. The global burden of trachoma: a review. *PLoS Negl. Trop. Dis.* **2009**, *3*, e460.
64. Bastidas, R. J.; Elwell, C. A.; Engel, J. N.; Valdivia, R. H. Chlamydial Intracellular Survival Strategies. *Cold Spring Harbor Perspect. Med.* **2013**, *3*, a010256.
65. Wright, H. R.; Turner, A.; Taylor, H. R. Trachoma. *Lancet* **2008**, *371*, 1945-1954.
66. WHO Alliance for the Global Elimination of Trachoma by 2020: progress report on elimination of trachoma, 2014–2016. *Weekly epidemiological record*; World Health Organisation: Geneva, Switzerland 30 June **2017**; pp 359-368.
67. Global incidence and prevalence of selected curable sexually transmitted infections – 2008; 978 92 4 150383 9; World Health Organization: Geneva, Switzerland, **2012**.
68. Sexually Transmitted Disease Surveillance 2016; Centers for Disease Control and Prevention. U.S. Department of Health and Human Services: Atlanta, **2017**.
69. Folkhälsomyndigheten. 2018. Klamydiainfektion. <https://www.folkhalsomyndigheten.se/folkhalsorapportering-statistik/statistikdatabaser-och-visualisering/sjukdomsstatistik/klamydiainfektion/>. (2018-06-21).
70. Batteiger, B. E.; Tu, W.; Ofner, S.; Van Der Pol, B.; Stothard, D. R.; Orr, D. P.; Katz, B. P.; Fortenberry, J. D. Repeated *Chlamydia trachomatis* genital infections in adolescent women. *J. Infect. Dis.* **2010**, *201*, 42-51.
71. Whittington, W. L. H.; Kent, C.; Kissinger, P.; Oh, M. K.; Fortenberry, J. D.; Hillis, S. E.; Litchfield, B.; Bolan, G. A.; St. Louis, M. E.; Farley, T. A.; Handsfield, H. H. Determinants of persistent and recurrent *Chlamydia trachomatis* infection in young women: results of a multicenter cohort study. *Sex. Transm. Dis.* **2001**, *28*, 117-123.
72. Burstein, G. R.; Gaydos, C. A.; Diener-West, M.; Howell, M.; Zenilman, J. M.; Quinn, T. C. Incident *Chlamydia trachomatis* infections among inner-city adolescent females. *JAMA* **1998**, *280*, 521-526.
73. Niccolai, L. M.; Hochberg, A. L.; Ethier, K. A.; Lewis, J. B.; Ickovics, J. R. Burden of recurrent *Chlamydia trachomatis* infections in young women: Further uncovering the “hidden epidemic”. *Arch. Pediatr. Adolesc. Med.* **2007**, *161*, 246-251.

74. Valdivia, R. H. Thinking outside the box: new strategies for antichlamydial control. *Future Microbiol.* **2012**, *7*, 427-429.
75. Lan, J.; Melgers, I.; Meijer, C. J.; Walboomers, J. M.; Roosendaal, R.; Burger, C.; Bleker, O. P.; van den Brule, A. J. Prevalence and serovar distribution of asymptomatic cervical *Chlamydia trachomatis* infections as determined by highly sensitive PCR. *J. Clin. Microbiol.* **1995**, *33*, 3194-3197.
76. Gratrix, J.; Brandley, J.; Dane, M.; Plitt, S. S.; Smyczek, P.; Read, R.; Singh, A. E. A retrospective review of treatment failures using azithromycin and doxycycline in the treatment of rectal *Chlamydia infections* in women and men who have sex with men. *Sex. Transm. Dis.* **2016**, *43*, 110-112.
77. Haggerty, C. L.; Gottlieb, S. L.; Taylor, B. D.; Low, N.; Xu, F.; Ness, R. B. Risk of sequelae after *Chlamydia trachomatis* genital infection in women. *J. Infect. Dis.* **2010**, *201*, 134-155.
78. Ceovic, R.; Gulin, S. J. Lymphogranuloma venereum: diagnostic and treatment challenges. *Infect. Drug Resist.* **2015**, *8*, 39-47.
79. Somani, J.; Bhullar, V. B.; Workowski, K. A.; Farshy, C. E.; Black, C. M. Multiple drug-resistant *Chlamydia trachomatis* associated with clinical treatment failure. *J. Infect. Dis.* **2000**, *181*, 1421-1427.
80. Abdelrahman, Y. M.; Belland, R. J. The chlamydial developmental cycle. *FEMS Microbiol. Rev.* **2005**, *29*, 949-959.
81. Beeckman, D. S.; De Puyseleir, L.; De Puyseleir, K.; Vanrompay, D. Chlamydial biology and its associated virulence blockers. *Crit. Rev. Microbiol.* **2014**, *40*, 313-328.
82. Eiting, M.; Hagelüken, G.; Schubert, W.-D.; Heinz, D. W. The mutation G145S in PrfA, a key virulence regulator of *Listeria monocytogenes*, increases DNA-binding affinity by stabilizing the HTH motif. *Mol. Microbiol.* **2005**, *56*, 433-446.
83. Vega, Y.; Rauch, M.; Banfield, M. J.; Ermolaeva, S.; Scortti, M.; Goebel, W.; Vázquez-Boland, J. A. New *Listeria monocytogenes* prfA* mutants, transcriptional properties of PrfA* proteins and structure–function of the virulence regulator PrfA. *Mol. Microbiol.* **2004**, *52*, 1553-1565.
84. Hall, M.; Grundström, C.; Begum, A.; Lindberg, M. J.; Sauer, U. H.; Almqvist, F.; Johansson, J.; Sauer-Eriksson, A. E. Structural basis for glutathione-mediated activation of the virulence regulatory protein PrfA in *Listeria*. *Proc. Natl. Acad. Sci. U. S. A.* **2016**, *113*, 14733-14738.
85. Reniere, M. L.; Whiteley, A. T.; Hamilton, K. L.; John, S. M.; Lauer, P.; Brennan, R. G.; Portnoy, D. A. Glutathione activates virulence gene expression of an intracellular pathogen. *Nature* **2015**, *517*, 170-173.
86. Reniere, M. L.; Whiteley, A. T.; Portnoy, D. A. An *in vivo* selection identifies *Listeria monocytogenes* genes required to sense the intracellular environment and activate virulence factor expression. *PLOS Pathog.* **2016**, *12*, e1005741.
87. Portman, J. L.; Dubensky, S. B.; Peterson, B. N.; Whiteley, A. T.; Portnoy, D. A. Activation of the *Listeria monocytogenes* Virulence Program by a Reducing Environment. *mBio* **2017**, *8*, e01595-01517.
88. Waring, M. J. Lipophilicity in drug discovery. *Expert Opin. Drug Discovery* **2010**, *5*, 235-248.

89. Andersson, C.; Gripenland, J.; Johansson, J. Using the chicken embryo to assess virulence of *Listeria monocytogenes* and to model other microbial infections. *Nat. Protoc.* **2015**, *10*, 1155-1164.
90. Bjørnstad, S.; Austdal, L. P. E.; Roald, B.; Glover, J. C.; Paulsen, R. E. Cracking the egg: Potential of the developing chicken as a model system for nonclinical safety studies of pharmaceuticals. *J. Pharmacol. Exp. Ther.* **2015**, *355*, 386-396.
91. Janse, E. M.; Jeurissen, S. H. M. Ontogeny and function of two non-lymphoid cell populations in the chicken embryo. *Immunobiology* **1991**, *182*, 472-481.
92. Arunan, E.; Desiraju Gautam, R.; Klein Roger, A.; Sadlej, J.; Scheiner, S.; Alkorta, I.; Clary David, C.; Crabtree Robert, H.; Dannenberg Joseph, J.; Hobza, P.; Kjaergaard Henrik, G.; Legon Anthony, C.; Mennucci, B.; Nesbitt David, J. Defining the hydrogen bond: An account (IUPAC Technical Report). *Pure Appl. Chem.* **2011**, *83*, 1619-1636.
93. Arunan, E.; Desiraju Gautam, R.; Klein Roger, A.; Sadlej, J.; Scheiner, S.; Alkorta, I.; Clary David, C.; Crabtree Robert, H.; Dannenberg Joseph, J.; Hobza, P.; Kjaergaard Henrik, G.; Legon Anthony, C.; Mennucci, B.; Nesbitt David, J. Definition of the hydrogen bond (IUPAC Recommendations 2011). *Pure Appl. Chem.* **2011**, *83*, 1637-1641.
94. Desiraju G. R.; Steiner, T. *The Weak Hydrogen Bond: In Structural Chemistry and Biology*. Oxford University Press: New York, 1999.
95. Dougherty, D. A. The cation- π interaction. *Acc. Chem. Res.* **2013**, *46*, 885-893.
96. Berg, L.; Mishra, B. K.; Andersson, C. D.; Ekström, F.; Linusson, A. The nature of activated non-classical hydrogen bonds: A case study on acetylcholinesterase-ligand complexes. *Chem. – Eur. J.* **2016**, *22*, 2672-2681.
97. Trott, O.; Olson, A. J. AutoDock Vina: Improving the speed and accuracy of docking with a new scoring function, efficient optimization, and multithreading. *J. Comput. Chem.* **2010**, *31*, 455-461.
98. Åberg, V.; Hedenström, M.; Pinkner, J. S.; Hultgren, S. J.; Almqvist, F. C-Terminal properties are important for ring-fused 2-pyridones that interfere with the chaperone function in uropathogenic *E. coli*. *Org. Biomol. Chem.* **2005**, *3*, 3886-3892.
99. Testa, B.; Mayer, J. M. The Hydrolysis of Amides. In *Hydrolysis in Drug and Prodrug Metabolism*, Verlag Helvetica Chimica Acta: Zürich, 2003; pp 81-162.
100. Mohammed, I.; Kummetha, I. R.; Singh, G.; Sharova, N.; Lichinchi, G.; Dang, J.; Stevenson, M.; Rana, T. M. 1,2,3-Triazoles as amide bioisosteres: discovery of a new class of potent HIV-1 Vif antagonists. *J. Med. Chem.* **2016**, *59*, 7677-7682.
101. Valverde, I. E.; Bauman, A.; Kluba, C. A.; Vomstein, S.; Walter, M. A.; Mindt, T. L. 1,2,3-Triazoles as amide bond mimics: triazole scan yields protease-resistant peptidomimetics for tumor targeting. *Angew. Chem., Int. Ed.* **2013**, *52*, 8957-8960.
102. Monceaux, C. J.; Hirata-Fukae, C.; Lam, P. C.; Totrov, M. M.; Matsuoka, Y.; Carlier, P. R. Triazole-linked reduced amide isosteres: an approach for the fragment-based drug discovery of anti-Alzheimer's BACE1 inhibitors. *Bioorg. Med. Chem. Lett.* **2011**, *21*, 3992-3996.

103. Meanwell, N. A. Synopsis of some recent tactical application of bioisosteres in drug design. *J. Med. Chem.* **2011**, *54*, 2529-2591.
104. Stepan, A. F.; Walker, D. P.; Bauman, J.; Price, D. A.; Baillie, T. A.; Kalgutkar, A. S.; Aleo, M. D. Structural alert/reactive metabolite concept as applied in medicinal chemistry to mitigate the risk of idiosyncratic drug toxicity: a perspective based on the critical examination of trends in the top 200 drugs marketed in the United States. *Chem. Res. Toxicol.* **2011**, *24*, 1345-1410.
105. Castanedo, G. M.; Seng, P. S.; Blaquiére, N.; Trapp, S.; Staben, S. T. Rapid synthesis of 1,3,5-substituted 1,2,4-triazoles from carboxylic acids, amidines, and hydrazines. *J. Org. Chem.* **2011**, *76*, 1177-1179.
106. Tornøe, C. W.; Christensen, C.; Meldal, M. Peptidotriazoles on solid phase: [1,2,3]-triazoles by regiospecific copper(I)-catalyzed 1,3-dipolar cycloadditions of terminal alkynes to azides. *J. Org. Chem.* **2002**, *67*, 3057-3064.
107. Rostovtsev, V. V.; Green, L. G.; Fokin, V. V.; Sharpless, K. B. A stepwise Huisgen cycloaddition process: Copper(I)-catalyzed regioselective "ligation" of azides and terminal alkynes. *Angew. Chem., Int. Ed.* **2002**, *41*, 2596-2599.
108. Good, J. A. D.; Kulén, M.; Silver, J.; Krishnan, K. S.; Bahnan, W.; Núñez-Otero, C.; Nilsson, I.; Wede, E.; de Groot, E.; Gylfe, Å.; Bergström, S.; Almqvist, F. Thiazolino 2-pyridone amide isosteres as inhibitors of *Chlamydia trachomatis* infectivity. *J. Med. Chem.* **2017**, *60*, 9393-9399.
109. Ames, B. N.; McCann, J.; Yamasaki, E. Methods for detecting carcinogens and mutagens with the *Salmonella*/mammalian-microsome mutagenicity test. *Mutat. Res.* **1975**, *31*, 347-364.
110. Abràmoff, M. D.; Magalhães, P. J.; Ram, S. J. Image Processing with ImageJ. *Biophotonics Int.* **2004**, *11*, 36-42.
111. Evans, M. D.; Ring, J.; Schoen, A.; Bell, A.; Edwards, P.; Berthelot, D.; Nicewonger, R.; Baldino, C. M. The accelerated development of an optimized synthesis of 1,2,4-oxadiazoles: application of microwave irradiation and statistical design of experiments. *Tetrahedron Lett.* **2003**, *44*, 9337-9341.
112. Code: logP(o/w). *Molecular Operating Environment (MOE)*, version 2016.08; Chemical Computing Group: Quebec, Canada.
113. Bergström, C. A. S.; Strafford, M.; Lazorova, L.; Avdeef, A.; Luthman, K.; Artursson, P. Absorption classification of oral drugs based on molecular surface properties. *J. Med. Chem.* **2003**, *46*, 558-570.
114. Zahedifar, M.; Sheibani, H. Reaction of α -oxoketenes with 2-substituted benzothiazoles and benzimidazoles: synthesis of benzo[4,5]thiazolo[3,2-a]pyridinone and N-(1,3-benzothiazol-2-yl)-3-oxopropanamide derivatives. *Chem. Heterocycl. Comp.* **2016**, *52*, 41-44.
115. Huang, Z.-T.; Shi, X. Synthesis of heterocyclic ketene N,S-acetals and their reactions with esters of α,β -unsaturated acids. *Synthesis* **1990**, *1990*, 162-167.
116. Emsley, P.; Lohkamp, B.; Scott, W. G.; Cowtan, K. Features and development of Coot. *Acta Crystallogr., Sect. D: Biol. Crystallogr.* **2010**, *66*, 486-501.
117. Mattsson, S.; Dahlström, M.; Karlsson, S. A mild hydrolysis of esters mediated by lithium salts. *Tetrahedron Lett.* **2007**, *48*, 2497-2499.

